



The research for this thesis was performed within the framework of the
Erasmus Postgraduate School Molecular Medicine

Printing of the thesis was financially supported by



Functional Analysis of Molecular Alterations in Brain Tumours: from fishing to function

Functionele analyse van moleculaire afwijkingen in hersentumoren;
van 't vissen naar de functie

Proefschrift

ter verkrijging van de graad van doctor aan de
Erasmus Universiteit Rotterdam
op gezag van de
rector magnificus

prof.dr. H.G. Schmidt

en volgens besluit van het College voor Promoties.

De openbare verdediging zal plaatsvinden op

dinsdag 24 september 2013 om 15.30 uur

Nanne Krispijn Kloosterhof
geboren te Schiedam



Promotiecommissie

Promotor: Prof.dr. P.A.E. Sillevius Smitt

Overige leden: Prof.dr. M.J. van den Bent

Prof.dr. S. Leenstra

Prof.dr. J.V.M.G. Bovée

Copromotoren: Dr. E.M.C. Michiels

Dr. P.J. French

"move with the cheese"

Who moved my cheese, Spencer Johnson

Table of Contents

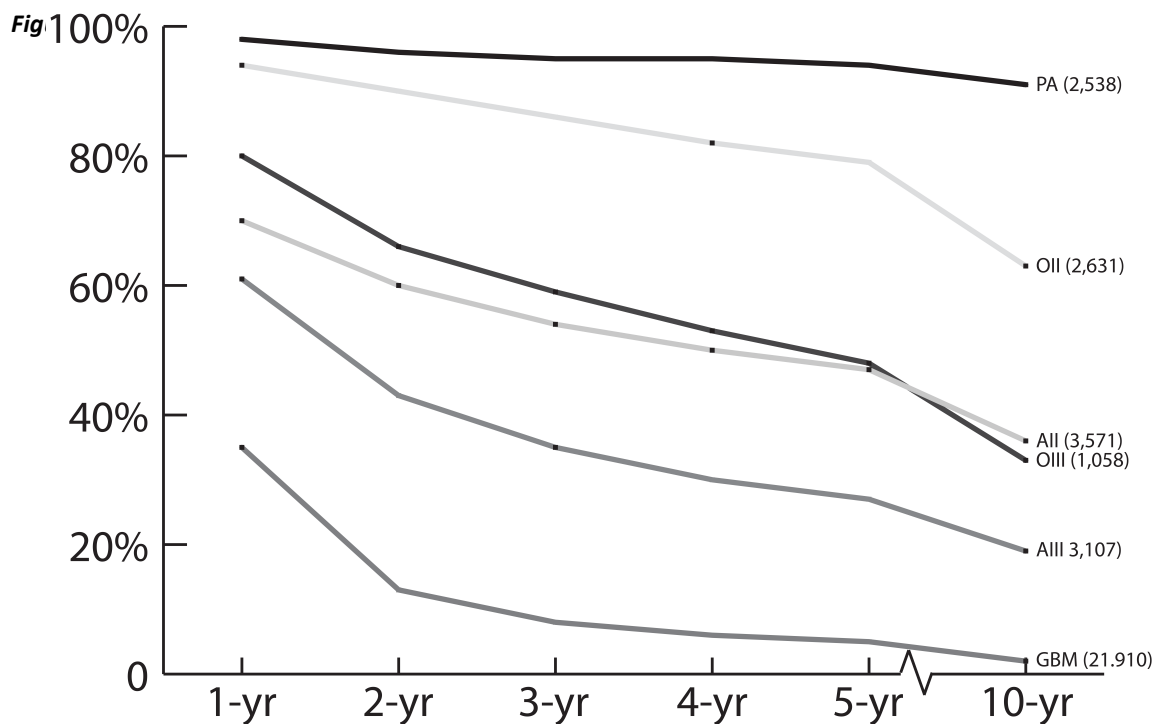
Introduction	7
Chapter One	17
<i>Subgroup Specific Alternative Splicing in Medulloblastoma</i>	
Chapter Two	37
<i>Isocitrate dehydrogenase-1 mutations: a fundamentally new understanding of diffuse glioma?</i>	
Chapter Three	53
<i>Segregation of non-p.R132H mutations in IDH1 in distinct molecular subtypes of glioma</i>	
Chapter Four	63
<i>IDH1 R132H Decreases Proliferation of Glioma Cell Lines In Vitro and In Vivo</i>	
Chapter Five	77
<i>Mutation specific functions of EGFR result in a mutation-specific downstream pathway activation</i>	
Discussion	101
Addendum	111
<i>Summary</i>	<i>112</i>
<i>Samenvatting</i>	<i>113</i>
<i>PhD portfolio</i>	<i>114</i>
<i>List of publications</i>	<i>115</i>
<i>About the author</i>	<i>116</i>

Introduction

Brain tumours consist of primary or de novo tumours, and secondary tumours. The latter group consists of metastasis derived from primary tumours at another location within the body, for example breast or lung. The primary brain tumours form a heterogeneous group of different tumour types with variable prognoses. In adults, the most common types of brain tumour are the meningiomas (mainly benign) and gliomas. In children, although gliomas occur, other tumours are more frequent and include primitive neuroectodermal tumours (PNETs) and medulloblastoma. Pilocytic astro-cytomas and ependymomas, a specific type of glioma, also mainly occur in children.

Gliomas

Gliomas are a common type of brain tumour with a slightly higher frequency in males compared to females, 7.17 and 5.07 per 100,000 in the US (cbtrus.org). Pathologists subdivide gliomas into pilocytic astrocytomas, astrocytomas (A), oligodendrogliomas (O), oligoastrocytomas (OA) and glioblastoma (GBM). Gliomas can be further separated into grades I-IV tumours depending on the number of malignant features present, such as anaplasia, microvascular proliferation and necrosis. (1) Pilocytic astrocytomas (PA) are grade I tumours; astrocytomas, oligodendrogliomas and oligoastrocytomas are either grade II (low grade) or III (anaplastic). GBMs are grade IV. (1) However, the subtyping of gliomas based on histological appearance is difficult and there is intraobserver variation. Molecular diagnostics may aid the pathologist in classifying gliomas. For example, *IDH1* mutations do not occur in PAs but are common events in low grade glioma. (2) Loss of 1p/19q is more frequently seen in oligodendrogliomas than in astrocytomas. (3)



The survival rates of different histologies from CBTRUS.org, estimated from the SEER program. (PA – pilocytic astrocytoma, OII – oligodendroglioma grade II, OIII – oligodendroglioma grade III, AII – astrocytoma grade II, AIII – astrocytoma grade III, GBM – glioblastoma multiforme)

The survival of patients with a brain tumour is associated with of the histological diagnosis. The most frequently occurring glioma, GBM, has a median survival of less than one year and a five years survival of less than 5% (cbtrus.org). Other gliomas have a better prognosis, but apart from PAs all subtypes are eventually fatal. (figure 1)

The treatment options for low grade gliomas include surgery, radiotherapy and chemotherapy. Early radiation results in longer progression free survival but not overall survival. (<http://www.oncoline.nl/gliomen>). In GBM, which grow faster, surgical resection is followed by combined chemoradiation with temozolomide. Recently, in anaplastic oligodendroglial tumors, the benefit of adjuvant PCV chemotherapy was demonstrated, in particular in tumors with 1p/19q codeletion. (4) (<http://www.oncoline.nl/gliomen>)

Medulloblastoma

Medulloblastoma belong to the group embryonal brain tumours. Apart from medulloblastoma, this group consists of CNS primitive neuroectodermal tumours (PNETs) and atypical teratoid/rhabdoid tumours. Based on their histology, medulloblastoma can be further subdivided into classic, desmoplastic/nodular, anaplastic, large cell medulloblastoma and medulloblastoma with extensive nodularity. (1)

Although medulloblastoma most frequently occur in children (median age of 7 at diagnosis), they can occur in adults. (5) The vast majority of the medulloblastoma cases are sporadic, though Li-Fraumeni, Gorlin and Turcot syndromes as well as *SUFU* mutations are all associated with medulloblastoma. (see table 1) (1, 6, 7) The treatment options are surgical resection and chemotherapy for children under 3. In older patients, additional radiotherapy is used. (8, 9) The prognosis for medulloblastoma patients is better than for glioma patients; up to 70-80% of the patients do not have an incurable disease. (8) However, the side effects of the treatment are grave for those who survive the cancer. (9, 10) Treatment for medulloblastoma patients therefore requires improvement

Molecular background of medulloblastoma

There are many genetic and proteomic markers associated with medulloblastoma, see de Bont *et al* for an exhaustive list and Northcott *et al* for a more recent overview of the novel molecular developments. (9, 11) Two well-established pathways, Sonic Hedgehog (SHH) pathway and Wnt pathway, are associated with two groups of medulloblastoma found in expression profiling. (7, 12, 13) Alterations in these pathways consist of mutations, overexpression or deletions. Examples of frequent alterations are PTCH1 mutations, Gli1 overexpression and Axin1 deletions and mutations. (14-16) Syndromes with mutations in PTCH and *SUFU*, both proteins are involved in the SHH pathway, are associated with medulloblastoma. Furthermore, although frequent alterations are found in the Notch pathways, these alterations do not seem to be restricted to a single group. (7, 13)

Other proteins are frequently affected in medulloblastoma, such as mutations in TP53, members of the IGF signaling pathway, and OTX2. (11, 17, 18) Deletion of genes is rare in medulloblastoma, frequent deletions are PTEN, PTCH1 and CDKN2A/B, the former two occurring mainly in tumours associated with the SHH pathway. (17) Amplifications are more frequent, such as MYC proteins in various types of medulloblastoma. (17) Another frequent alteration found in medulloblastoma is isochromosome 17q. Various alterations

have been associated with favourable or unfavourable outcome, such as Wnt pathway activation, through for example β -catenin mutations, with improved survival and, rather ironically, overexpression of survivin is associated with an unfavourable outcome. (19-21)

Molecular background of gliomas

Several hereditary syndromes have been described that are associated with gliomas and medulloblastomas, which can give potential clues which genes are involved in tumourigenesis. Syndromes include neurofibromatosis type I and II, Li-Fraumeni, Tuberous sclerosis and Turcot. (1) (table 1)

Table 1: Familial (brain) tumour syndromes

Name	Gene(s) involved	Most frequent brain tumours
Li-Fraumeni	<i>TP53</i>	Astrocytoma; medulloblastoma, PNET (1)
Turcot	<i>MLH1, MSH2, MSH6 or PMS2</i>	Astrocytoma; GBM; medulloblastoma (1)
Melanoma-astrocytoma syndrome	<i>CDKN2A, CDKN2B, ANRIL</i>	Astrocytoma (22-25)
Tuberous sclerosis	<i>TSC1; TSC2</i>	Subependymal Giant Cell Astrocytoma(1)
Neurofibromatose type 1	<i>NF1</i>	Optic pathway glioma, astrocytoma; GBM (1)
Neurofibromatose type 2	<i>NF2</i>	Vestibular schwannoma, astrocytoma, meningioma (1)
SUFU mutations	<i>SUFU</i>	Medulloblastoma (6)
Gorlin syndrome	<i>PTCH</i>	Medulloblastoma (1)

This table lists several syndromes that have been described to be associated with gliomas and medulloblastomas

Of the genes involved in hereditary syndromes only *TP53* (35%) and *NF1* (18%) are frequently somatically mutated in gliomas. In contrast, genes affected by the hereditary syndromes in medulloblastoma are also affected in sporadic cases (*PCTH1, SUFU, TP53*). The remaining genes found in hereditary glioma syndromes, only *TSC2* and *MSH6* were found to be mutated in a single sample in large sequencing studies of both GBMs and oligodendrogliomas. (26-28) Of note, D-2-hydroxyglutaric aciduria (D-2-HGA), caused by mutations in the *IDH2* gene does not have an increased frequency of gliomas whereas the gene is mutated at significant frequency in this tumor type. (29, 30) However, only 9 D-2-HGA patients have been diagnosed with *IDH2* mutations, all with a reduced lifespan. (29) Therefore the number of patients affected may be too low to show an increased frequency of glioma. Nonetheless, these patients display enchondroma like lesions, which could indicate that gliomas require additional mutations. In 2008, two groups have screened for genes that are somatically mutated in GMBs and have identified three core pathways that are commonly affected in this tumour type: the RTK/RAS/PI(3)K signalling, TP53 signalling and the RB signalling pathway. (28) Interestingly not all genes involved in familial glioma syndromes are part of these three core pathways or are otherwise frequently mutated. (28) This suggests that additional core pathways are still to be uncovered or that new connections can be found between known genes and known pathways. Some caution should be taken however as these studies examined selected histologies such as GBMs (mostly primary GBM) or oligodendrogliomas.

Somatically mutated genes in GBMs include *TP53* (35%), *PTEN* (26%), *NF1* (18%), *EGFR* (14%), *PIK3CA* (10%), *PIK3R1* (8%), *RB1* (8%) and *IDH1* (5%). (26, 31) In GBMs genomic

amplifications include the *EGFR*, *CDK4* and *MDM2* loci (23%), deletions are common in the *CDKN2A*, *TP53*, *PTEN* and *RB1* loci. Fewer genes are mutated in lower grade gliomas. The loss of 1p and 19q is a frequent occurrence in oligodendroglioma and oligoastrocytoma, whereas *TP53* mutation is more frequently found in astrocytomas. (32) Three frequently mutated genes have been found in oligodendroglioma: *FUBP1* (20%), *CIC* (83%) and *IDH1*. (27, 31, 33) Interestingly, *CIC* is also overexpressed in medulloblastoma. (34) In astrocytomas, frequently mutated genes include *IDH1*, *TP53* and *ATRX*. (35)

EGFR

The epidermal growth factor receptor (EGFR) belongs to a family of epidermal growth factor receptors. Other members of this family include ERBB2 (HER2), ERBB3 (HER3) and ERBB4 (HER4). All EGFR family members are characterised by two extracellular cysteine rich domains and an intracellular tyrosine kinase domain. (36) In order to activate EGFR, a ligand (e.g. EGF and TGF- α) has to bind the extracellular domain which results in a conformational change allowing dimerisation on a newly exposed interface. (37-39) This results in an activation of the downstream signalling pathways.

Due to its causal role in cancer, anti-EGFR treatments have been developed. A first indication of the efficacy of targeted therapies (gefitinib, erlotinib) directed against EGFR was observed in cell lines. (40) These therapies are effective in pulmonary adenocarcinomas with activating mutations in the TK domain of *EGFR* (5-10%). In gliomas however, clinical benefit to EGFR inhibitors has been limited. (41)

EGFR is frequently amplified and mutated in several cancer types including breast cancer, pulmonary adenocarcinomas and GBMs. (42) Although *EGFR* mutations are found in many different cancer types, not all cancer types have the same type of mutation. For example, *EGFR* mutations in lung cancer are small activating mutations (point mutations or small deletions in exon 19) in the tyrosine kinase domain. (43) In GBMs the most common mutation is an in-frame deletion of exons 2-7 affecting the extracellular domain (*EGFRvIII*). (26, 44) Both mutation types in lung cancer and GBM result in an activation of the EGFR pathway. (40) A differential distribution of the mutation spectrum in EGFR may be a result of different types of genetic stress per cell type. Alternatively the different mutations have different functional consequences.

IDH1

Point mutations in the gene encoding isocitrate dehydrogenase 1 (*IDH1*) were recently discovered in gliomas. (26) The normal function of IDH1 is to convert isocitrate into α -ketoglutarate and generating NADPH in the process in the cytoplasm. Two other enzymes with similar function exist in eukaryotic cells, IDH2 and IDH3 (the latter being a complex of IDH3 alpha, IDH3 beta and IDH3 gamma (ratio 2:1:1)). Both IDH2 and the IDH3 complex are located in the mitochondria, the former using NADP⁺ while the latter uses NAP⁺.

The mutations found both in *IDH1* and IDH2 are located at highly conserved codons that are involved in substrate binding. The mutated protein has a novel substrate, α -ketoglutarate, and product, D-2-hydroxyglutarate (D-2-HG). (45) D-2-HG is thought to contribute to tumourigenesis as it is a competitive inhibitor of aKG in a-KG-dependent dioxygenases such as TET2. This inhibition results in decreased 5-hydroxymethylcytosine which is the first step in the demethylation of DNA. Ultimately, IDH1 mutation results in

an increased genome wide methylation. Indeed, IDH1 mutations are associated with and cause a CpG island methylator phenotype (CIMP). (60, 61)

In glioma, the point mutations in *IDH1* nearly always occur at codon 132 resulting in a transition of an arginine to a histidine. (46) *IDH1* mutations are also found in other tumour types including acute myeloid leukaemia (AML), cholangiocarcinoma and cartilaginous tumours. (47-50) It is interesting to note that *IDH2* mutations are also frequently found in homologous and conserved codon R172 as well as in codon R140 in AML. *IDH2* mutations are rarely found in glioma. (48, 51) Although mutations are restricted to a single hotspot in IDH1, the frequency distribution of the type of mutation for IDH1 is different for glioma compared to AML. In AML the R132H:R132C ratio is approximately 1:1 whereas in glioma the ratio is approximately 9:1. (32, 46, 48) Similar to the differential distribution of mutations in *EGFR*, it remains to be determined whether these differences are due to external factors, or if these changes have a functional consequence.

Molecular diagnostics in gliomas

The number of molecular markers is increasingly used in glioma diagnostics. The most common alterations known in glioma, used in diagnostics, are the codeletion of chromosome arms 1p and 19q (1p/19q), the methylation of the *MGMT* promotor and more recently *IDH1* mutations. The 1p/19q alterations are most frequently found in oligodendrogliomas. Apart from an improved survival, the codeletion of 1p/19q predicts a better response to chemotherapy. (4) *MGMT* promotor methylation (the addition of a methyl (-CH₃) group to a cytosine) occurs in a subgroup of GBMs. If methylation is present in a tumour, these tumours have a better prognosis and respond better to chemotherapy. (52)

Molecular subgroups of brain tumours

High-throughput data (gene expression, genome wide methylation) allow researchers to group various tumours together based on unbiased approaches. The determination of tumour subgroups depends on the methodological approach, be it looking at gene expression, genome wide methylation or histology. When using big data the number of data points used (partially) determines the subgroups found. Therefore, we usually sort by variance per data point. What has been done using single markers can also be done using multiple markers, thereby finding subgroups with improved survival, or groups that display response to therapy. Using gene expression arrays we were able to identify six subgroups of gliomas. In a heterogeneous group of gliomas, consisting of different histological subtypes, our clustering method was able to predict survival better than histology. (53) Other investigators have found different glioma subgroups ranging from three, four to six. (28, 54, 55) The differences in number of groups depend on the statistical and molecular techniques used. The true value of these molecular subgroups remains to be proven in a clinical setting. What we, and others, have found is that the known single markers, for example EGFR amplification, is absent in some groups and very frequent in others. (56) This indicates that these molecular subgroups based on gene expression arrays are also distinguishing between single markers. Similar to adult gliomas, different molecular subtypes of medulloblastoma have been identified by expression profiling. (7, 12, 13) One of the more commonly used molecular classifications of medulloblastoma identifies four major subtypes WNT, SHH, group C and group D. (12)

Another alteration found in tumours is differential splicing. This is similar to EGFRvIII in which the exons are used differently to generate an mRNA. Using those subgroups we have determined whether specific cases of differential splicing occur more frequently as described in chapter one.

Using another technique, genome wide methylation, one is able to detect two major groups, namely CIMP- and CIMP+. (57-59) These groups correlate strongly with survival in patients with a better survival for the latter. Methylation profiling can so far subdivide gliomas in two major subtypes. (57) However, each tumour is unique, therefore it is a matter of time before more groups will be defined. Whether another subgroup of gliomas is useful in a clinical setting remains to be demonstrated. The initial future research should be focussed on whether molecular classification performs better or worse than histology and which type of molecular classification, gene expression or methylation, should be used for which situation.

Scope of this thesis

In this thesis we wish to further elucidate the molecular changes in adult and paediatric brain tumors. In chapter one we start with a discovery study on subtype specific splice variants in medulloblastoma in order to aid classification and identify novel treatment targets. In chapters two to five we focus on single causal genetic changes in gliomas. We first give an overview on the clinical and molecular implications of *IDH1* and *IDH2* mutations (chapter two). In chapter three we performed an in-depth analysis on the prevalence and distribution of mutations in *IDH1* in gliomas. Little is known on the cellular function of *IDH1* mutations. Therefore, in chapter four we performed a functional analysis on this gene. The advent of large datasets with mutational data reveals a novel complexity: different tumour types have different mutations in the same gene. To determine whether the different mutations have different consequences, in chapter five we have looked at the molecular and functional consequences of different mutations in *IDH1* and *EGFR*. The overall aim was to discover if different mutations have different functions that could influence the tumour.

References

1. David N. Louis HO, Otmar D. Wiestler, Webster K. Cavenee. World Health Organization Classification of Tumours of the Nervous System: IARC; 2007.
2. Korshunov A, Meyer J, Capper D, Christians A, Remke M, Witt H, et al. Combined molecular analysis of BRAF and IDH1 distinguishes pilocytic astrocytoma from diffuse astrocytoma. *Acta Neuropathol.* 2009 Sep;118(3):401-5.
3. Smith JS, Perry A, Borell TJ, Lee HK, O'Fallon J, Hosek SM, et al. Alterations of chromosome arms 1p and 19q as predictors of survival in oligodendrogliomas, astrocytomas, and mixed oligoastrocytomas. *J Clin Oncol.* 2000 Feb;18(3):636-45.
4. van den Bent MJ, Brandes AA, Taphoorn MJ, Kros JM, Kouwenhoven MC, Delattre JY, et al. Adjuvant procarbazine, lomustine, and vincristine chemotherapy in newly diagnosed anaplastic oligodendroglioma: long-term follow-up of EORTC brain tumor group study 26951. *J Clin Oncol.* 2013 Jan 20;31(3):344-50.
5. Bourdeaut F, Miquel C, Alapetite C, Roujeau T, Doz F. Medulloblastomas: update on a heterogeneous disease. *Curr Opin Oncol.* 2011 Nov;23(6):630-7.
6. Taylor MD, Liu L, Raffel C, Hui CC, Mainprize TG, Zhang X, et al. Mutations in *SUFU* predispose to medulloblastoma. *Nat Genet.* 2002 Jul;31(3):306-10.

7. Kool M, Koster J, Bunt J, Hasselt NE, Lakeman A, van Sluis P, et al. Integrated genomics identifies five medulloblastoma subtypes with distinct genetic profiles, pathway signatures and clinicopathological features. *PLoS One*. 2008;3(8):e3088.
8. Gilbertson RJ. Medulloblastoma: signalling a change in treatment. *Lancet Oncol*. 2004 Apr;5(4):209-18.
9. Northcott PA, Jones DT, Kool M, Robinson GW, Gilbertson RJ, Cho YJ, et al. Medulloblastomics: the end of the beginning. *Nat Rev Cancer*. 2012 Dec;12(12):818-34.
10. Palmer SL, Goloubeva O, Reddick WE, Glass JO, Gajjar A, Kun L, et al. Patterns of intellectual development among survivors of pediatric medulloblastoma: a longitudinal analysis. *J Clin Oncol*. 2001 Apr 15;19(8):2302-8.
11. de Bont JM, Packer RJ, Michiels EM, den Boer ML, Pieters R. Biological background of pediatric medulloblastoma and ependymoma: a review from a translational research perspective. *Neuro Oncol*. 2008 Dec;10(6):1040-60.
12. Northcott PA, Korshunov A, Witt H, Hielscher T, Eberhart CG, Mack S, et al. Medulloblastoma comprises four distinct molecular variants. *J Clin Oncol*. 2011 Apr 10;29(11):1408-14.
13. Thompson MC, Fuller C, Hogg TL, Dalton J, Finkelstein D, Lau CC, et al. Genomics identifies medulloblastoma subgroups that are enriched for specific genetic alterations. *J Clin Oncol*. 2006 Apr 20;24(12):1924-31.
14. Vorechovsky I, Tingby O, Hartman M, Stromberg B, Nister M, Collins VP, et al. Somatic mutations in the human homologue of *Drosophila* patched in primitive neuroectodermal tumours. *Oncogene*. 1997 Jul 17;15(3):361-6.
15. Hallahan AR, Pritchard JI, Hansen S, Benson M, Stoeck J, Hatton BA, et al. The SmoA1 mouse model reveals that notch signaling is critical for the growth and survival of sonic hedgehog-induced medulloblastomas. *Cancer Res*. 2004 Nov 1;64(21):7794-800.
16. Baeza N, Masuoka J, Kleihues P, Ohgaki H. AXIN1 mutations but not deletions in cerebellar medulloblastomas. *Oncogene*. 2003 Jan 30;22(4):632-6.
17. Northcott PA, Shih DJ, Peacock J, Garzia L, Morrissy AS, Zichner T, et al. Subgroup-specific structural variation across 1,000 medulloblastoma genomes. *Nature*. 2012 Aug 2;488(7409):49-56.
18. Michiels EM, Oussoren E, Van Groenigen M, Pauws E, Bossuyt PM, Voute PA, et al. Genes differentially expressed in medulloblastoma and fetal brain. *Physiol Genomics*. 1999 Aug 31;1(2):83-91.
19. Clifford SC, Lusher ME, Lindsey JC, Langdon JA, Gilbertson RJ, Straughton D, et al. Wnt/Wingless pathway activation and chromosome 6 loss characterize a distinct molecular sub-group of medulloblastomas associated with a favorable prognosis. *Cell Cycle*. 2006 Nov;5(22):2666-70.
20. Pizem J, Cort A, Zdravec-Zaletel L, Popovic M. Survivin is a negative prognostic marker in medulloblastoma. *Neuropathol Appl Neurobiol*. 2005 Aug;31(4):422-8.
21. Ellison DW, Onilude OE, Lindsey JC, Lusher ME, Weston CL, Taylor RE, et al. beta-Catenin status predicts a favorable outcome in childhood medulloblastoma: the United Kingdom Children's Cancer Study Group Brain Tumour Committee. *J Clin Oncol*. 2005 Nov 1;23(31):7951-7.
22. Kaufman DK, Kimmel DW, Parisi JE, Michels VV. A familial syndrome with cutaneous malignant melanoma and cerebral astrocytoma. *Neurology*. 1993 Sep;43(9):1728-31.
23. Randerson-Moor JA, Harland M, Williams S, Cuthbert-Heavens D, Sheridan E, Aveyard J, et al. A germline deletion of p14(ARF) but not CDKN2A in a melanoma-neural system tumour syndrome family. *Hum Mol Genet*. 2001 Jan 1;10(1):55-62.
24. Bahuau M, Vidaud D, Kujas M, Palangie A, Assouline B, Chaignaud-Lebreton M, et al. Familial aggregation of malignant melanoma/dysplastic naevi and tumours of the nervous system: an original syndrome of tumour proneness. *Ann Genet*. 1997;40(2):78-91.
25. Pasmant E, Laurendeau I, Heron D, Vidaud M, Vidaud D, Bieche I. Characterization of a germ-line deletion, including the entire INK4/ARF locus, in a melanoma-neural system tumor family: identification of ANRIL, an antisense noncoding RNA whose expression coclusters with ARF. *Cancer Res*. 2007 Apr 15;67(8):3963-9.
26. Parsons DW, Jones S, Zhang X, Lin JC, Leary RJ, Angenendt P, et al. An integrated genomic analysis of human glioblastoma multiforme. *Science*. 2008 Sep 26;321(5897):1807-12.
27. Bettgowda C, Agrawal N, Jiao Y, Sausen M, Wood LD, Hruban RH, et al. Mutations in CIC and FUBP1 contribute to human oligodendroglioma. *Science*. 2011 Sep 9;333(6048):1453-5.
28. Comprehensive genomic characterization defines human glioblastoma genes and core pathways. *Nature*. 2008 Oct 23;455(7216):1061-8.

29. Kranendijk M, Struys EA, van Schaftingen E, Gibson KM, Kanhai WA, van der Knaap MS, et al. IDH2 mutations in patients with D-2-hydroxyglutaric aciduria. *Science*. 2010 Oct 15;330(6002):336.
30. Struys EA, Salomons GS, Achouri Y, Van Schaftingen E, Grosso S, Craigen WJ, et al. Mutations in the D-2-hydroxyglutarate dehydrogenase gene cause D-2-hydroxyglutaric aciduria. *Am J Hum Genet*. 2005 Feb;76(2):358-60.
31. Kloosterhof NK, Bralten LB, Dubbink HJ, French PJ, van den Bent MJ. Isocitrate dehydrogenase-1 mutations: a fundamentally new understanding of diffuse glioma? *Lancet Oncol*. 2011 Jan;12(1):83-91.
32. Gravendeel AM, Kloosterhof NK, Bralten LB, Marion Rv, Dubbink HJ, Dinjens WN, et al. Segregation of non-R132H mutations in IDH1 into distinct molecular subtypes of glioma. *Human Mutation*. 2009 Mar;31(3):E1186-99.
33. Sahm F, Koelsche C, Meyer J, Pusch S, Lindenberg K, Mueller W, et al. CIC and FUBP1 mutations in oligodendrogliomas, oligoastrocytomas and astrocytomas. *Acta Neuropathol*. 2012 Jun;123(6):853-60.
34. Lee CJ, Chan WI, Scotting PJ. CIC, a gene involved in cerebellar development and ErbB signaling, is significantly expressed in medulloblastomas. *J Neurooncol*. 2005 Jun;73(2):101-8.
35. Liu XY, Gerges N, Korshunov A, Sabha N, Khuong-Quang DA, Fontebasso AM, et al. Frequent ATRX mutations and loss of expression in adult diffuse astrocytic tumors carrying IDH1/IDH2 and TP53 mutations. *Acta Neuropathol*. 2012 Nov;124(5):615-25.
36. Alberts B. *Molecular biology of the cell*. 4th ed. New York: Garland Science; 2002.
37. Mi LZ, Lu C, Li Z, Nishida N, Walz T, Springer TA. Simultaneous visualization of the extracellular and cytoplasmic domains of the epidermal growth factor receptor. *Nat Struct Mol Biol*. 2011 Sep;18(9):984-9.
38. Burgess AW, Cho HS, Eigenbrot C, Ferguson KM, Garrett TP, Leahy DJ, et al. An open-and-shut case? Recent insights into the activation of EGF/ErbB receptors. *Mol Cell*. 2003 Sep;12(3):541-52.
39. Harris RC, Chung E, Coffey RJ. EGF receptor ligands. *Exp Cell Res*. 2003 Mar 10;284(1):2-13.
40. Lee JC, Vivanco I, Beroukhir R, Huang JH, Feng WL, DeBiasi RM, et al. Epidermal growth factor receptor activation in glioblastoma through novel missense mutations in the extracellular domain. *PLoS Med*. 2006 Dec;3(12):e485.
41. van den Bent MJ, Brandes AA, Rampling R, Kouwenhoven MC, Kros JM, Carpentier AF, et al. Randomized phase II trial of erlotinib versus temozolomide or carmustine in recurrent glioblastoma: EORTC brain tumor group study 26034. *J Clin Oncol*. 2009 Mar 10;27(8):1268-74.
42. Sen M, Joyce S, Panahandeh M, Li C, Thomas SM, Maxwell J, et al. Targeting Stat3 Abrogates EGFR Inhibitor Resistance in Cancer. *Clin Cancer Res*. 2012 Sep 15;18(18):4986-96.
43. Sharma SV, Bell DW, Settleman J, Haber DA. Epidermal growth factor receptor mutations in lung cancer. *Nat Rev Cancer*. 2007 Mar;7(3):169-81.
44. Gan HK, Kaye AH, Luwor RB. The EGFRvIII variant in glioblastoma multiforme. *J Clin Neurosci*. 2009 Jun;16(6):748-54.
45. Dang L, White DW, Gross S, Bennett BD, Bittinger MA, Driggers EM, et al. Cancer-associated IDH1 mutations produce 2-hydroxyglutarate. *Nature*. 2009 Nov 22.
46. Kloosterhof NK, Bralten LB, Dubbink HJ, French PJ, van den Bent MJ. Isocitrate dehydrogenase-1 mutations: a fundamentally new understanding of diffuse glioma? *Lancet Oncol*. 2011 Jan;12(1):83-91.
47. Mardis ER, Ding L, Dooling DJ, Larson DE, McLellan MD, Chen K, et al. Recurring Mutations Found by Sequencing an Acute Myeloid Leukemia Genome. *N Engl J Med*. 2009 Aug 5.
48. Abbas S, Lugthart S, Kavelaars FG, Schelen A, Koenders JE, Zeilemaker A, et al. Acquired mutations in the genes encoding IDH1 and IDH2 both are recurrent aberrations in acute myeloid leukemia: prevalence and prognostic value. *Blood*. 2012 Sep 23;116(12):2122-6.
49. Borger DR, Tanabe KK, Fan KC, Lopez HU, Fantin VR, Straley KS, et al. Frequent mutation of isocitrate dehydrogenase (IDH)1 and IDH2 in cholangiocarcinoma identified through broad-based tumor genotyping. *Oncologist*. 2012 17(1):72-9.
50. Amary MF, Bacsi K, Maggiani F, Damato S, Halai D, Berisha F, et al. IDH1 and IDH2 mutations are frequent events in central chondrosarcoma and central and periosteal chondromas but not in other mesenchymal tumours. *2011 J Pathol*. Jul;224(3):334-43.
51. Yan H, Parsons DW, Jin G, McLendon R, Rasheed BA, Yuan W, et al. IDH1 and IDH2 mutations in gliomas. *N Engl J Med*. 2009 Feb 19;360(8):765-73.

52. Hegi ME, Diserens AC, Gorlia T, Hamou MF, de Tribolet N, Weller M, et al. MGMT gene silencing and benefit from temozolomide in glioblastoma. *N Engl J Med*. 2005 Mar 10;352(10):997-1003.
53. Gravendeel LA, Kouwenhoven MC, Gevaert O, de Rooij JJ, Stubbs AP, Duijm JE, et al. Intrinsic gene expression profiles of gliomas are a better predictor of survival than histology. *Cancer Res*. 2009 Dec 1;69(23):9065-72.
54. Phillips HS, Kharbanda S, Chen R, Forrest WF, Soriano RH, Wu TD, et al. Molecular subclasses of high-grade glioma predict prognosis, delineate a pattern of disease progression, and resemble stages in neurogenesis. *Cancer Cell*. 2006 Mar;9(3):157-73.
55. Li A, Walling J, Ahn S, Kotliarov Y, Su Q, Quezado M, et al. Unsupervised analysis of transcriptomic profiles reveals six glioma subtypes. *Cancer Res*. 2009 Mar 1;69(5):2091-9.
56. Gravendeel LA, Kouwenhoven MC, Gevaert O, de Rooij JJ, Stubbs AP, Duijm JE, et al. Intrinsic Gene Expression Profiles of Gliomas Are a Better Predictor of Survival than Histology. *Cancer Res*. 2009 Nov 17.
57. Noshmehr H, Weisenberger DJ, Diefes K, Phillips HS, Pujara K, Berman BP, et al. Identification of a CpG island methylator phenotype that defines a distinct subgroup of glioma. *Cancer Cell*. 2012 May 18;17(5):510-22.
58. van den Bent MJ, Gravendeel LA, Gorlia T, Kros JM, Lapre L, Wesseling P, et al. A hypermethylated phenotype is a better predictor of survival than MGMT methylation in anaplastic oligodendroglial brain tumors: a report from EORTC study 26951. *Clin Cancer Res*. 2011 Nov 15;17(22):7148-55.
59. Christensen BC, Smith AA, Zheng S, Koestler DC, Houseman EA, Marsit CJ, et al. DNA methylation, isocitrate dehydrogenase mutation, and survival in glioma. *J Natl Cancer Inst*. 2012 Jan 19;103(2):143-53.
60. Turcan S, Rohle D, Goenka A, Walsh LA, Fang F, Yilmaz E, et al. IDH1 mutation is sufficient to establish the glioma hypermethylator phenotype. *Nature*. Mar 22;483(7390):479-83.
61. Xu Y, Hu B, Choi AJ, Gopalan B, Lee BH, Kalady MF, et al. Unique DNA methylome profiles in CpG island methylator phenotype colon cancers. *Genome Res*. Feb;22(2):283

Chapter One

Subgroup Specific Alternative Splicing in Medulloblastoma

Adrian M Dubuc, A. Sorana Morrissy, Nanne K Kloosterhof, Paul A Northcott, Emily PY Yu, David Shih, John Peacock, Wieslawa Grajkowska, Timothy van Meter, Charles G Eberhart, Stefan Pfister, Marco A Marra, William A Weiss, Stephen W Scherer, James T Rutka, Pim J French and Michael D Taylor

Acta Neuropathol 2012 Apr;123(4):485-499.

Abstract

Medulloblastoma is comprised of four distinct molecular variants: WNT, SHH, Group 3, and Group 4. We analyzed alternative splicing usage in 14 normal cerebellar samples and 103 medulloblastomas of known subgroup. Medulloblastoma samples have a statistically significant increase in alternative splicing as compared to normal fetal cerebella (2.3-times; $P < 6.47E-8$). Splicing patterns are distinct and specific between molecular subgroups. Unsupervised hierarchical clustering of alternative splicing events accurately assigns medulloblastomas to their correct subgroup. Subgroup-specific splicing and alternative promoter usage was most prevalent in Group 3 (19.4%) and SHH (16.2%) medulloblastomas, while observed less frequently in WNT (3.2%), and Group 4 (9.3%) tumors. Functional annotation of alternatively spliced genes reveals over-representation of genes important for neuronal development. Alternative splicing events in medulloblastoma may be regulated in part by the correlative expression of antisense transcripts, suggesting a possible mechanism affecting subgroup specific alternative splicing. Our results identify additional candidate markers for medulloblastoma subgroup affiliation, further support the existence of distinct subgroups of the disease, and demonstrate an additional level of transcriptional heterogeneity between medulloblastoma subgroups.

Introduction

Medulloblastoma (MB) is the most common malignant brain tumor in children [12, 41, 45] and has recently been demonstrated to exhibit considerable inter-tumoral heterogeneity [7, 14]. Recent publications have dissected medulloblastoma at a molecular level into four distinct variants – namely WNT, SHH, Group 3 and Group 4 [9, 27, 41, 43, 53]. These subgroups differ in their epidemiology, copy number profiles, transcriptional networks, mutational spectra, and clinical characteristics [42, 45, 48]. The study of subgroup specific gene expression has assisted in the identification of cells of origin for WNT [20] and SHH medulloblastomas [63]. Subgroup specific targeted therapy is imminent, with promising preliminary responses to SHH-pathway inhibitors in humans and mice [8, 49]. However, nearly half of all medulloblastoma are represented by Group 3 or 4 tumors [13, 43] with dismal overall survival and in which the molecular mechanisms driving tumorigenesis remain largely unknown [21]. The optimal mechanism for ‘real time’ assignment of subgroup affiliation in the setting of a clinical trial is not currently settled. To further understand the transcriptional dissimilarity between subgroups we undertook an analysis of alternative splicing and promoter use in medulloblastoma.

Alternative splicing of pre-mRNA is a dynamic mechanism that adds complexity to the human transcriptome, thereby significantly increasing the diversity of expressed proteins [28]. Transcriptional selection of splice sites usage occurs through the processes of: exon skipping, alternative transcriptional start site usage, intron retention, and alternative polyadenylation sites, collectively referred to in the current manuscript as alternative splicing [28, 35, 40, 62]. One or more of these alternative splicing mechanisms are estimated to affect 75% [19] to 92% [62] of all genes in the human genome. Tight regulation of normal, tissue-specific, and developmental splicing is mediated by a complex network of RNA-binding proteins that recognize exonic or intronic cis-regulatory elements, enhancing or repressing inclusion of an exon in a transcript [19]. Recent

evidence has also shown that transcription of an overlapping gene, encoded on the opposite DNA strand (antisense transcription) can affect splicing outcomes [57, 58].

Alternative splicing has been reported to be “cancer-specific”, producing protein isoforms that favor cellular growth, or metastasis [4, 11, 36, 59, 60]. Research efforts to target cancer specific isoforms are ongoing [2, 23], and in notable cases have led to clinical trials addressing the efficacy of isoform-specific monoclonal antibodies [54]. A limited number of studies detailing medulloblastoma-restricted isoform-expression have been conducted. Notable findings include alternative splicing of *ERBB4* [17], *PTC* [56], and *GLI1* [65], which impact critical signaling and developmental pathways relevant to the pathogenesis of medulloblastoma. We undertook a comprehensive investigation of alternative splicing across medulloblastoma subgroups in a large cohort of primary tumours (n=103). Using data from the Affymetrix exon array platform, we identified multiple, recurrent, subgroup-specific alternative start site, and exon dropping events. Furthermore, we identified sense-antisense (S-AS) transcription, with subgroup specific expression of antisense transcripts correlating with alternative splicing in medulloblastoma, which may represent a putative mechanism contributing to isoform variability. Our data further highlights the transcriptional dissimilarity between subgroups, suggests additional markers for assignment of subgroup affiliation, provide additional tools for cell of origin studies, and provides a hypothesis based on S-AS transcription that may explain patterns of subgroup specific alternative splicing.

Materials and Methods

Tissue Samples and RNA preparation

Primary medulloblastoma (n=103) and normal cerebella (fetal - n=9, adult - n=5) samples were profiled on Affymetrix Genechip Human Exon 1.0ST Arrays. Samples, obtained in accordance with Hospital for Sick Children (Toronto, Canada) Research Ethic Board, were snap frozen with liquid nitrogen at local host institutions and stored at -80°C. RNA was extracted using standard TRIzol (Invitrogen) protocol and quantification was performed using a Nanodrop ND-1000 Spectrophotometer. The quality of RNA was assessed on an Agilent 2100 Bioanalyzer by The Toronto Centre for Applied Genomics (TCAG, Toronto, Canada).

Expression Profiling and Molecular Subgrouping

As previously described in Northcott *et al.*, 2009 [41], Affymetrix Genechip Human Exon 1.0ST Array were processed at the TCAG (Toronto, Canada). Molecular subgroups were established as previously described [43].

Subgroup Specific Splice Variant Detection

Pattern-Based Correlation

Pattern-based Correlation (PAC) splice variant values, which represent the theoretical expression of each probe in relation to gene expression levels, were generated for each probe set and used to identify putative alternative-splicing. PAC values were calculated for each probe set in each sample except for samples where its meta-probe set level was < 8.5. In this manner, PAC values are calculated only in samples where the meta-probe set (a measure for gene-level expression) is expressed. We further focused only on probe sets whose expression is correlated with its meta-probe set ($R^2 > 0.64$) as a measure to filter out poor performing and cross-hybridizing probe sets. ANOVA analysis was performed to

identify differentially expressed splice variants between molecular subgroups of MBs. Differentially expressed splice variants were then further selected based on the degree of alternative-splicing (PAC values > 2 criteria, corresponding to 4-fold difference in relative expression), see also French *et al*, 2007 [18]. Our analysis detected distinct changes in intra-transcript levels, revealing 1986 probe sets mapping to 1286 genes demonstrating ≥ 1 probe with a statistically significant PAC-score, suggestive of alternative-splicing.

Splice Index (SI)

As an alternative bioinformatic approach, we re-processed the data to generate Splice Index values for each probe set. First, to filter out probe sets with poor performance or low signal, we calculated the median intensity across samples for each of the 287,189 core probe sets on the array. 161,720 probe sets with an average intensity above the median of these values (6.58) were retained for further analysis. Next, probe sets were mapped to Ensembl genes (hg18). A total of 12,209 genes that (1) were represented by a minimum of 6 core probe sets on the array, and (2) had a minimum of 20% of probe sets above the filtering threshold, were retained for further analysis. A splice index (SI) value was calculated for each probe set in these 12,209 genes as previously described [37]. Briefly, in each sample, probe set intensity values were normalized by the corresponding gene expression value. The resulting SI value indicates whether the exon is included in the transcript (higher SI) or excluded (lower SI). SI values were first filtered to retain probe sets with a high dynamic range across samples, as described next. For each probe set, we calculated the difference between the 5th percentile and 95th percentile of the SI values across the 117 samples. The top 5% of probe sets (7464) with the largest 95th-5th percentile differences were selected as a probable target of alternative splicing. To determine the number of alternative splicing events across each sample, a z-score was calculated for each probe set. Samples with probe sets whose z-score fell two standard deviations away from the mean ($-2 > z\text{-score} >= 2$) were identified as alternative splicing events.

Comparing alternatively spliced probe sets identified by PAC or SI predictions a collective splice series was generated, whereas probe sets/genes identified by both algorithms were defined as the consensus splice series. The collective splice series was used to identify subgroup-specific alternative splicing events and hypersplice medulloblastomas whereas the consensus splice series permitted the identification of hallmark alternative splicing events prevalent in each molecular subgroup.

Unsupervised Clustering of Splice Index values

Splice Index (SI) values for medulloblastoma (n=103) and normal cerebella (n=14) samples were used for clustering analysis. We performed unsupervised Hierarchical Clustering (HCL) using Pearson's Correlation as a distance metric with bootstrapping analysis (100 iterations) with all 7464 probe sets using TM4 Microarray SoftwareSuite (MeV v4.6, Dana-Farber Cancer Institute, Boston). We repeated this analysis with the top 50% of probe sets (3732) with the highest standard deviation, as well as the top 25% of probe sets (1866), 13.4% (1000 probe sets) and 6.25% of probe sets (467). We identified the strongest support for clustering using 1000 probe sets which identified 6 core clusters, composed of 2 normal subgroups (fetal and adult cerebella) and 4 medulloblastoma subgroups. Non-negative matrix factorization (NMF) (Dana-Farber Cancer Institute,

Boston) was used as second, unsupervised clustering algorithm. Using both the top 1000 probe sets with the highest standard deviation, as well as all 7464 probe sets, we determined the cophenetic correlation for k=2 to k=8 subgroups. We identified the strongest support for k=7 for both the filtered (1000 probe sets 0.9629) and unfiltered (7464 probe sets 0.8801), producing 2 normal clusters and 5 medulloblastoma subgroups.

qRT-PCR Validation of Alternative Start Sites and Exon Dropping Events

Validation of splice isoforms was performed using qRT-PCR. In brief, cDNA was synthesized from RNA using Superscript III First-Strand Synthesis supermix (Invitrogen). Five-hundred (500ng) nanograms of RNA was incubated with 2xFirst Strand Reaction mix (Invitrogen) and random hexamers (50ng/ μ L) for 10-minutes at 25°C and then 1-hour at 50°C prior to heat-inactivation of the enzyme mixture at 85°C for 5-minutes. Primers designed using Primer Express software were generated targeting regions at the 5' and 3' end of the transcript. Primer sequences can be found in supplemental data (Table S5). Fifty-nanograms (50ng) of cDNA was profiled on ABI Step One qRT-PCR instrumentation using SYBR green. A transcript ratio was calculated as the fold-change difference between the 5' versus 3' end. All transcript ratios were normalized to pooled fetal cerebellar cDNA.

Bioinformatic Analysis of Over-represented Genes and Pathways

Ingenuity Pathway Analysis (IPA) (Ingenuity Systems) was used to annotate predominant themes and pathways. Specifically, the top statistically significant canonical pathways and molecular functions were used to classify genes. Over representation of Gene Ontology (GO) groups targeted by alternative splicing were assessed using BINGO v2.3 (A Biological Network Gene Ontology Tool) [31] a Cytoscape plug-in [10]. In brief, a hypergeometric test was used to assess over represented GO Biological Processes. Benjamini & Hochberg False Discovery Rate (FDR) correction was applied and only themes with a statistical significance of $P < 0.05$ were included in the analysis.

Sense-Antisense Transcription

Filtered Affymetrix exon array probe sets were mapped to ~1,765 sense-antisense gene pairs (defined as overlapping by a minimum of 1bp, and encoded on opposing strands, as in Morrissy et al., 2011 [37]). A total of 376 genes with at least 20% of probe sets expressed above the filtering threshold were further considered. These genes had a total of 4,344 filtered probe sets. SI values for these probe sets were calculated as described above. Spearman's rank correlation coefficients were calculated between the SI values of each probe set in a sense gene, and the expression values of the antisense gene (across all samples). P-values for correlations were calculated using the cor.test function in R (R Development Core Team 2008), and were multiple-test corrected using the stringent Bonferroni method. For each S-AS gene pair, each gene partner was, in turn, analyzed as the sense gene and as the antisense gene (in order to identify cases where both genes had antisense-correlated splicing events).

Results

Alternative Splicing in Medulloblastoma is Subgroup Specific

To further highlight the transcriptional differences between medulloblastoma subgroups we analyzed alternative splicing consisting of the differential use of exons, promoters and polyadenylation sites in a large cohort of medulloblastomas (n=103) and normal cerebella

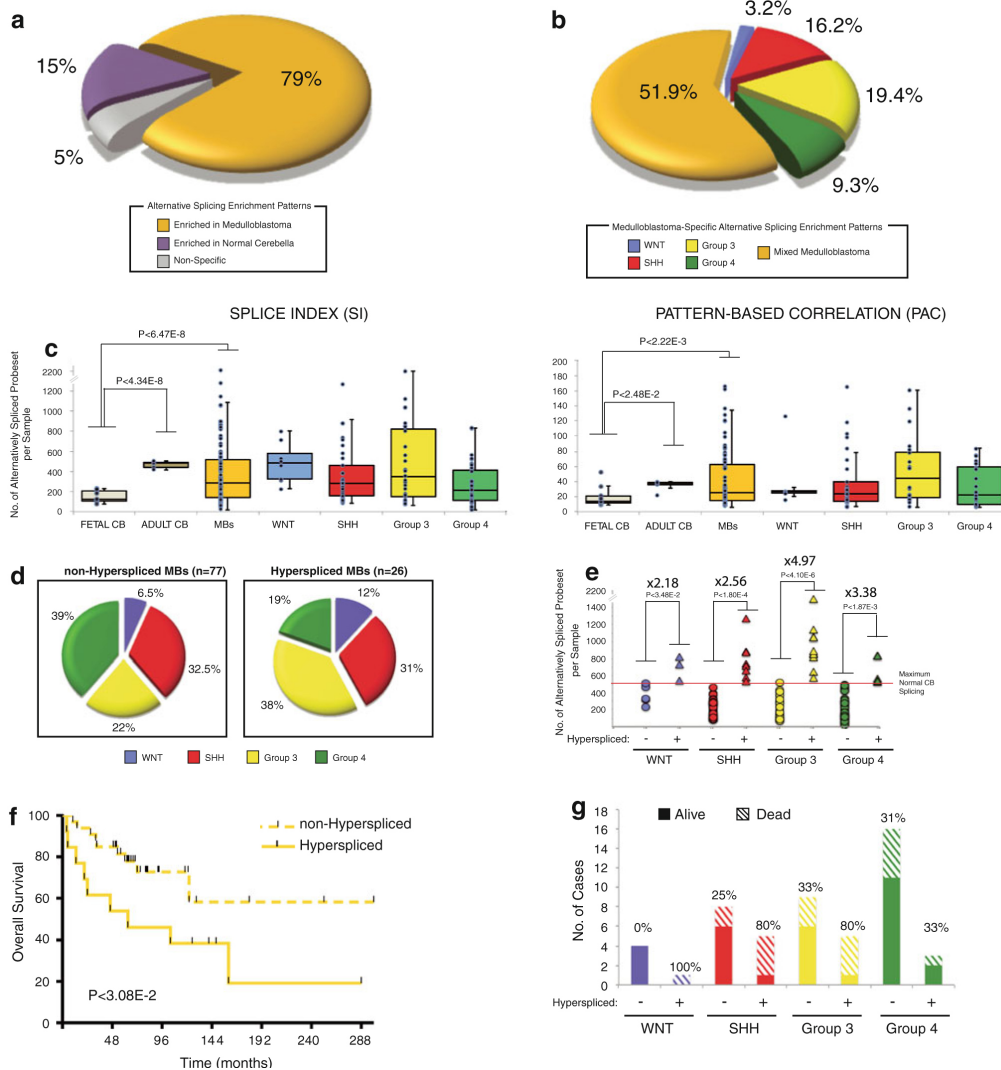
(n=14). Using two independent bioinformatics algorithms – Splice Index (SI) [37] and Pattern Based Correlation (PAC) [18] – we created a ‘collective splicing series’ of 9096 putatively spliced probe sets that map to well annotated exons in 4622 genes (Figure S1a; Table S3). The majority of these alternatively spliced probe sets (64%) mapped to non-terminal exons, whereas 15% and 21% of our collective splice series affected probe sets which could be mapped to the first or last exon, respectively (Figure S2). Most of the identified alternative splicing occurred in medulloblastoma samples (79%), while only a minority (15%) was specifically enriched in the normal cerebella (Figure 1a). Subgroup-specific splicing events were most prevalent in Group 3 and SHH tumors (19.4% and 16.2% respectively) and less abundant in Group 4 (9.3%) and WNT (3.2%) medulloblastomas. Half (51.9%) of all medulloblastoma-enriched splicing events occurred across subgroups in a mixed population of medulloblastomas (Figure 1b). We identified genes with known roles in medulloblastoma and cerebellar development including: *AXIN2* (WNT), *GLI1* [47], *TSC1* [5] and *PTCH1* (SHH) [24](Table S5; Table S6). We also observed the previously reported medulloblastoma-specific splicing affecting *ERBB4* [17].

During cerebella development, a significant increase in alternative splicing is observed as the normal cerebellum develops from the fetus to adulthood ($P < 4.34E-8$) (Figure 1c). The adult cerebella demonstrates 3.93-times higher median levels of alternative splicing (Figure 1c; Figure S3a) relative to the fetal cerebella, however within fetal or adult samples there exists no direct correlation between age and the observed frequency of alternative splicing (Figure S3b; Figure S3c).

Medulloblastomas display on average 2.3-times the median levels present in the developing fetal cerebella ($P < 6.47E-8$), which nonetheless remain 0.59-times lower than those observed within the developed, adult cerebella ($P < 1.89E-2$). A subgroup-specific analysis of medulloblastoma alternative splicing reveals no statistically significant differences in the observed number of spliced probe sets across WNT, SHH and Group 3 tumors whereas Group 4 medulloblastomas possess a reduced frequency of alternative splicing ($P < 2.31E-2$). Although medulloblastoma is largely a pediatric disease, adult tumors (age > 16) represent 13.6% (14/102) of our tumor cohort. Pediatric versus adult medulloblastomas do not display any statistically significant differences ($P < 4.92E-1$) in the observed frequency of alternative splicing events (Figure S4a). Furthermore, there is no correlation between the age of the patient and the frequency of alternative splicing when medulloblastoma is analyzed as a single disease, (Figure S4b) however a weak, positive trend towards increasing alternative splicing with age was observed in non-Group 4 tumors (Figure S4c).

The extensive intra-subgroup variance in abundance of alternative spliced probesets permits stratification of medulloblastomas into two broader groups, distinguished by the frequency of alternative splicing. The first group, referred to as “hyperspliced”, is composed of 26 samples with splicing frequencies above the 75th percentile across all medulloblastomas. The second group, with splicing frequencies comparable to those present in normal cerebella, is referred as “non-hyperspliced”. Notably, we observed relative differences in the distributions of Group 3 and 4 subgroups across both hyperspliced and non-hyperspliced medulloblastomas. An increase (+16%) in the distribution of Group 3 tumors was observed in the hyperspliced group with the inverse

Figure 1. Subgroup-Specific Alternative Splicing in Medulloblastoma



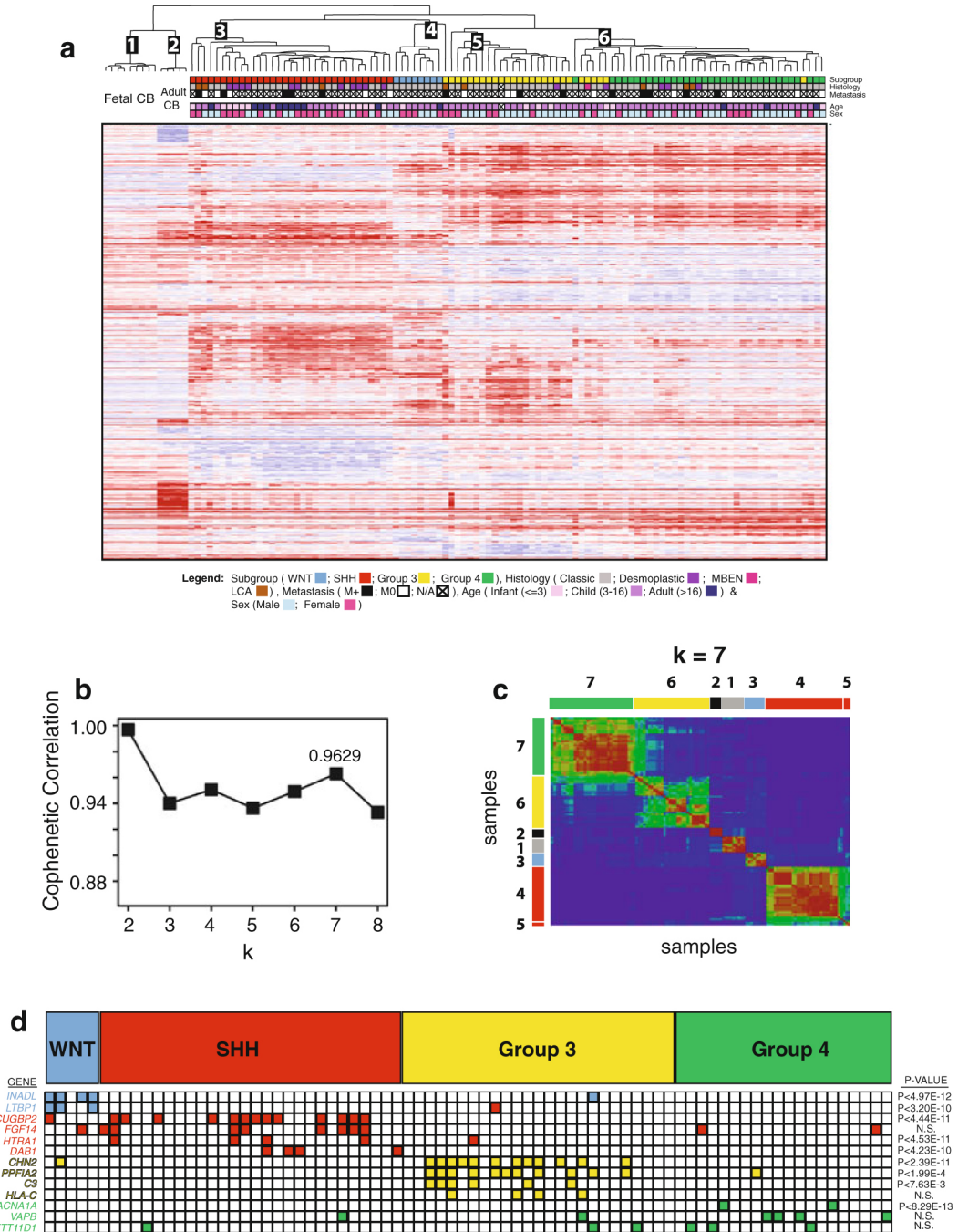
(a) Distribution of 9096 alternatively spliced probe sets, identified by Splice Index (SI) and Pattern-Based Correlation (PAC) algorithms, across 103 primary medulloblastoma and 14 normal cerebella samples demonstrates strong enrichment patterns in medulloblastoma (79%) with a minority of alternative splicing events restricted to the normal cerebella (15%). (b) Subgroup association of 7509 probe sets with medulloblastoma-enriched splicing patterns identifies elevated levels of Group 3 (19.4%, 1454 probe sets) and SHH (16.2%, 1216 probe sets) enriched alternative splicing with lower levels present in WNT (3.2%, 241 probe sets) and Group 4 (9.3%, 697 probe sets) tumors. Half of all medulloblastoma-enriched splicing events (51.9%, 3901 probe sets) were identified in medulloblastomas from multiple subgroups. (c) Using Splice Index (SI) and Pattern Based Correlation (PAC) algorithms the number of alternative splicing events per sample was identified, producing similar trends for both algorithms. Subgroup-specific splicing patterns revealed a significant developmental increase in alternative splicing from the fetal to adult normal cerebella with a further increase in splicing observed in medulloblastomas. (d) Distribution of the molecular subgroups of medulloblastoma in hyperspliced (n=26) and non-hyperspliced tumors (n=77) reveals an increased frequency of WNT (+6%) and Group 3 tumors (+16%) in hyperpliced medulloblastomas, and a decreased frequency in Group 4 tumors (-20%). (e) Subgroup-specific distribution of alternative splicing per sample for hyperspliced versus non-hyperspliced tumors. Hyperspliced tumors demonstrate a significant increased number of alternatively spliced exons across each subgroup – ranging from 2.18 (WNT) to 4.97 (Group 3) times higher levels of splicing. (f) Hyperspliced medulloblastomas display a significantly decreased overall survival ($P < 3.08E-2$) relative to non-hyperspliced medulloblastomas. (g) Each molecular subgroup of medulloblastomas demonstrates a trend towards increased mortality for hyperspliced tumors, with an 80% or greater increase in mortality for WNT, SHH and Group 3 medulloblastomas.

relationship (-20%) for Group 4 medulloblastomas (Figure 1d). Hyperspliced medulloblastomas demonstrate 2.18 (WNT) to 4.97 (Group 3) times greater frequency of median splicing events relative to non-hyperspliced tumors in the same sub-group (Figure 1e). Strikingly, there is a significant decrease in the overall survival of patients with hyperspliced tumors ($P < 3.08E-2$) (Figure 1f) with a trend towards increased mortality across all molecular subgroups of the disease (Figure 1g). There exists no significant change in the frequency of alternative splicing that occurs in the presence of metastasis (Figure S5a), nor is there any change in the incidence of metastasis which correlates with the presence of the hyperspliced phenotype (Figure S5b). Whether this hyperspliced phenomena is a true biological event with clinical significance, or an artifact associated with the current sample cohort, the algorithms used for analysis, or the platform used, remains to be proven through identification and validation of the hyperspliced phenotype on a separate cohort of medulloblastomas with exon level expression data derived from another hybridization or sequencing-based platform.

Unsupervised Clustering of Splice Indices Identifies Four Medulloblastoma Subgroups

Through unsupervised hierarchical clustering (HCL) of Splice Index (SI) values, we were able to recapitulate the clustering pattern produced by gene-level transcriptional data [41, 43], generating six major clusters with four clear medulloblastoma subgroups, in addition to normal fetal and adult cerebella clusters (Figure 2a). Ninety-two percent (92%, 95/103) of samples clustered according to their predicted molecular subgroup, while six samples (8%, 8/103) were misclassified. Clustering discrepancies occurred largely (87.5%, 7/8) between Group 3 and 4 medulloblastomas – two molecular subgroups previously shown to display a higher concordance in copy number and transcriptional profiles. The clustering pattern observed was highly robust (Figure S6a) with >98% confidence associated with the clustering patterns of WNT, SHH and normal cerebellar samples (Figure S6b). Fetal and adult normal cerebella clustered together with confidence scores >81% irrespective of the number of probe sets used to generate the clusters, suggesting they display a distinct alternative splicing pattern from the medulloblastoma samples profiled (Figure S6a). There is clear sub-structure identified within Group 3 medulloblastomas, with half of all Group 3 hyperspliced tumors clustering with a high confidence (77%) (Figure S6b), further supporting the necessity of characterizing intra-subgroup heterogeneity. Using an independent and unsupervised learning algorithm, Non-negative Matrix Factorization (NMF), we were able to reproduce our HCL clustering patterns. NMF provided the highest support (Cophenetic correlation 0.9629) for 7 molecular subgroups consisting of the 6 major groups identified by HCL (Fetal cerebella, Adult cerebella, WNT, SHH, Group 3, Group 4) and one additional subgroup (Figure 2b). The additional subgroup consisted of a minority ($n=3$) of SHH cases clustering separately from other SHH tumors (Figure 2c). NMF produced an accuracy similar to that of HCL, with 93% (96/103) of medulloblastomas clustering as expected. Importantly, the clustering pattern produced by alternative splicing is not driven by gene expression, as there is only 47.2% (244/516) overlap in the genes sets used to generate stable alternative splicing clustering and gene-level transcriptional clustering (Table S10). Using information generated from both HCL and NMF clustering, we identified highly recurrent hallmark alternative splicing events enriched in each of the molecular subgroups (Figure 2d).

Figure 2. Unsupervised Clustering of Splice Indices Identifies Four Subgroups of Medulloblastomas



(a) Unsupervised Hierarchical Clustering (HCL) of the top 1000 probe sets with the highest standard deviation across Splice Index (SI) values generates robust clustering of four core medulloblastoma subgroups with two normal cerebella clusters. (b) Non-Negative Matrix Factorization using the same 1000 probe sets used for HCL clustering produces the highest support (cophenetic correlation) for 7 subgroups. (c) Non-Negative Matrix Factorization demonstrates 7 core subgroups composed of the adult and fetal normal samples, the corresponding four subgroups identified by HCL, and one additional subgroup composed of a small set of SHH medulloblastomas (n=3). (d) Medulloblastoma subgroup-enriched alternative splicing events identified by SI and PAC analysis revealing events present in >50-70% of each subgroup.

Extensive Alternative Splicing of Cerebellar Development Genes in Non-WNT Medulloblastoma.

To identify genes and pathways disproportionately affected by alternative splicing we performed Ingenuity Pathway Analysis (IPA) in a subgroup specific manner (Figure 3a). We identified pathways with known roles in the pathogenesis of medulloblastoma, including p53 signaling (WNT tumors, $P < 1.09E-2$) [44] and CREB signaling (SHH tumors; $P < 1.70E-4$) [46]. Among medulloblastomas, *TP53* mutations are most common in the WNT subgroup [44]. In non-WNT medulloblastomas, we identified a high incidence of neuronal development pathways affected by alternative splicing. Of the top ten statistically significant pathways, 60% (6/10) in both SHH and Group 3 medulloblastomas, and 40% (4/10) of Group 4 tumors, affected neuronal functions (Figure S7). Normal cerebella exhibited some overlap with these findings, however neuronal functions are less frequently targeted (30%, 3/10). Instead, cell cycle pathways (30%, 3/10) are enriched in the normal cerebella (Table S11).

Using Cytoscape BINGO [10, 31], an independent algorithm for the visualization of Gene Ontology (GO) functions, we performed a subtractive analysis, removing gene ontologies present in the normal cerebella and identifying biological processes enriched exclusively in medulloblastoma. The results complemented our pathway analysis demonstrating a strong enrichment of neuronal networks, including nervous system development ($P < 1.30E-2$), axonal guidance ($P < 3.36E-3$) and glutamatergic synaptic transmission ($P < 2.19E-2$) in Group 3 medulloblastomas (Figure 3b). Additionally, this analysis identified signaling pathways previously implicated in medulloblastoma pathogenesis including the Roundabout (*ROBO-SLIT*, Group 3, $P < 1.13E-2$) [61] and *PDGF* pathways (Group 3, $P < 2.53E-2$) [1, 30]. Similarly, alternative splicing events in SHH and Group 4 tumors comprised a high percentage of neuronal pathways, and networks such as the regulation of cell migration ($P < 8.06E-3$, SHH) and extracellular structure organization ($P < 1.65E-2$, Group 4) (Figure S7, Table S12-S15).

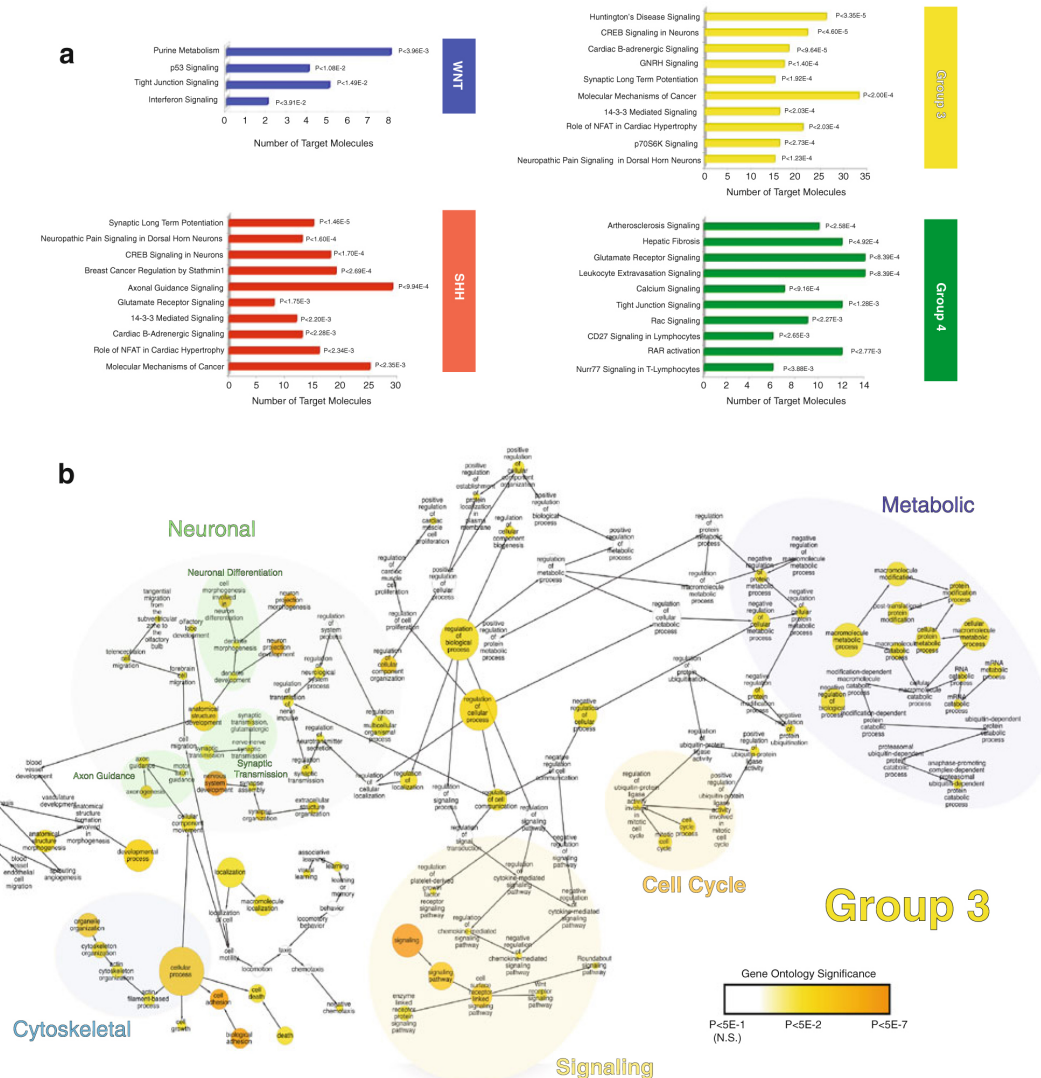
Given the high incidence of mortality associated with hyperspliced medulloblastomas, we analyzed differential use of exons, alternative polyadenylation sites and alternative start sites between hyperspliced and non-hyperspliced tumors in an effort to identify possible molecular changes contributing to this phenotype. Using supervised clustering, we first identified the top 5% of probesets with the greatest differential splice indices between the two groups (Figure S9a; Figure S9b). We then examined the molecular function of the most differential probesets using Ingenuity Pathway Analysis (IPA). The majority of the top canonical pathways differentiating hyperspliced from non-hyperspliced tumours affected known cancer signaling pathways (60%, 6/10) (Figure S9c).

Validation of Subgroup-Specific Alternative Splicing Events

We selected high confidence subgroup specific splicing candidates from our consensus splicing series to validate. These events were predominantly found in a single molecular subgroup (>75%), and displayed gross changes in transcript structure of isoforms. To assess subgroup-specific isoform expression, a transcript ratio was calculated as change in 3' versus 5' expression levels, and normalized to fetal cerebellar levels. Exon-specific primers were then designed to distinguish between 3' and 5' exon cassettes. We validated alternative splicing events for *INADL* (WNT), *CHN2* (Group 3), *NBEA* (Group 4)

and *SNAP25* (Mixed MB). *INADL* is a cell polarity and tight junction protein [52] with a 3' alternative promoter isoform that is present in >80% of WNT tumors and a minority of

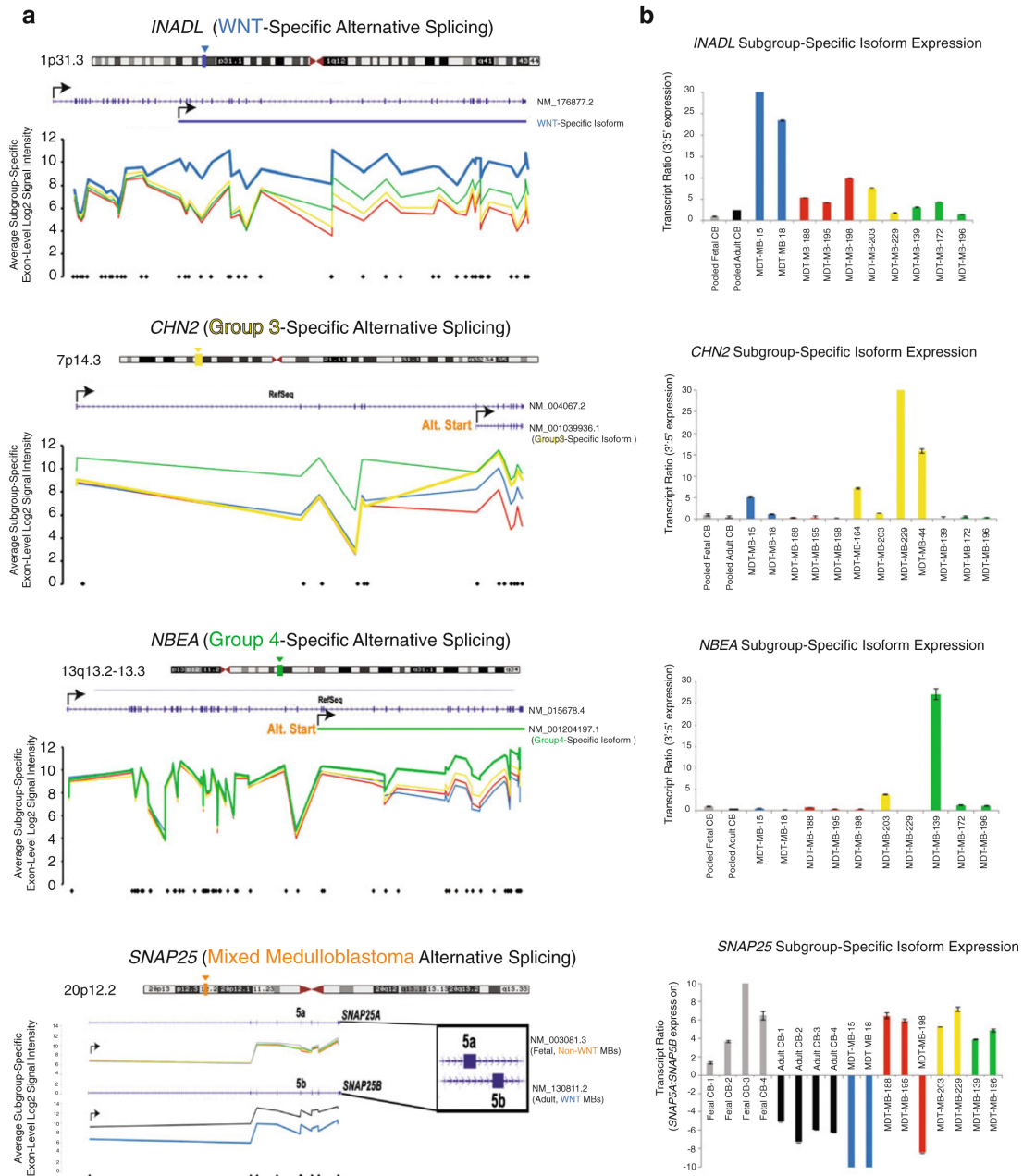
Figure 3: Pathway and Gene Ontology analysis of Subgroup-Specific Splicing Events Identifies Recurrent Targeting of Cere-bellar Development Pathways in non-WNT medulloblastomas



(a) Ingenuity Pathway Analysis (IPA) of the top ten pathways affected by alternative splicing across each molecular subgroup of medulloblastoma. Known signaling pathways: such as Tight junction signaling (WNT, $P < 1.49E-2$) and CREB signaling (SHH, $P < 1.70E-4$) were identified in our analysis as well as an abundance of neuronal pathways in non-WNT medulloblastomas. (b) Cytoscape BINGO analysis of the significant Gene Ontologies (GO) targeted by alternative splicing in Group 3 tumors, after subtracting events present in the normal cerebella, identifies neuronal pathways targeting axonogenesis and glutamatergic synaptic transmission.

Group 4 tumors (8%) (Figure 4a). Upon validation, WNT medulloblastomas displayed a 2-10 times greater transcript ratio (i.e. higher levels of the shorter isoform) relative to non-WNT tumors and normal cerebella (Figure 4b). *CHN2*, a Rho-GTPase Activating Protein [6, 25, 29] and *NBEA*, a neuronal differentiation protein [33] also demonstrated 3' alternative promoters enriched in Group 3 and Group 4 subgroups, respectively (Figure 4a). The *NBEA* truncated isoform was predicted to occur

Figure 4. Validation of Subgroup-Specific Hallmark Alternative Splicing Events in Medulloblastoma



(a) Exon array RMA signal intensity plots of highly frequent and subgroup-specific alternative transcripts. Alternative promoter usage generates a WNT-specific 3' isoform of *INADL*, while alternative promoter usages in Group 3 and Group 4 tumors produce known isoforms of *CHN2* and *NBEA*, respectively. *SNAP25* demonstrates subgroup-specific expression of a known exon cassette with Fetal and non-WNT medulloblastomas expressing elevated levels of *SNAP25a* and Adult and WNT tumors expressing higher levels of *SNAP25b*. (b) Primers generated against the 5' and 3' gene regions of the full transcript were used to assess the intra-transcript variability. A transcript ratio, based on the 3':5' expression, was calculated and normalized to normal fetal cerebella permitting the identification of subgroup specific isoform expression. For each of the reported genes we observe the expected isoform expression restricted to the predicted subgroups.

In 91% of Group 4 tumors and a minority of Group 3 medulloblastomas (37%), whereas the 3' *CHN2* isoform predominated in Group 3 (74%) and WNT (37%) medulloblastomas, evident in our validation (Figure 4b). Finally, we validated alternative splicing targeting *SNAP25*, a synaptosomal protein necessary for neurotransmitter exocytosis [3], with a

known exon-5 cassette (*SNAP25a* versus *SNAP25b*). We observed a greater 5a to 5b ratio in normal fetal cerebella and the majority non-WNT medulloblastomas. In contrast, adult cerebella and WNT tumors demonstrate higher 5b levels. Each of these splicing events causes the disruption of one or more protein domains, likely resulting in a significant change in gene function (Figure S10).

Sense-Antisense (S-AS) Transcription Correlates with Alternative Splicing

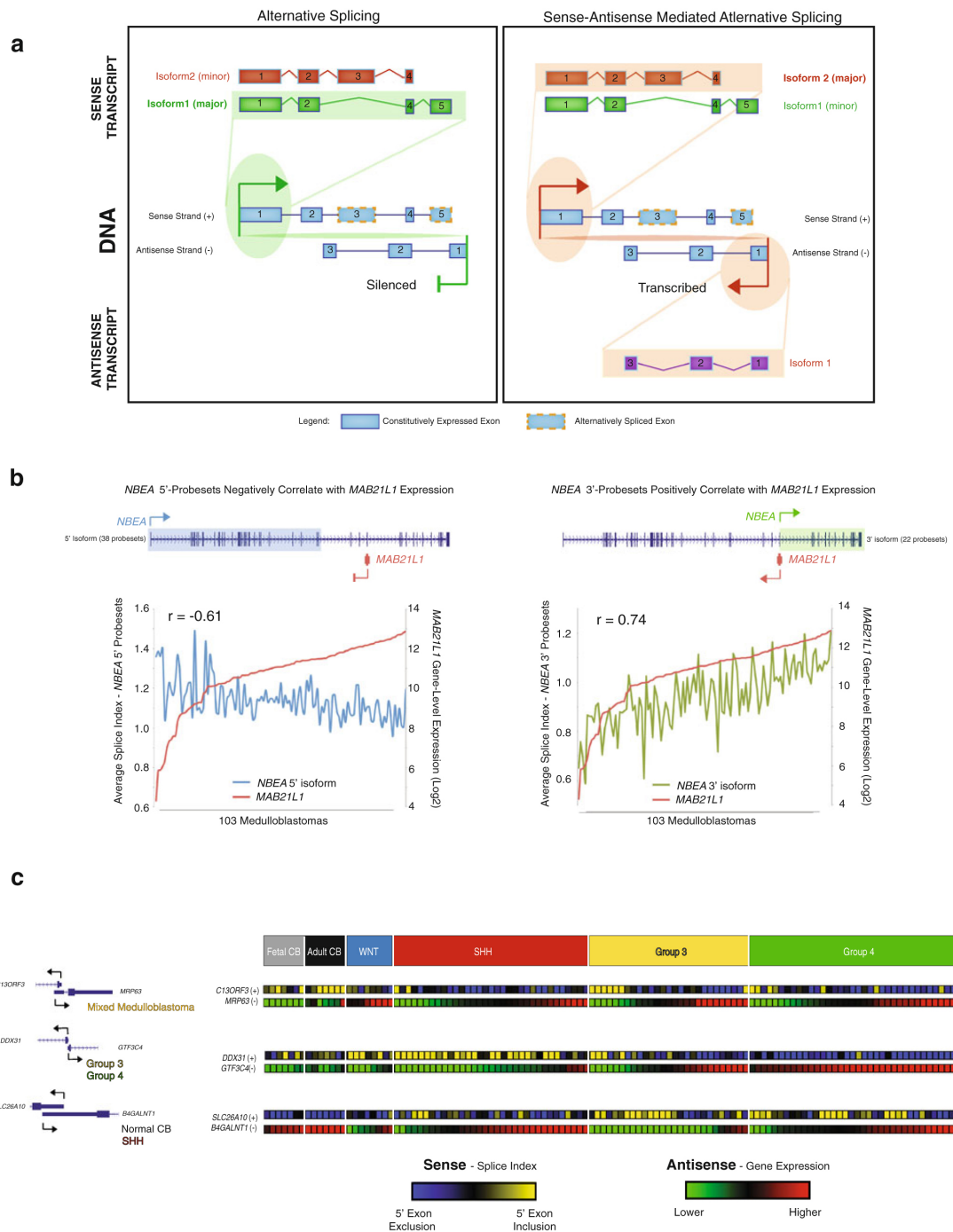
Recent reports have demonstrated changes in alternative splicing patterns that correlate with the expression of an antisense gene [37]. Sense-antisense (S-AS) transcription occurs when overlapping genes on opposing DNA strands are co-expressed in the same cell [26, 51]. Antisense transcription can regulate splicing decisions and alter the balance of isoforms expressed from the sense strand through a variety of mechanisms, such as direct transcriptional interference based on the physical consequences of convergent polymerase complexes (PolII) transcribing both strands of the sense-antisense gene locus [50]. In normal human cells, antisense transcription is significantly correlated to splicing at hundreds of loci, showing that this is likely a common mechanism of transcriptional regulation (Figure 5a), occurring in >75% of all genes and often altered in a cancer-specific context [32].

To determine whether antisense transcription contributes to alternative splicing in medulloblastoma, we analyzed 188 overlapping gene pairs (i.e. 376 genes) that are encoded in opposing orientations and simultaneously expressed in a given tumor. Alternative splicing was predicted to occur in either the sense or antisense gene in 88 (46.8%) sense-antisense partners. We measured the correlation between exon inclusion in the sense genes (splice index (SI) values; see Methods), and the expression of the antisense gene partner, across all 117 samples, identifying significant correlations between splicing and antisense gene expression in all (100%, 88/88) gene pairs ($p < 0.05$, after Bonferroni correction) (Figure S11a). Our results suggest that S-AS transcription may play a role in the regulation of alternative splicing of these genes in medulloblastoma.

Notable examples of such events include the well-annotated S-AS pairs *NBEA-MAB21L1*, *NNAT-BLCAP* and *BCL2L12-IRF3*. All three examples have previously been identified, and validated [15, 39, 55], using independent molecular techniques, demonstrating the validity and strength of our approach. Of specific interest to us was *NBEA*, previously identified as alternatively spliced in Group 4 medulloblastomas where it is enriched in isoforms distinguished by an alternative transcriptional start site located mid-gene (Figure 4). Analysis of the antisense-correlated splicing events identified the presence of two predominant *NBEA* isoforms (Figure 5b). Expression of the longer *NBEA* isoform was negatively correlated ($r = -0.61$) to the expression of the antisense gene (*MAB21L1*). In contrast, expression of the shorter *NBEA* isoform, previously identified as upregulated in Group C and Group D medulloblastomas (Figure 4b), was positively correlated ($r = 0.74$) to *MAB21L1* expression (also up-regulated in Group D tumors (Figure S11b)). These results suggest that subgroup specific expression of *MAB21L1* contributes to the regulation of subgroup specific alternative promoter usage of *NBEA*.

In the set of 88 S-AS gene pairs with significant correlations between alternative splicing and concomitant antisense transcription, there exist subgroup-restricted (Figure 5c, middle and bottom panels) and subgroup-independent events (Figure 5c, top panel). To

Figure 5: Sense-Antisense Transcription Correlates with Alternative Splicing in Medulloblastoma



(a) Schematic of sense-antisense (S-AS) transcription depicting overlapping genes on opposing strands with concomitant expression. A switch in the predominant sense-strand isoform occurs in the context of antisense transcription. (b) Analysis of *MAB21L1* transcription (antisense gene) and correlated NBEA (sense gene) alternative splicing events. The splice index values of 38 NBEA 5' exons are inversely correlated with expression of *MAB21L1* (i.e. these exons are excluded from the NBEA isoform when *MAB21L1* is expressed). Conversely, the 22 3' exons have splice index values that are positively correlated to *MAB21L1* expression (i.e. these exons are included in the NBEA isoform when *MAB21L1* is expressed). (c) Examples of S-AS gene pairs demonstrating inverse relationships between sense strand exon inclusion and antisense strand transcription. These correlations demonstrate mixed medulloblastomas (*C13ORF3-MRP63*) or subgroup-enriched (*DDX31-GTF3C4*, Group 3 & Group 4) patterns suggesting S-AS events may play a critical role in normal development (*SLC26A10-B4GALNT1*, Normal CB) and the pathogenesis of medulloblastoma.

understand the putative biological relevance of S-AS genes with antisense-correlated splicing events, we performed pathway analysis, and identified an enrichment of critical cellular functions such as cell death, cell cycle regulation and cellular development (Figure S11c). Further validation of the relationship between antisense transcription and the regulation of alternative splicing in larger datasets with more comprehensive AS transcriptional data will allow further testing of our model. Antisense genes that are expressed in a highly subgroup specific manner should be considered as candidate marker genes for subgroup assignment

Discussion

We present the first subgroup specific analysis of alternative splicing in medulloblastoma using two independent bioinformatic approaches. We identified differential splicing across each medulloblastoma subgroup as well as normal fetal and adult cerebella. While age-matched normal tissue was unavailable, normal fetal (20 to 40 weeks of age) and adult (22 to 82 years of age) cerebella were used as normal controls, representing the developing and developed cerebella. Based on the distribution of alternative splicing events across all tumors, we were able to identify a ‘hypersliced’ phenotype evident in one-quarter of all medulloblastomas. Although hyperspliced medulloblastomas are evident across all molecular subgroups, they are significantly under-represented in Group 4 tumors. Notably, they display decreased overall survival and a strong trend towards increased mortality in non-Group 4 medulloblastomas, indicating that survival trends are not influenced by the over-representation of a single aggressive molecular variant. Hyperspliced tumors do not display any change in the observed frequency of metastatic disease (M+), nor do we observe higher levels of alternative splicing in M+ tumors. Bioinformatic analysis of probesets differentiating hyperspliced from non-hyperspliced medulloblastomas identified numerous cancer-signaling pathways whose instability may, in part, explain the aggressive nature of hyperspliced tumors. Clinical and biological relevance of the observed hyperspliced phenotype awaits its validation on a separate set of tumors studied using an independent technology.

Exon arrays were designed to allow complementary analyses to be performed, both at the level of gene expression as well as alternative splicing [16]. For the latter purpose, the relative difference in exon-level probeset expression can be effectively interpreted as alternative splicing, alternative promoter usage, and alternative polyadenylation events [11, 19, 34, 38]. Although a comprehensive survey of transcript structures cannot be conducted using this platform, particularly in genes with low expression values or in genes with numerous co-expressed isoforms, obvious and consistent events corresponding to the above categories can be measured reliably and reproducibly [16, 64]. Although sequencing technologies can explicitly profile exon-exon junctions, their comparatively prohibitive cost ensures that array-based approaches are an efficient and informative method for rapidly assaying large numbers of tumors, in an effort to address the known heterogeneity of this disease. However, a complete catalog of alternative splicing events remains to be identified through the use of alternative technologies.

Our results are supported by previous research demonstrating a role for alternative splicing in medulloblastoma. Most recently, Menghi et al, 2011 [34] examined alternative splicing in a modest cohort of 14 medulloblastomas using the Splice Index algorithm which differentiated SHH from non-SHH medulloblastomas. The authors identified 174

high confidence splicing events, with an additional 285 probable events. Of these, they validated 11/14 alternatively spliced exons present in a SHH-specific (3/11) or in a medulloblastoma-enriched (8/11) manner. Our analysis identified 100% of the validated events presented by Menghi et al. [34], largely following the subgroup associations reported in their investigation. There are some discrepancies, such as the presence of a SHH-restricted isoform of *TRRAP* reported by the Menghi study, which was observed in all molecular subgroups of medulloblastoma in our dataset.

We examined whether the variation in alternative splicing patterns reflected the transcriptional heterogeneity that defines the four molecular subgroups of medulloblastoma using two independent methods of unsupervised clustering: Hierarchical Clustering (HCL) and Non-negative Matrix Factorization (NMF). HCL produced the most robust clustering with four molecular subgroups of medulloblastoma, findings largely recapitulated by NMF, which identified the four core subgroups and one additional minor medulloblastoma cluster. The extra NMF cluster composed of three SHH medulloblastomas, two of which are large cell anaplastic and hyperspliced, while the remaining SHH tumor is classic and non-hyperspliced. These tumors cluster apart from other SHH tumors in our HCL analysis, suggesting they may represent outliers. As the clustering patterns produced were largely driven by exon from genes independent from those used to produce transcriptional clustering, our results suggest that subgroup-specific alternative splicing events are an independent and equally informative measure of the heterogeneity that exists within the medulloblastoma transcriptome.

By examining alternative splicing events that predominate within each medulloblastoma subgroup, we identified hallmark events, many of which have neuronal functions. These prevalent splicing events, found in >50-70% of tumors in each molecular variant, may identify genes important in tumorigenesis, and may aid in the identification of the cell type of origin. WNT and non-WNT tumors display significantly different pathways affected by alternative splicing. Pathway analysis of WNT medulloblastomas revealed genes important to cerebellar development and medulloblastomas pathogenesis targeting tight junction signaling ($P < 1.49E-2$) and p53 signaling ($P < 1.08E-2$) [44]. In non-WNT medulloblastomas there was a high incidence of pathways affecting nervous system development and differentiation. Important neuronal signaling pathways include CREB signaling in neurons (SHH tumors, $P < 1.70E-4$) and RAR activation (Group 4 tumors, $P < 2.77E-3$), both of which are core or peripheral elements of retinoic acid (RA) signaling. Retinoid treatment has been previously used to induce differentiation in medulloblastoma cells [22]. Furthermore, our analysis has identified subgroup-specific pathways targeting Roundabout (ROBO/SLIT) in Group 3 tumors. Deregulation of ROBO/SLIT genes may contribute to the high incidence of metastasis and brain tumor invasion observed in aggressive Group 3 medulloblastomas [61].

We suggest a model in which antisense transcription may represent one mechanism able to mediate alternative splicing outcomes. We found that approximately 47% of S-AS gene pairs expressed in medulloblastoma had a significant relationship between sense gene splicing outcomes, and expression of the antisense gene partner. An example of this relationship is the alternative splicing of *NBEA*, a neuronal development protein. Our data show that a majority of Group 4 (91%) tumors express a truncated *NBEA* isoform containing only 27% of the full length coding sequence, lacking important functional

domains. Expression of this short *NBEA* isoform is significantly correlated to expression of *MAB21L1*, a gene encoded on the opposite strand of *NBEA*, and believed to function in embryonal development [55]. Many of the identified S-AS events occurred in a subgroup specific manner, indicating that antisense transcription is likely an important component in the regulation of subgroup-specific alternative splicing and medulloblastoma tumorigenesis.

Our data reveals important clinical and biological trends associated with alternative splicing in the medulloblastoma transcriptome, suggests a putative mechanism for subgroup specific alternative splicing, and further highlights the transcriptional heterogeneity present across, and within, subgroups of medulloblastoma

References

1. Abouantoun TJ, MacDonald TJ (2009) Imatinib blocks migration and invasion of medulloblastoma cells by concurrently inhibiting activation of platelet-derived growth factor receptor and transactivation of epidermal growth factor receptor. *Mol Cancer Ther* 8(5): 1137–1147.
2. Alló M, Buggiano V, Fededa JP, Petrillo E, Schor I, et al. (2009) Control of alternative splicing through siRNA-mediated transcriptional gene silencing. *Nat Struct Mol Biol* 16(7): 717–724.
3. Bark C, Bellinger FP, Kaushal A, Mathews JR, Partridge LD, et al. (2004) Developmentally regulated switch in alternatively spliced SNAP-25 isoforms alters facilitation of synaptic transmission. *J Neurosci* 24(40): 8796–8805.
4. Bartel F, Taubert H, Harris LC (2002) Alternative and aberrant splicing of MDM2 mRNA in human cancer. *Cancer cell* 2(1): 9–15.
5. Bhatia B, Northcott PA, Hambarzumyan D, Govindarajan B, Brat DJ, et al. (2009) Tuberous sclerosis complex suppression in cerebellar development and medulloblastoma: separate regulation of mammalian target of rapamycin activity and p27 Kip1 localization. *Cancer Res* 69(18): 7224–7234.
6. Bruinsma SP, Baranski TJ (2007) Beta2-chimaerin in cancer signaling: connecting cell adhesion and MAP kinase activation. *Cell Cycle* 6(20): 2440–2444.
7. Bueren AO, von Hoff K, Pietsch T, Gerber NU, Warmuth-Metz M, et al. (2011) Treatment of young children with localized medulloblastoma by chemotherapy alone: results of the prospective, multicenter trial HIT 2000 confirming the prognostic impact of histology. *Neuro Oncol* 13(6): 669–679.
8. Buonamici S, Williams J, Morrissey M, Wang A, Guo R, et al. (2010) Interfering with resistance to smoothed antagonists by inhibition of the PI3K pathway in medulloblastoma. *Sci Transl Med* 2(51): 51ra70.
9. Cho Y-J, Tsherniak A, Tamayo P, Santagata S, Ligon A, et al. (2011) Integrative genomic analysis of medulloblastoma identifies a molecular subgroup that drives poor clinical outcome. *J Clin Oncol* 29(11): 1424–1430.
10. Cline MS, Smoot M, Cerami E, Kuchinsky A, Landys N, et al. (2007) Integration of biological networks and gene expression data using Cytoscape. *Nat protoc* 2(10): 2366–2382.
11. David CJ, Manley JL (2010) Alternative pre-mRNA splicing regulation in cancer: pathways and programs unhinged. *Genes Dev* 24(21): 2343–2364.
12. Dubuc AM, Northcott PA, Mack S, Witt H, Pfister S, et al. (2010) The genetics of pediatric brain tumors. *Curr Neurol Neurosci Rep* 10(3): 215–223.
13. Eberhart CG (2011) Molecular diagnostics in embryonal brain tumors. *Brain Pathol* 21(1): 96–104.
14. Ellison DW (2010) Childhood medulloblastoma: novel approaches to the classification of a heterogeneous disease. *Acta Neuropathol* 120(3): 305–316.
15. Evans HK, Weidman JR, Cowley DO, Jirtle RL (2005) Comparative phylogenetic analysis of *blcap/nnat* reveals eutherian-specific imprinted gene. *Mol Biol Evol* 22(8): 1740–1748.
16. Fan W, Khalid N, Hallahan AR, Olson JM, Zhao LP (2006) A statistical method for predicting splice variants between two groups of samples using GeneChip expression array data. *Theor Biol Med Model* 3: 19.

17. Ferretti E, Di Marcotullio L, Gessi M, Mattei T, Greco a, et al. (2006) Alternative splicing of the ErbB-4 cytoplasmic domain and its regulation by hedgehog signaling identify distinct medulloblastoma subsets. *Oncogene* 25(55): 7267–7273.
18. French PJ, Peeters J, Horsman S, Duijm E, Siccama I, et al. (2007) Identification of differentially regulated splice variants and novel exons in glial brain tumors using exon expression arrays. *Cancer Res* 67(12): 5635–5642.
19. Gardina PJ, Clark T a, Shimada B, Staples MK, Yang Q, et al. (2006) Alternative splicing and differential gene expression in colon cancer detected by a whole genome exon array. *BMC Genomics* 7: 325.
20. Gibson P, Tong Y, Robinson G, Thompson MC, Currle DS, et al. (2010) Subtypes of medulloblastoma have distinct developmental origins. *Nature* 468(7327): 1095–1099.
21. Gilbertson RJ (2011) Finding the perfect partner for medulloblastoma prognostication. *J Clin Oncol* 29(29): 3841–3842.
22. Hallahan AR, Pritchard JI, Chandraratna R a S, Ellenbogen RG, Geyer JR, et al. (2003) BMP-2 mediates retinoid-induced apoptosis in medulloblastoma cells through a paracrine effect. *Nat Med* 9(8): 1033–1038.
23. Hilmi C, Guyot M, Pagès G (2012) VEGF spliced variants: possible role of anti-angiogenesis therapy. *J Nucleic Acids* 2012: 162692.
24. Ingham PW (1998) The patched gene in development and cancer. *Curr Opin Genet Dev* 8(1): 88–94.
25. Kai M, Yasuda S, Imai S-I, Kanoh H, Sakane F (2007) Tyrosine phosphorylation of beta2-chimaerin by Src-family kinase negatively regulates its Rac-specific GAP activity. *Biochim Biophys Acta* 1773(9): 1407–1415.
26. Katayama S, Tomaru Y, Kasukawa T, Waki K, Nakanishi M, et al. (2005) Antisense transcription in the mammalian transcriptome. *Science* 309(5740): 1564–1566.
27. Kool M, Koster J, Bunt J, Hasselt NE, Lakeman A, et al. (2008) Integrated genomics identifies five medulloblastoma subtypes with distinct genetic profiles, pathway signatures and clinicopathological features. *PLoS one* 3(8): e3088.
28. Kwan T, Benovoy D, Dias C, Gurd S, Serre D, et al. (2007) Heritability of alternative splicing in the human genome. *Genome Res* 17(8): 1210–1218.
29. Leung T, How BE, Manser E, Lim L (1994) Cerebellar beta 2-chimaerin, a GTPase-activating protein for p21 ras-related rac is specifically expressed in granule cells and has a unique N-terminal SH2 domain. *J Biol Chem* 269(17): 12888–12892.
30. Li X-N, Shu Q, Su JM, Adesina a M, Wong KK, et al. (2007) Differential expression of survivin splice isoforms in medulloblastomas. *Neuropathol Appl Neurobiol* 33(1): 67–76.
31. MacDonald TJ, Brown KM, LaFleur B, Peterson K, Lawlor C, et al. (2001) Expression profiling of medulloblastoma: PDGFRA and the RAS/MAPK pathway as therapeutic targets for metastatic disease. *Nat Genet* 29(2): 143–152.
32. Maere S, Heymans K, Kuiper M (2005) BiNGO: a Cytoscape plugin to assess overrepresentation of gene ontology categories in biological networks. *Bioinformatics* 21(16): 3448–3449.
33. Mata MD, Alonso CR, Fededa JP, Pelisch F, Cramer P, et al. (2003) A Slow RNA Polymerase II Affects Alternative Splicing In Vivo. *Mol Cell* 12(2): 525–532.
34. Medrihan L, Rohlmann A, Fairless R, Andrae J, Döring M, et al. (2009) Neurobeachin, a protein implicated in membrane protein traffic and autism, is required for the formation and functioning of central synapses. *J Physiol* 587(Pt 21): 5095–5106.
35. Menghi F, Jacques TS, Barenco M, Schwalbe EC, Clifford SC, et al. (2011) Genome-wide analysis of alternative splicing in medulloblastoma identifies splicing patterns characteristic of normal cerebellar development. *Cancer Res* 71(6): 2045–2055.
36. Modrek B, Lee C (2002) A genomic view of alternative splicing. *Nat Genet* 30(1): 13–19.
37. Morrissy AS, Morin RD, Delaney A, Zeng T, McDonald H, et al. (2009) Next-generation tag sequencing for cancer gene expression profiling. *Genome Res* 19(10): 1825–1835.
38. Morrissy AS, Griffith M, Marra MA. (2011) Extensive relationship between antisense transcription and alternative splicing in the human genome. *Genome Res*: 21(8):1203–1212.

39. Nagao K, Togawa N, Fujii K, Uchikawa H, Kohno Y, et al. (2005) Detecting tissue-specific alternative splicing and disease-associated aberrant splicing of the PTCH gene with exon junction microarrays. *Hum Mol Genet* 14(22): 3379–3388.
40. Nakajima A, Nishimura K, Nakaima Y, Oh T, Noguchi S, et al. (2009) Cell type-dependent proapoptotic role of Bcl2L12 revealed by a mutation concomitant with the disruption of the juxtaposed Irf3 gene. *Proc Natl Acad Sci USA* 106(30): 12448–12452.
41. Nilsen TW, Graveley BR (2010) Expansion of the eukaryotic proteome by alternative splicing. *Nature* 463(7280): 457–463.
42. Northcott PA, Fernandez-L A, Hagan JP, Ellison DW, Grajkowska W, et al. (2009) The miR-17/92 polycistron is up-regulated in sonic hedgehog-driven medulloblastomas and induced by N-myc in sonic hedgehog-treated cerebellar neural precursors. *Cancer Res* 69(8): 3249–3255.
43. Northcott P a, Hielscher T, Dubuc A, Mack S, Shih D, et al. (2011) Pediatric and adult sonic hedgehog medulloblastomas are clinically and molecularly distinct. *Acta Neuropathol* 122(2): 231–240.
44. Northcott P a, Korshunov A, Witt H, Hielscher T, Eberhart CG, et al. (2011) Medulloblastoma comprises four distinct molecular variants. *J Clin Oncol* 29(11): 1408–1414.
45. Pfaff E, Remke M, Sturm D, Benner A, Witt H, et al. (2010) TP53 mutation is frequently associated with CTNNB1 mutation or MYCN amplification and is compatible with long-term survival in medulloblastoma. *J Clin Oncol* 28(35): 5188–5196.
46. Pfister SM, Korshunov A, Kool M, Hasselblatt M, Eberhart C, et al. (2010) Molecular diagnostics of CNS embryonal tumors. *Acta Neuropathol* 120(5): 553–566.
47. Pons S, Trejo JL, Martínez-Morales JR, Martí E (2001) Vitronectin regulates Sonic hedgehog activity during cerebellum development through CREB phosphorylation. *Development* 128(9): 1481–1492.
48. Raffel C (2004) Medulloblastoma: molecular genetics and animal models. *Neoplasia* 6(4): 310–322.
49. Remke M, Hielscher T, Korshunov A, Northcott P a, Bender S, et al. (2011) FSTL5 Is a Marker of Poor Prognosis in Non-WNT/Non-SHH Medulloblastoma. *J Clin Oncol* 29(29): 3852–3861.
50. Rudin CM, Hann CL, Laterra J, Yauch RL, Callahan C a, et al. (2009) Treatment of medulloblastoma with hedgehog pathway inhibitor GDC-0449. *N Engl J Med* 361(12): 1173–1178.
51. Shearwin KE, Callen BP, Egan JB (2005) Transcriptional interference--a crash course. *Trends Genet* 21(6): 339–345.
52. Shendure J, Church GM (2002) Computational discovery of sense-antisense transcription in the human and mouse genomes. *Genome Biol* 3(99): RESEARCH0044.
53. Storrs CH, Silverstein SJ (2007) PATJ, a tight junction-associated PDZ protein, is a novel degradation target of high-risk human papillomavirus E6 and the alternatively spliced isoform 18 E6. *J Virol* 81(8): 4080–4090.
54. Thompson MC, Fuller C, Hogg TL, Dalton J, Finkelstein D, et al. (2006) Genomics identifies medulloblastoma subgroups that are enriched for specific genetic alterations. *J Clin Oncol* 24(12): 1924–1931.
55. Tijink BM, Buter J, de Bree R, Giaccone G, Lang MS, et al. (2006) A phase I dose escalation study with anti-CD44v6 bivatuzumab mertansine in patients with incurable squamous cell carcinoma of the head and neck or esophagus. *Clin Cancer Res* 12(20 Pt 1): 6064–6072.
56. Tsang WH, Shek KF, Lee TY, Chow KL (2009) An evolutionarily conserved nested gene pair - Mab21 and Lrba/Nbea in metazoan. *Genomics* 94(3): 177–187..
57. Uchikawa H, Toyoda M, Nagao K, Miyauchi H, Nishikawa R, et al. (2006) Brain- and heart-specific Patched-1 containing exon 12b is a dominant negative isoform and is expressed in medulloblastomas. *Biochem Biophys Res Commun* 349(1): 277–283.
58. Wang ET, Sandberg R, Luo S, Khrebtkova I, Zhang L, et al. (2008) Alternative isoform regulation in human tissue transcriptomes. *Nature* 456(7221): 470–476.
59. Wang Z, Burge CB (2008) Splicing regulation: from a parts list of regulatory elements to an integrated splicing code. *RNA* 14(5): 802–813.
60. Wei J, Zaika E, Zaika A (2012) p53 Family: Role of Protein Isoforms in Human Cancer. *J Nucleic Acids* 2012: 687359.
61. Werbowetski-Ogilvie TE, Seyed Sadr M, Jabado N, Angers-Loustau a, Agar NYR, et al. (2006) Inhibition of medulloblastoma cell invasion by Slit. *Oncogene* 25(37): 5103–5112.

62. Xin D, Hu L, Kong X (2008) Alternative promoters influence alternative splicing at the genomic level. *PLoS one* 3(6): e2377.
63. Yang Z-J, Ellis T, Markant SL, Read T-A, Kessler JD, et al. (2008) Medulloblastoma can be initiated by deletion of Patched in lineage-restricted progenitors or stem cells. *Cancer cell* 14(2): 135–145.
64. Zhang C, Li H-R, Fan J-B, Wang-Rodriguez J, Downs T, et al. (2006) Profiling alternatively spliced mRNA isoforms for prostate cancer classification. *BMC Bioinformatics* 7: 202.
65. Zhu H, Lo H-W (2010) The Human Glioma-Associated Oncogene Homolog 1 (GLI1) Family of Transcription Factors in Gene Regulation and Diseases. *Curr Genomics* 11(4): 238–245.

Chapter Two

Isocitrate dehydrogenase-1 mutations: a fundamentally new understanding of diffuse glioma?

Nanne K Kloosterhof, Linda B C Bralten, Hendrikus J Dubbink, Pim J French, Martin J van den Bent

Lancet Oncol 2011 Jan;12(1):83-91

Abstract

The discovery of somatic mutations in the gene encoding isocitrate dehydrogenase-1 (IDH1) in glioblastomas was remarkable because the enzyme was not previously identified with any known oncogenic pathway. *IDH1* is mutated in up to 75% of grade II and grade III diffuse gliomas. Apart from acute myeloid leukaemia, other tumour types do not carry *IDH1* mutations. Mutations in a homologous gene, *IDH2*, have also been identified, although they are much more rare. Although *TP53* mutations and 1p/19q codeletions are mutually exclusive in gliomas, in both of these genotypes *IDH1* mutations are common. *IDH1* and *IDH2* mutations are early events in the development of gliomas. Moreover, *IDH1* and *IDH2* mutations are a major prognostic marker for overall and progression-free survival in grade II–IV gliomas. Mutated IDH1 has an altered catalytic activity that results in the accumulation of 2-hydroxyglutarate. Molecularly, *IDH1* and *IDH2* mutations are heterozygous, affect only a single codon, and rarely occur together. Because *IDH1* does not belong to a traditional oncogenic pathway and is specifically and commonly mutated in gliomas, the altered enzymatic activity of IDH1 may provide a fundamentally new understanding of diffuse glioma.

Introduction

In 2008, a genome-wide sequencing study identified mutations in a gene encoding isocitrate dehydrogenase (IDH1) in 18 (12%) of 149 samples of glioblastoma multiforme.¹ The mutations were most common in young patients with glioblastomas that had progressed from lowgrade gliomas to secondary glioblastoma multiforme. Patients with *IDH1* mutations were also associated with a longer survival than patients with glioblastomas without *IDH1* mutations. Several papers have since identified the *IDH1* mutations in other glioma subtypes and in various tumour types (table 1). Functional studies^{2–17} on *IDH1* found that *IDH1* mutations in the gene are highly glioma specific. Investigations of large numbers of other tumour types showed that acute myeloid leukaemia (AML) was the only cancer other with a high incidence of *IDH1* mutations (table 1). *IDH1* is the most commonly mutated gene in many types of glioma, with incidences of up to 75% in grade II and grade III glioma (table 1). *IDH1* mutations are always heterozygous missense mutations that affect aminoacid residue 132 (figure 1) and are associated with longer survival in patients with glioma than patients with glioma without *IDH1* mutations (table 2, figure 2). *IDH1* mutations result in a reduced enzymatic activity towards the native substrate, isocitrate, and mutant IDH1 catalyses the formation of 2-hydroxyglutarate from α -ketoglutarate.

In addition to *IDH1*, mutations in a homologous gene, *IDH2*, with a different subcellular distribution have been identified in gliomas. *IDH2* mutation is much less common than *IDH1* mutation; the two rarely occur together, but both seem to be specific to gliomas.^{5,6,11,24} Inactivating mutations in another gene, *IDH3B*, have been identified in patients with retinitis pigmentosa, but they do not seem to be associated with tumour formation.²⁵

Structure and function

In human beings, five genes encode for isocitrate dehydrogenase: *IDH1*, *IDH2*, *IDH3A*, *IDH3B*, and *IDH3G*. These genes encode three catalytic isozymes: IDH1, IDH2, and IDH3. Both IDH1 and IDH2 function as homodimers whereas IDH3 functions as a heterotetramer

composed of two α , one β , and one γ subunit.²⁶ The function of all isocitrate dehydrogenases is to catalyse the oxidative decarboxylation of isocitrate into α -

Table 1. IDH1 and IDH2 mutation frequencies

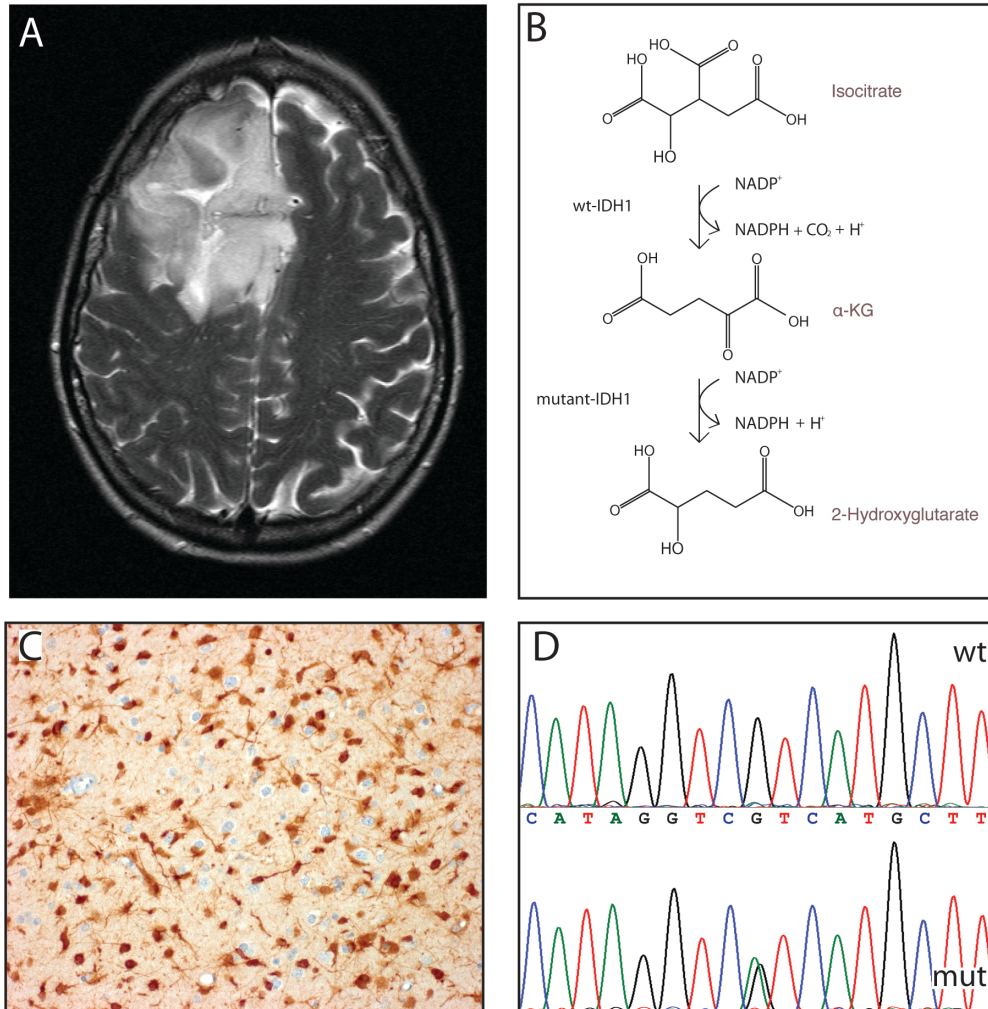
	IDH1		IDH2	
	mutations (%) median (range)	Total/# mutations	mutations (%) median (range)	Total/# mutations
Astrocytic tumours				
Pilocytic astrocytoma ²⁻⁵	1% (0% - 10%)	131/4	0%	21/0
Pleomorphic	7% (0% - 14%)	14/1		
Subependymal giant-cell	0%	14/0		
Diffuse astrocytoma ²⁻⁸	74% (0% - 88%)	405/309	0.88% (0% - 7%)	259/4
Anaplastic astrocytoma ²⁻⁹	60% (0% - 78%)	525/324	4% (0.9% - 5%)	301/5
Glioblastoma				
Primary ^{2-5,7-11}	5% (3% - 12%)	1153/61	0%	139/0
Primary pediatric ^{2,5}	4% (0% - 7%)	29/1	0%	15/0
Secondary ^{2-5,7-10}	75% (50% - 88%)	126/96	0%	11/0
Giant cell glioblastoma	25%	8/2		
Gliosarcoma ²	0%	5/0		
Oligodendroglial				
Oligodendroglioma ²⁻⁸	76% (67% - 82%)	366/283	4% (0% - 5%)	188/8
Anaplastic	67% (49% - 86%)	388/260	5% (0% - 8%)	224/12
Oligoastrocytoma ²⁻⁷	80% (50% - 100%)	196/153	1%	76/1
Anaplastic	74% (63%- 100%)	391/269	5% (0% - 9%)	181/11
Ependymal tumours				
Subependymoma ²⁻⁸	0%	8/0		
Myxopapillary	0%	14/0		
Ependymoma ²⁻⁵	0%	92/0	0%	30/0
Anaplastic	0%	17/0		
Neuronal and mixed				
Ganglioglioma ⁸	37.5%	8/3	0%	8/0
Anaplastic ganglioglioma ⁷	60%	5/3	0%	5/0
DNET ³	0%	4/0		
Paraganglioma	0%	21/0		
Paraganglioma	0%	203/0		
Embryonal tumours				
Medulloblastoma IV ^{2,3-5}	0%	149/0	0%	55/0
PNET ^{2,3}	17% (0% -33%)	17/3		
Tumours of the cranial				
Schwannoma I ²	0%	17/0		
Vestibular Schwannoma ³	0%	48/0		
Meningeal tumours				
Meningioma I ^{2,3,11}	0%	86/0	0%	14/0
Atypical meningioma II ²	0%	17/0		
Anaplastic meningioma	0%	17/0		
Tumours of the sellar				
Pituitary adenoma I ²	0%	23/0		
Hematological disorders				
Acute leukemia ¹¹			0%	166/0
Acute myelogenous	0% (0% - 9%)	389/21		

Listed are the median and range of the percentages of *IDH1* mutations from individual studies. The total number of mutations is a sum of all samples from all relevant studies. The study of Parsons et al. is excluded from this table due to partly overlapping sample sets with Yan et al.

ketoglutarate, with oxalosuccinate formed as an intermediate product (figure 1).²⁷ In mitochondria this reaction is part of the tricarboxylic-acid cycle (also know as the Krebs cycle). During the enzymatic reaction, either nicotinamide adenine dinucleotide (NAD+) in the case of IDH3 or nicotinamide adenine dinucleotide phosphate (NADP+) for IDH1 and IDH2 function as the electron acceptor. Distinct isocitrate dehydrogenase (IDH) isozymes

also differ in subcellular localisation; IDH1 is located in the cytoplasm and peroxisomes whereas IDH2 and IDH3 are found in mitochondria. Neither IDH1 nor IDH2 function as monomers, and both require a divalent metal ion, preferably Mn^{2+} , for enzymatic activity.²⁸⁻³⁴

Figure 1: Isocitrate dehydrogenase 1 mutations in gliomas



Example of a MRI of a patient with a glial brain tumour. B: The enzymatic reaction catalyzed by isocitrate dehydrogenase. Isocitrate is first converted into oxalosuccinate and subsequently into α -ketoglutarate. During the reaction, $NADP^+$ is converted into $NADPH + CO_2 + H^+$. C: Immunohistochemistry on formalin fixed, paraffin embedded glioma tissue using an antibody specific for R132H mutated IDH1. At the infiltrating edge of the tumour into the cortex, only glioma cells stain positive for the antibody and not the normal brain parenchyma (courtesy of A. von Deimling, university of Heidelberg, Germany, see also references (36-38)). D: Example of a chromatogram of a tumour that harbours a heterozygous mutation (G>G/A) on position 395 of IDH1 (mut, lower trace). The upper trace shows a wildtype glioma around the same nucleotides for comparison (wt).

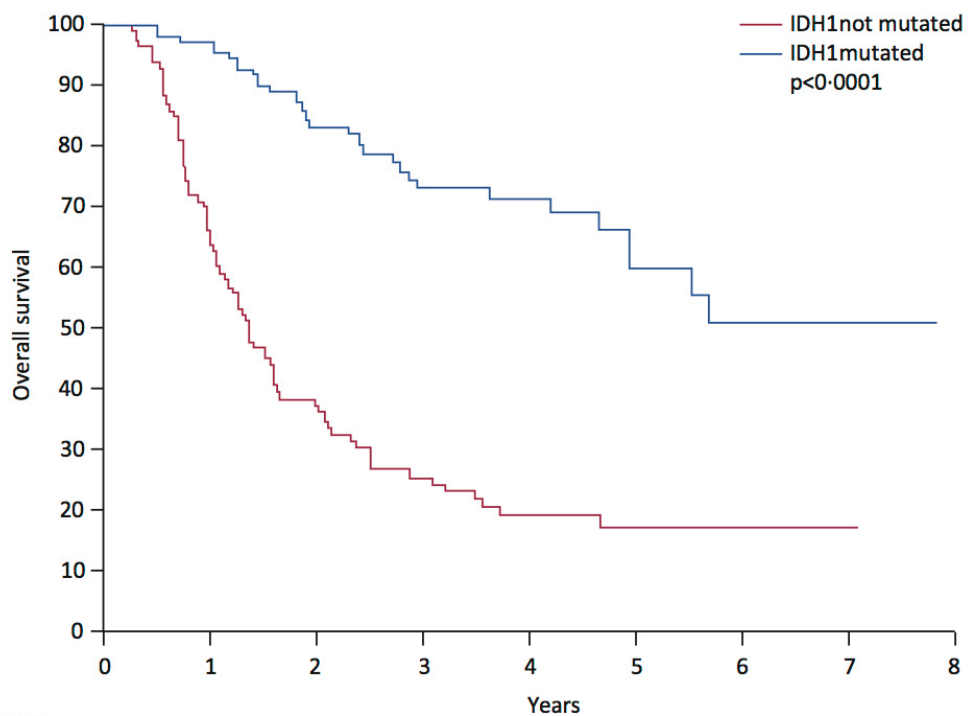
Mutation frequency

Diffuse gliomas are the most common primary brain cancer in adults and typically have a poor prognosis.^{35,36} On the basis of histology, gliomas are classified into astrocytic tumours (75%) and oligodendroglial tumours (25%). Oligodendroglial tumours comprise both classic oligodendrogliomas and mixed oligoastrocytic tumours.³⁷ Diffuse gliomas are further classified into grade II (or low grade), grade III (anaplastic), and grade IV

(glioblastoma multiforme) depending on the presence of malignant features. Grade IV tumours, are the most common and aggressive type of glioma and are distinguished between those that occur de novo (primary glioblastoma multiforme) and those that have progressed from lowgrade gliomas (secondary).³⁸

IDH1 mutation is common in almost all glioma subtypes, ranging from 50% to 80%, except in primary glioblastoma multiforme (table 1). *IDH1* is among the few genes that are commonly mutated in grade II and grade III gliomas.^{39,40} The prevalence of *IDH1* mutation is much lower in primary (about 5%) than in secondary gliomas than in anaplastic gliomas.^{7,41} *IDH2* mutations (about 75%) glioblastoma multiforme. Furthermore, are much less common than *IDH1* mutations and are *IDH1* mutation seems to be more common in grade II associated with oligodendrogliomas (table 1).⁶ *IDH1* mutations are rarely seen in pilocytic astrocytomas, which are circumscript (non-diffuse) grade I gliomas.⁴² Molecularly, *IDH1* mutations are associated with MGMT (O⁶-methylguanine-DNA methyltransferase) methylation status, *TP53* mutations, and deletions of both 1p and 19q.^{3,4,7,22} *TP53* mutations and deletions of both 1p and 19q are mutually exclusive and are thought to be early events in the development of astrocytomas and oligodendrogliomas respectively.

Figure 2: The prognostic value of isocitrate dehydrogenase 1 mutation status



Overall survival in 159 patients (univariate analysis) from a prospective randomised phase 3 study (22) on procarbazine, lomustine, and vincristine chemotherapy for anaplastic oligodendroglioma (EORTC study 26951), in whom isocitrate dehydrogenase mutations could be determined.²² Observed events 70 in IDH1 not mutated, 26 events in IDH1 mutated.

IDH1 mutations are almost exclusively detected in gliomas. However, of 224 patients with AML in one study,¹⁴ 21 (9%) had *IDH1* mutations, which occurred predominantly (13 of 80 patients) in otherwise cytogenetically normal cells.¹⁴ No other major subtype of

leukaemia (chronic-lymphoid leukaemia, acute-lymphoid leukaemia, and chronic-myeloid leukaemia) was associated with *IDH1* mutation (table 1). *IDH1* mutations do not seem to occur in any of the other tumour types examined, although sporadic mutations have been found in paraganglioma, prostate carcinomas, and in a colon cancer metastasis.^{12,13,43}

Table 2. Prognostic value of *IDH1* and *IDH2* mutations in glioma

Tumour	No. of patients	HR (mutant vs wildtype)	HR (mutant vs PFS wildtype)	median PFS (months)	median OS (months)
Grade II-IV					
Multivariate ^{7*}	397	0.4	0.3		
GBM					
Multivariate ^{10†}	407				11.3 vs 27.1
Multivariate ^{20‡}	301	0.4	0.4	6.5 vs 16.2	11.2 vs 30.2 (trend)
Multivariate ^{15§}	159		0.1		8.4 vs 24.0
Univariate ⁷	183			8.8 vs 55	14 vs 27.4
Univariate ⁵	129§§				15 vs 31
Univariate ^{1¶}	105§§				13.2 vs 45.6
Grade III gliomas					
Multivariate ²¹	318	0.4	0.5		
Univariate ^{7**}	121			9.2 vs 37	19.4 vs 81.1
Anaplastic					
Univariate ⁵	52				20 vs 65
Univariate ⁸	21				22 vs 50
Anaplastic oligodendroglioma and anaplastic astrocytoma					
Multivariate ^{22††}	159	0.3	0.2	7.8 vs 50	16 vs not
Grade II gliomas					
Univariate ⁷	100				60.1 vs 150.9
Progressive low-grade astrocytoma					
Univariate ^{23‡‡}	49				48 vs 98

Prognostic value of *IDH1* and *IDH2* mutations for progression-free survival and overall survival, according to tumour type. HR=hazard ratio. PFS=progression free survival. OS=overall survival. GBM=glioblastoma multiforme. KPS=Karnofsky performance score. *Tumour grade, age, *MGMT* methylation status, genomic profile (1p and 19q co-deletion, epidermal growth factor receptor [EGFR] amplification) and treatment were included in the multivariate analysis. †Age and gender were included in the multivariate analysis. ‡*MGMT* methylation status, age, KPS, extent of resection, and adjuvant therapy were included. §Molecular cluster, KPS, age, sex, extent of surgery, chemotherapy, epidermal growth factor receptor amplification, and 1p and 19q loss were included. ¶This was also significant in *TP53* mutated group younger than 35 years. ||Age, KPS, mini-mental status, resection, histology, *MGMT* methylation status, 1p and 19q codeletion, and *IDH1 R132H* mutation were included. **Significant in the non-1p–19q codeleted and non-EGFR amplified group (n=80). ††Necrosis, frontal localisation, and 1p and 19q co-deletion were included. ‡‡Age, presenting clinical symptoms, and treatment were the same in the two groups. §§Parsons and colleagues¹ and Yan and colleagues⁵ have a partly overlapping sample set.

Clinical implications

Histological diagnosis of gliomas is subject to substantial interobserver variation,⁴⁴ thus *IDH1* mutation status can provide an objective marker to identify the glioma subtype. *IDH1* mutations are rare in primary glioblastoma multiforme and are common in secondary glioblastoma multiforme; therefore, *IDH1* mutation status can distinguish between these two subtypes (sensitivity 71.0–73%, specificity 96%).¹⁸ The low incidence of *IDH1* mutation in pilocytic astrocytomas also allows clinically relevant differentiation between diffuse and pilocytic astrocytomas (sensitivity 73–83%, specificity 100%).¹⁸ Furthermore, *IDH1* mutations can have a role in distinguishing anaplastic astrocytomas from primary glioblastoma multiforme, or astrocytomas from ependymomas.¹⁸ Several techniques have been developed to detect *IDH1* mutations (figure 1).^{18,19,45,46} These

techniques might aid diagnosis, even if samples contain little tumour tissue, and allow differentiation between tumour and reactive gliosis.

Extensive research has been done to determine the prognostic value of *IDH1* mutations (table 2). Patients with *IDH1* mutated glioblastoma multiforme have a better prognosis than those without *IDH1* mutations,¹ with respect to both overall survival^{1,5,7,8,10,15,20–23} (figure 2) and progression-free survival.^{7,20,22} Although patients with an *IDH1* mutation are generally younger, and that age alone is an independent prognostic factor in gliomas, several studies have confirmed by multivariate analyses the independent prognostic value of *IDH1* mutations.^{7,10,15,20–22} The major prognostic importance of *IDH1* mutation status suggests that it should be used as a stratification factor in controlled clinical trials.

Two studies have examined whether *IDH1* mutation status can predict response to treatment in gliomas. In a group of patients with dedifferentiated low-grade astrocytomas progressive after radiotherapy response to temozolomide did not differ between *IDH1* mutant and wild-type tumours.²³ In patients with anaplastic oligodendroglial tumours treated with radiotherapy alone or radiotherapy with adjuvant PCV (procarbazine, lomustine, and vincristine), the presence of *IDH1* mutations had no predictive value for outcome to PCV.²² Whether *IDH1* mutations have a predictive value in other subgroups or treatment regimens needs to be investigated; at present *IDH1* mutations seem to be mostly prognostic.

Are *IDH1* and *IDH2* mutations causal?

Despite the high mutation frequency, whether *IDH1* mutations cause disease is unknown. Several observations suggest a causal role for *IDH1* and *IDH2* in tumorigenesis. The prevalence and nature of somatically acquired mutations does not suggest a bystander mutation.⁴⁷ Moreover, *IDH1* and *IDH2* mutations rarely occur together.⁶ Mutant *IDH1* causes an accumulation of 2-hydroxyglutarate, high concentrations of which are associated with brain tumours.^{16,48,49} Specific mutation types segregate into distinct tumour types;^{6,41} *IDH1* mutations are early events in glioma development and have been reported to precede both the loss of 1p and 19q and the acquisition of *TP53* mutations.^{3,4} Furthermore, the incidence of *IDH1* mutations is higher in grade II than in grade III gliomas.^{7,41} Thus, mutation type and incidence, as well as the timing of the mutation suggests a causal role for *IDH1* and *IDH2* in tumours.

Mutations of a single codon

All mutations in *IDH1* and *IDH2* are somatic, missense, heterozygous, and affect codon 132 (*IDH1*) or codon 172 (*IDH2*). Moreover, both codons have analogous positions in the isozymes.^{50–52} Most mutations are single base transition substitutions: 395G→A for *IDH1* (about 90%), and 515G→A for *IDH2* (about 60%). These mutations result in an arginine to histidine (R132H) substitution in *IDH1* or an arginine to lysine (R172K) substitution in *IDH2*. The remaining *IDH1* mutations are, with the exception of R132V (1 of 1630, 0.1%), single nucleotide substitutions on neighbouring bases that result in a substitution of arginine with cysteine (77 of 1630, 4.7%), glycine (34 of 1630, 2.1%), serine (27 of 1630, 1.7%), or leucine (13 of 1630, 0.8%).^{2–10}

Although more than 90% of all mutations in *IDH1* are R132H substitutions, several studies

reported an increased prevalence of other mutation types in specific histological subtypes. In gliomas, R132C mutations seem to be much more common in astrocytomas (32 of 591, 5.4%) than in oligodendrogliomas (2 of 662, 0.3%).^{6,41} Additionally, all five *IDH1*-mutated astrocytomas in patients with Li-Fraumeni syndrome (ie, patients with a germline *TP53* mutation), had R132C substitutions.⁵³ In AML and in sporadic mutations of non-gliomas, only 11 of 26 mutations were R132H; R132C comprise most of the remaining mutations.^{12–14,43} Genetic and epigenetic differences might explain differences in the incidence of mutation types in various tumour types and subtypes. However, functional differences between R132H and non-R132H mutated *IDH1* might also explain the segregation of distinct mutation subtypes.

Because only R132 in *IDH1* and R172 in *IDH2* are mutated in cancer, they probably confer unique properties on the enzyme. Both codons are highly conserved and have analogous positions in the isozymes.^{50–52} In IDH, R132 and R172 are needed for the electrostatic attraction of isocitrate (both α -carboxylates and β -carboxylates)⁵² and the actual enzymatic reaction; arginine (ie, R132 and R172) lowers the pK of nearby aspartic acids, which accept the cleaved proton of the hydroxyl group (OH⁻) before transfer to NADP⁺. Under high pH conditions, the enzyme function is conserved by site directed mutagenesis of porcine R133 (corresponding to R172 in human *IDH2*).⁵² R132 seems to be a structurally important residue when changing between the different conformational states of the enzyme. Substitution of histidine for arginine is likely to shift the equilibrium to the closed (ligand and NADP⁺ bound) conformation.¹⁶ Therefore, R132 and R172 are involved in both the substrate binding and the enzymatic reaction.

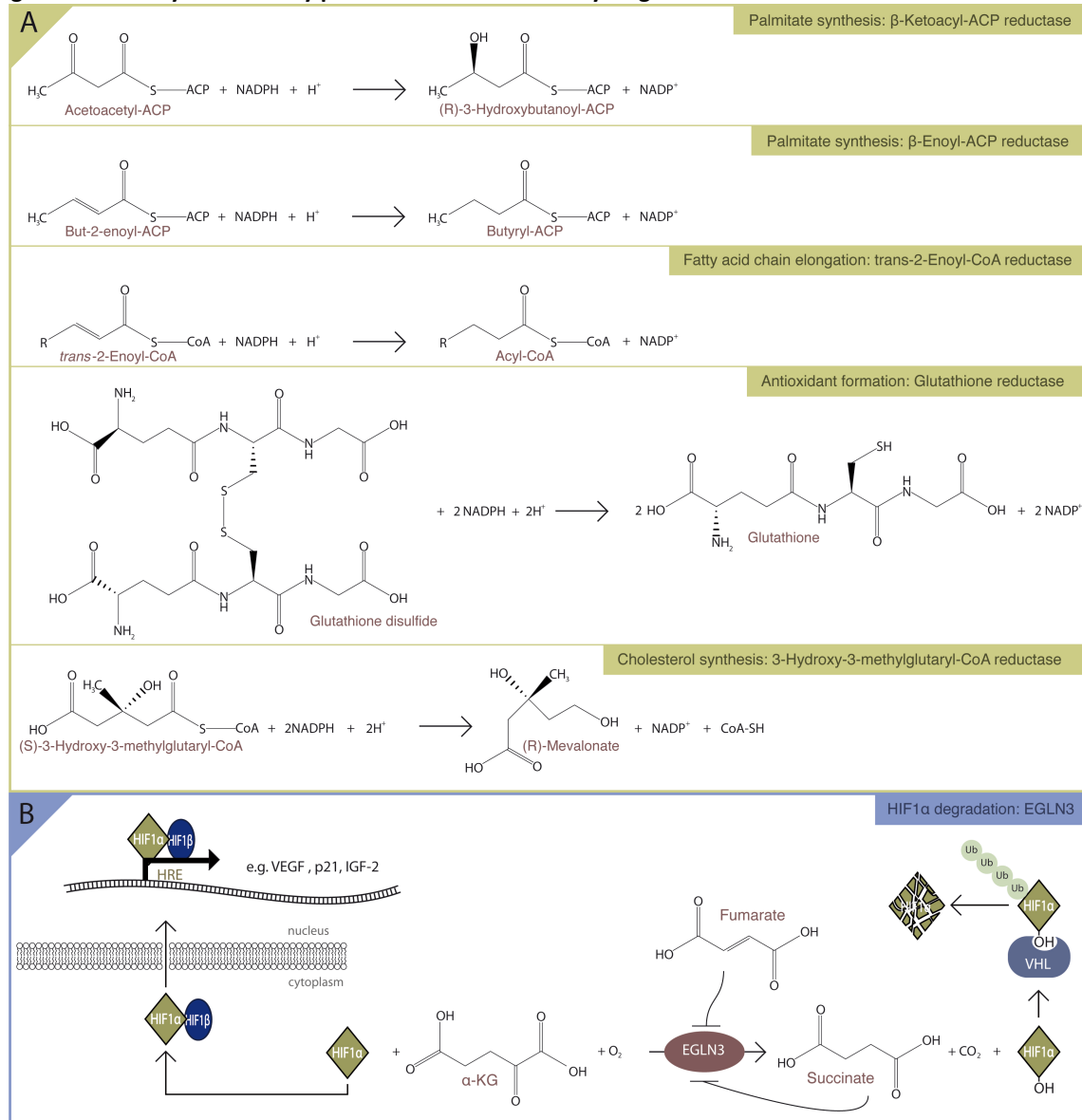
Altered enzymatic activity

Results of studies examining the functional consequences of *IDH1* and *IDH2* mutant proteins have shown a strong decrease in the isocitrate-dependent production of reduced NADPH production.^{3,5,17} Such a decrease in enzymatic activity suggests that both *IDH1* and *IDH2* are tumour suppressor genes; however, mutant *IDH1* has altered substrate specificity and is more compatible with an oncogenic function.¹⁶

A tumour suppressor function of wild-type *IDH1* is possible because the mutant protein exerts a dominant negative effect on its activity. Because *IDH1* mutations are heterozygous, both wild-type and mutant *IDH1* are expressed in a single cell.¹⁴ When dimers are formed between a mutant and a wild-type protein (heterodimers), mutant *IDH1* substantially reduces the activity of the wild-type protein.¹⁷ Similar findings have been reported for *IDH2*.⁵⁴ However, many other mutations generated in *IDH1* or *IDH2*, which are scattered across the various domains of the *IDH1* and *IDH2* proteins, also strongly reduce enzymatic activity.^{27,52,55–58} Therefore, if *IDH1* and *IDH2* do function as tumour suppressor genes, then this enzymatic activity is only susceptible to mutation in R132 and R172, respectively.

Two observations contradict a dominant negative effect for *IDH1*. First, overexpression of recombinant mutant *IDH1* or *IDH2* in a cell line with two normal copies of the isozymes does not seem to reduce isocitrate dehydrogenase activity.^{3,5} Zhao and colleagues¹⁷ showed that the dominant negative effect of mutant *IDH1* is dependent on the isocitrate concentration,¹⁷ but the isocitrate concentration in enzymatic activity measurements

Figure 3: Pathways affected by products of isocitrate dehydrogenase 1



Products of isocitrate dehydrogenase 1 (IDH1) are used in various processes. NADPH is used as a cofactor in palmitate synthesis (A), fatty-acid chain elongation (B), and antioxidant formation (C). NADPH is also used as a cofactor in the rate limiting step of cholesterol synthesis by the enzyme 3-hydroxy-3-methylglutaryl-coenzyme A reductase (D). Hypoxia-inducible factor 1 α (HIF1 α) degradation; under normoxic conditions HIF1 α is hydroxylated by egl nine homologue 3 (EGLN3), in a reaction that requires α -ketoglutarate as a substrate. This reaction results in the generation of succinate and hydroxylated HIF1 α , which allow the von Hippel-Lindau (VHL) tumour suppressor to bind HIF1 α , resulting in the proteasomal degradation of HIF1 α . The reaction catalysed by EGLN is inhibited by succinate and fumarate. Under hypoxic conditions the hydroxylation does not occur and allows HIF1 α to form a complex with HIF1 β . This complex binds to hypoxia-responsive elements (HRE) in the DNA to promote transcription of HIF responsive genes such as those encoding vascular endothelial growth factor (VEGF), p21, and insulin-like growth factor 2 (E; IGF2). ACP=acyl-carrier protein. Ub=ubiquitin.

(using lysates of cells overexpressing recombinant mutant IDH1) were too high for such a dominant negative effect to be seen. Additional experiments on cell lysates with lower isocitrate concentrations are needed to confirm the dominant negative effect of mutant IDH1. Second, a dominant negative tumour-suppressor function is difficult to reconcile with the reported segregation of R132C mutations in tumour subtypes; however

differences in mutation frequency might be explained by genetic and epigenetic differences.^{6,14,41} Nevertheless, the possibility of a dominant negative function of mutant IDH1 or IDH2 in vivo requires further analysis.

An oncogenic role of IDH1 is most compatible with the reported range of mutations; hotspot mutations, with the exception of *TP53*, are commonly identified in oncogenes (eg, H-Ras59, PIK3CA60). This oncogenic role of IDH1 could result from altered substrate specificity. Site directed mutagenesis of the *Escherichia coli* NADP⁺-dependent isocitrate dehydrogenase has shown that point mutations can result in altered specificity for this enzyme.^{61,62} Mutant IDH1 uses α -ketoglutarate as a substrate to produce 2-hydroxyglutarate (figure 1).¹⁶ Concentrations of 2-hydroxyglutarate increase to over 50 times that of normal concentrations in IDH1 mutated tumours.¹⁶ Mutated IDH1 generates the (R)-enantiomer of 2-hydroxyglutarate (R-2HG). Accumulation of R-2HG is associated with D-2-hydroxyglutaric aciduria, a rare neurometabolic disorder with highly variable phenotypes, caused by a defect in D-2-hydroxyglutarate dehydrogenase. The S-enantiomer of 2-hydroxyglutarate (S-2HG) is dehydrated to α -ketoglutarate by the metabolic repair enzyme L-2-hydroxyglutarate dehydrogenase.⁶³ L-2-hydroxyglutaric aciduria, a hereditary encephalopathy due to a defect in L-2-hydroxyglutarate dehydrogenase, is associated with different brain tumour types, some of which are not associated with *IDH1* mutations (ependymomas and medulloblastomas).^{48,49} S-2HG is not a known intermediate in any mammalian pathway.⁶³ Moreover, S-2HG and R-2HG exert different biological effects.⁶⁴ Unlike L-2-hydroxyglutaric aciduria, D-2-hydroxyglutaric aciduria is not associated with tumour formation. Thus, how an increase in R-2HG contributes to tumour formation needs to be investigated.

Cellular functions affected by mutant IDH1 and IDH2

Although IDH1 mediates a reaction identical to that which happens in the tricarboxylic acid cycle, IDH1 does not play a direct part in the reaction because it is localised in the cytosol. Thus, IDH1 does not seem to mediate the Warburg effect (the observation that even under normoxic conditions tumour cells preferentially use glycolysis over aerobic respiration).⁶⁵ Other tumour-associated mutations in metabolic enzymes have been described in hereditary pheochromocytoma-paraganglioma syndrome, hereditary leiomyomatosis, and renal-cell cancer. Hereditary pheochromocytoma-paragangliomas have dysfunctional succinate-dehydrogenase complexes, and hereditary leiomyomatosis and renal-cell cancer have dysfunctional fumarate hydratase.^{65,66} Because IDH1 is not part of the tricarboxylic-acid cycle, the *IDH1* mutations in gliomas are different from the inactivating mutations in the metabolic pathways of other tumour types.

Little is known about cytosolic IDH1 and its cellular function in tumours. Homozygous deletions are embryonically lethal in *Drosophila melanogaster*.⁶⁷ The biochemical role of IDH1 in α -ketoglutarate and NADPH production allow the cellular function of IDH1 to be inferred. Biochemical pathways might be affected by and fatty-acid biosynthetic pathways (figure 3).^{68,69} In changes in cellular α -ketoglutarate and NADPH nucleic acid synthesis, IDH1 competes with the pentose concentrations. The anabolic pathways of lipid synthesis, phosphate pathway for NADP⁺ as an electron acceptor,⁷⁰ cholesterol synthesis, and fatty-acid-chain elongation Cytosolic IDH attenuates the glucose-induced

increase depend on cytoplasmic NADPH. *IDH1* knock-in mice in pyruvate cycling in the tricarboxylic-acid cycle, show substantial changes in lipid metabolism perhaps by affecting the concentrations of organic acid, (eg, hyperlipidaemia, fatty liver, and obesity), and is involved in glucose-stimulated insulin secretion.⁷¹ Furthermore, *IDH1* activity is regulated by cholesterol in pancreatic islet cells.⁷¹ α -Ketoglutarate might affect the activity of *IDH* isozymes by end product inhibition.⁷² Finally, 2-hydroxyglutarate metabolism might be affected as mutant *IDH1* converts α -ketoglutarate to 2-hydroxyglutarate.¹⁶

Several biochemical pathways might be affected by changes in α -ketoglutarate and NADPH concentrations (figure 3). Overexpression of *IDH1* results in increased protection against reactive-oxygen species as well as protection against radiation, whereas inhibition of *IDH1* results in increased sensitivity.⁷³⁻⁷⁷ Similarly, overexpression of *IDH2* result in a decrease of intracellular reactiveoxygen species.⁷⁵ Although cellular response to oxidative stress might be altered in tumours with mutated *IDH*, this is not reflected in an increase in the number of mutations.^{1,47,77} *IDH1* expression also changes in response to other kinds of stressors, such as protein excretion by *Helicobacter pylori* and heat.^{78,79} *IDH* mutations might also play a part in the cellular migration and cellular response to hypoxia. For example, inhibition of cytosolic *IDH1* has been reported to increase lactate production, which promotes migration of glioma cells.^{71,80}

α -ketoglutarate promotes the degradation of hypoxiainducible factor (HIF)1 α , through EGLN (egl nine homologue) prolyl hydroxylases (figure 3). Activation of the HIF pathway results in the induction of vasucular endothelial growth factor (VEGF).⁸¹ However, the most vascularised gliomas (primary glioblastoma multiforme) have the lowest incidence of *IDH1* mutation among glioma. This finding suggests that decreased α -ketoglutarate concentrations might affect other HIF dependent (energy metabolism) or independent pathways (EGLN-related apoptosis).^{17,65,81-83} Nonetheless, the HIF path way is likely to be affected in tumours with mutations in metabolic enzymes, such as in phaeochromocytomaparaganglioma syndrome.⁸⁴ By contrast with glioma, *IDH1* mutated AML does not show an increased expression of *HIF1* α downstream target genes.^{14,17} Moreover, other biochemical and cellular pathways are affected by mutations in *IDH1* and *IDH2*, and the alternative products generated by mutated *IDH1* or *IDH2* might affect entirely different pathways. Further investigation is needed to establish whether *IDH1* and *IDH2* are functionally important to tumour formation and tumour progression.

Conclusion

The incidence of *IDH1* mutation is very high in most diffuse gliomas, but not in primary glioblastomas, and to a lesser extent in AML. Mutations in the homologous *IDH2* gene also occur albeit with a much lower incidence than *IDH1*. These mutations are early events in gliomagenesis, and arise both in *TP53* mutated astrocytomas and in 1p and 19q codeleted oligodendrogliomas. *IDH1* is a strong prognostic marker for overall survival and progression-free survival in gliomas, suggesting that future clinical trials might need stratification by *IDH1* mutation status. Molecularly, *IDH1* and *IDH2* mutations are inversely correlated, heterozygous, affect a single codon, and result in different catalytic properties. Because of the high mutation frequency, mutated *IDH1* could potentially form a good target for new treatments. *IDH1* is expressed at high levels and seems to be expressed in all tumour cells. The three-dimensional structure of the native protein has

also been identified. However, for effective pharmacological intervention, research into tumour-cell biology and biochemical defects associated with *IDH1* and *IDH2* mutations is needed. Further clinical research will identify the diagnostic relevance of these mutations.

Acknowledgments

We acknowledge Prof Andreas von Deimling for providing figure 1C.

References

- 1 Parsons DW, Jones S, Zhang X, et al. An integrated genomic analysis of human glioblastoma multiforme. *Science*. 2008; **321**: 1807–12.
- 2 Balss J, Meyer J, Mueller W, Korshunov A, Hartmann C, von Deimling A. Analysis of the IDH1 codon 132 mutation in brain tumors. *Acta Neuropathol* 2008; **116**: 597–602.
- 3 Ichimura K, Pearson DM, Kocialkowski S, et al. IDH1 mutations are present in the majority of common adult gliomas but rare in primary glioblastomas. *Neuro Oncol* 2009; **11**: 341–47.
- 4 Watanabe T, Nobusawa S, Kleihues P, Ohgaki H. IDH1 mutations are early events in the development of astrocytomas and oligodendrogliomas. *Am J Pathol* 2009; **174**: 1149–53.
- 5 Yan H, Parsons DW, Jin G, et al. IDH1 and IDH2 mutations in gliomas. *N Engl J Med* 2009; **360**: 765–73.
- 6 Hartmann C, Meyer J, Balss J, et al. Type and frequency of IDH1 and IDH2 mutations are related to astrocytic and oligodendroglial differentiation and age: a study of 1,010 diffuse gliomas. *Acta Neuropathol* 2009; **118**: 469–74.
- 7 Sanson M, Marie Y, Paris S, et al. Isocitrate dehydrogenase 1 codon 132 mutation is an important prognostic biomarker in gliomas. *J Clin Oncol* 2009; **27**: 4150–54.
- 8 Sonoda Y, Kumabe T, Nakamura T, et al. Analysis of IDH1 and IDH2 mutations in Japanese glioma patients. *Cancer Sci* 2009; **100**: 1996–98.
- 9 Bleeker FE, Lamba S, Leenstra S, et al. IDH1 mutations at residue p.R132 (IDH1(R132)) occur frequently in high-grade gliomas but not in other solid tumors. *Hum Mutat* 2009; **30**: 7–11.
- 10 Nobusawa S, Watanabe T, Kleihues P, Ohgaki H. IDH1 Mutations as molecular signature and predictive factor of secondary glioblastomas. *Clin Cancer Res* 2009; **15**: 6002–07.
- 11 Park SW, Chung NG, Han JY, et al. Absence of IDH2 codon 172 mutation in common human cancers. *Int J Cancer* 2009; **125**: 2485–6.
- 12 Gaal J, Burnichon N, Korpershoek E, et al. IDH mutations are rare in pheochromocytomas and paragangliomas. *JCEM* 2010; **95**: 1274–78.
- 13 Kang MR, Kim MS, Oh JE, et al. Mutational analysis of IDH1 codon 132 in glioblastomas and other common cancers. *Int J Cancer* 2009; **125**: 353–55.
- 14 Mardis ER, Ding L, Dooling DJ, et al. Recurring mutations found by sequencing an acute myeloid leukemia genome. *N Engl J Med* 2009; **361**: 1058–66.
- 15 Gravendeel AM, Kouwenhoven CM, Gevaert O, et al. Intrinsic gene expression profiles of gliomas are a better predictor of survival than histology. *Cancer Res* 2009; **69**: 9065–72.
- 16 Dang L, White DW, Gross S, et al. Cancer-associated IDH1 mutations produce 2-hydroxyglutarate. *Nature* 2009; **462**: 739–44.
- 17 Zhao S, Lin Y, Xu W, et al. Glioma-derived mutations in IDH1 dominantly inhibit IDH1 catalytic activity and induce HIF-1alpha. *Science* 2009; **324**: 261–65.
- 18 Capper D, Weissert S, Balss J, et al. Characterization of R132H Mutation-specific IDH1 Antibody Binding in Brain Tumors. *Brain Pathol* 2009. **20**: 245–54.
- 19 Capper D, Zentgraf H, Balss J, Hartmann C, von Deimling A. Monoclonal antibody specific for IDH1 R132H mutation. *Acta Neuropathol* 2009; **118**: 599–601.
- 20 Weller M, Felsberg J, Hartmann C, et al. Molecular predictors of progression-free and overall survival in patients with newly diagnosed glioblastoma: a prospective translational study of the german glioma network. *J Clin Oncol* 2009; **27**: 5743–50.
- 21 Wick W, Hartmann C, Engel C, et al. NOA-04 randomized phase III trial of sequential radiochemotherapy of anaplastic glioma with PCV or temozolomide. *J Clin Oncol* 2009; **27**: 5874–80.
- 22 van den Bent MJ, Dubbink HJ, Marie Y, et al. IDH1 and IDH2 mutations are prognostic but not predictive for outcome in anaplastic oligodendroglial tumors: a report of the EORTC Brain Tumor

- Group. *Clin Cancer Res* 2010; **16**: 1597–604.
- 23 Dubbink HJ, Taal W, van Marion R, et al. IDH1 mutations in astrocytomas predict survival but not
response to temozolomide. *Neurology* 2009; **73**: 1792–95.
- 24 Holdhoff M, Parsons DW, Diaz LA Jr. Mutations of IDH1 and IDH2 are not detected in brain
metastases of colorectal cancer. *J Neurooncol* 2009; **94**: 297.
- 25 Hartong DT, Dange M, McGee TL, Berson EL, Dryja TP, Colman RF. Insights from retinitis
pigmentosa into the roles of isocitrate dehydrogenases in the Krebs cycle. *Nat Genet* 2008; **40**:
1230–34.
- 26 Ramachandran N, Colman RF. Chemical characterization of distinct subunits of pig heart DPN-
specific isocitrate dehydrogenase. *J Biol Chem* 1980; **255**: 8859–64.
- 27 Bolduc JM, Dyer DH, Scott WG, et al. Mutagenesis and Laue structures of enzyme intermediates:
isocitrate dehydrogenase. *Science* 1995; **268**: 1312–18.
- 28 Villafranca JJ, Colman RF. Role of metal ions in reactions catalyzed by pig heart triphosphopyridine
nucleotide-dependent isocitrate dehydrogenase. I. Magnetic resonance and binding studies of the
complexes of enzyme, manganous ion, and substrates. *J Biol Chem* 1972; **247**: 209–14.
- 29 Colman RF. Role of metal ions in reactions catalyzed by pig heart triphosphopyridine nucleotide-
dependent isocitrate dehydrogenase. II. Effect on catalytic properties and reactivity of amino acid
residues. *J Biol Chem* 1972; **247**: 215–23.
- 30 Bailey JM, Colman RF. Distances among coenzyme and metal sites of NADP+-dependent isocitrate
dehydrogenase using resonance energy transfer. *Biochemistry* 1987; **26**: 4893–900.
- 31 Northrop DB, Cleland WW. The kinetics of pig heart triphosphopyridine nucleotideisocitrate
dehydrogenase. II. Deadend and multiple inhibition studies. *J Biol Chem* 1974; **249**: 2928–31.
- 32 Carlier MF, Pantaloni D. Slow association-dissociation equilibrium of NADP-linked isocitrate
dehydrogenase from beef liver in relation to catalytic activity. *Eur J Biochem* 1978; **89**: 511–16.
- 33 Kelly JH, Plaut GW. Kinetic evidence for the dimerization of the triphosphopyridine nucleotide-
dependent isocitrate dehydrogenase from pig heart. *J Biol Chem* 1981; **256**: 335–42.
- 34 Kelly JH, Plaut GW. Physical evidence for the dimerization of the triphosphopyridinespecific
isocitrate dehydrogenase from pig heart. *J Biol Chem* 1981; **256**: 330–34.
- 35 Parkin DM, Bray F, Ferlay J, Pisani P. Global cancer statistics, 2002. *CA Cancer J Clin* 2005; **55**: 74–
108.
- 36 Ohgaki H, Kleihues P. Epidemiology and etiology of gliomas. *Acta Neuropathol.* 2005; **109**: 93–108.
- 37 Louis DN, Ohgaki H, Wiestler OD, Cavenee WK. World Health Organization Classification of
Tumours of the Nervous System: IARC; 2007.
- 38 Ohgaki H, Kleihues P. Genetic pathways to primary and secondary glioblastoma. *Am J Pathol* 2007;
170: 1445–53.
- 39 Collins VP. Brain tumours: classification and genes. *J Neurol Neurosurg Psychiatry* 2004; **75** (suppl
2): 2–11.
- 40 Ohgaki H, Kleihues P. Genetic alterations and signaling pathways in the evolution of gliomas.
Cancer Sci 2009; **100**: 2235–41
- 41 Gravendeel AM, Kloosterhof NK, Bralten LB, et al. Segregation of non-R132H mutations in IDH1
into distinct molecular subtypes of glioma. *Hum Mutat* 2009; **31**:1186–99.
- 42 Korshunov A, Meyer J, Capper D, et al. Combined molecular analysis of BRAF and IDH1
distinguishes pilocytic astrocytoma from diffuse astrocytoma. *Acta Neuropathol* 2009; **118**: 401–
05.
- 43 Sjoblom T, Jones S, Wood LD, et al. The consensus coding sequences of human breast and
colorectal cancers. *Science* 2006; **314**: 268–74.
- 44 Kros JM, Gorlia T, Kouwenhoven MC, et al. Panel review of anaplastic oligodendroglioma from
European Organization For Research and Treatment of Cancer Trial 26951: assessment of
consensus in diagnosis, influence of 1p/19q loss, and correlations with outcome. *J Neuropathol Exp
Neurol* 2007; **6**: 545–51.
- 45 Kato Y, Jin G, Kuan CT, McLendon RE, Yan H, Bigner DD. A monoclonal antibody IMab-1 specifically
recognizes IDH1(R132H), the most common glioma-derived mutation. *Biochem Biophys Res
Commun* 2009; **390**: 547–51.
- 46 Meyer J, Pusch S, Bals J, et al. PCR- and Restriction Endonuclease-Based Detection of IDH1
Mutations. *Brain Pathol* 2010; **20**: 298–300.
- 47 Greenman C, Stephens P, Smith R, et al. Patterns of somatic mutation in human cancer genomes.
Nature 2007; **446**: 153–58.

- 48 Yazici N, Sarialioglu F, Alkan O, Kayaselcuk F, Erol I. L-2-hydroxyglutaric aciduria and brain tumors: a case report and review of the literature. *J Pediatr Hematol Oncol* 2009; **31**: 865–69.
- 49 Aghili M, Zahedi F, Rafiee E. Hydroxyglutaric aciduria and malignant brain tumor: a case report and literature review. *J Neurooncol* 2009; **91**: 233–36.
- 50 Ceccarelli C, Grodsky NB, Ariyaratne N, Colman RF, Bahnson BJ. Crystal structure of porcine mitochondrial NADP⁺-dependent isocitrate dehydrogenase complexed with Mn²⁺ and isocitrate. Insights into the enzyme mechanism. *J Biol Chem* 2002; **277**: 43454–62.
- 51 Jennings GT, Minard KI, McAlister-Henn L. Expression and mutagenesis of mammalian cytosolic NADP⁺-specific isocitrate dehydrogenase. *Biochemistry* 1997; **36**: 13743–47.
- 52 Soundar S, Danek BL, Colman RF. Identification by mutagenesis of arginines in the substrate binding site of the porcine NADP-dependent isocitrate dehydrogenase. *J Biol Chem* 2000; **275**: 5606–12.
- 53 Watanabe T, Vital A, Nobusawa S, Kleihues P, Ohgaki H. Selective acquisition of IDH1 R132C mutations in astrocytomas associated with Li-Fraumeni syndrome. *Acta Neuropathol* 2009; **117**: 653–56.
- 54 Yan H, Parsons DW, Jin G, et al. IDH1 and IDH2 mutations play a fundamental role in glioma development. *Neuro Oncol* 2009; **11**: 608.
- 55 Huang YC, Colman RF. Evaluation by mutagenesis of the roles of His309, His315, and His319 in the coenzyme site of pig heart NADP-dependent isocitrate dehydrogenase. *Biochemistry* 2002; **41**: 5637–43.
- 56 Huang YC, Grodsky NB, Kim TK, Colman RF. Ligands of the Mn²⁺ bound to porcine mitochondrial NADP-dependent isocitrate dehydrogenase, as assessed by mutagenesis. *Biochemistry* 2004; **43**: 2821–28.
- 57 Lee P, Colman RF. Implication by site-directed mutagenesis of Arg314 and Tyr316 in the coenzyme site of pig mitochondrial NADP-dependent isocitrate dehydrogenase. *Arch Biochem Biophys* 2002; **401**: 81–90.
- 58 Kim TK, Colman RF. Ser95, Asn97, and Thr78 are important for the catalytic function of porcine NADP-dependent isocitrate dehydrogenase. *Protein Sci* 2005; **14**: 140–47.
- 59 Weinberg RA. The biology of cancer. New York: Garland Science; 2007.
- 60 Samuels Y, Wang Z, Bardelli A, et al. High frequency of mutations of the PIK3CA gene in human cancers. *Science* 2004; **304**: 554.
- 61 Doyle SA, Beernink PT, Koshland DE Jr. Structural basis for a change in substrate specificity: crystal structure of S113E isocitrate dehydrogenase in a complex with isopropylmalate, Mg²⁺, and NADP. *Biochemistry* 2001; **40**: 4234–41.
- 62 Doyle SA, Fung SY, Koshland DE Jr. Redesigning the substrate specificity of an enzyme: isocitrate dehydrogenase. *Biochemistry* 2000; **39**: 14348–55.
- 63 Van Schaftingen E, Rzem R, Veiga-da-Cunha M. L: -2-Hydroxyglutaric aciduria, a disorder of metabolite repair. *J Inherit Metab Dis* 2009; **32**: 135–42.
- 64 Kolker S, Pawlak V, Ahlemeyer B, et al. NMDA receptor activation and respiratory chain complex V inhibition contribute to neurodegeneration in d-2-hydroxyglutaric aciduria. *Eur J Neurosci* 2002; **16**: 21–28.
- 65 Frezza C, Gottlieb E. Mitochondria in cancer: not just innocent bystanders. *Semin Cancer Biol* 2009; **19**: 4–11.
- 66 van Nederveen FH, Gaal J, Favier J, et al. An immunohistochemical procedure to detect patients with paraganglioma and pheochromocytoma with germline SDHB, SDHC, or SDHD gene mutations: a retrospective and prospective analysis. *Lancet Oncol* 2009; **10**: 764–71.
- 67 Merritt TJ, Kuczynski C, Sezgin E, Zhu CT, Kumagai S, Eanes WF. Quantifying interactions within the NADP(H) enzyme network in *Drosophila melanogaster*. *Genetics* 2009; **182**: 565–74.
- 68 Shechter I, Dai P, Huo L, Guan G. IDH1 gene transcription is sterol regulated and activated by SREBP-1a and SREBP-2 in human hepatoma HepG2 cells: evidence that IDH1 may regulate lipogenesis in hepatic cells. *J Lipid Res* 2003; **44**: 2169–80.
- 69 Koh HJ, Lee SM, Son BG, et al. Cytosolic NADP⁺-dependent isocitrate dehydrogenase plays a key role in lipid metabolism. *J Biol Chem* 2004; **279**: 39968–74.
- 70 Geer BW, Lindel DL, Lindel DM. Relationship of the oxidative pentose shunt pathway to lipid synthesis in *Drosophila melanogaster*. *Biochem Genet* 1979; **17**: 881–95.
- 71 Ronnebaum SM, Ilkayeva O, Burgess SC, et al. A pyruvate cycling pathway involving cytosolic NADP-dependent isocitrate dehydrogenase regulates glucose-stimulated insulin secretion. *J Biol*

- Chem* 2006; **281**: 30593–602.
- 72 Thompson CB. Metabolic enzymes as oncogenes or tumor suppressors. *N Engl J Med* 2009; **360**:
813–15.
- 73 Kim J, Kim KY, Jang HS, et al. Role of cytosolic NADP⁺-dependent isocitrate dehydrogenase in
ischemia-reperfusion injury in mouse kidney. *Am J Physiol Renal Physiol* 2009; **296**: 622–33.
- 74 Kil IS, Kim SY, Lee SJ, Park JW. Small interfering RNA-mediated silencing of mitochondrial NADP⁺-
dependent isocitrate dehydrogenase enhances the sensitivity of HeLa cells toward tumor necrosis
factor- α and anticancer drugs. *Free Radic Biol Med* 2007; **43**: 1197–207. 45
- 75 Yang ES, Park JW. Regulation of ethanol-induced toxicity by mitochondrial NADP(+) dependent
isocitrate dehydrogenase. *Biochimie* 2009; **91**: 1020–28.
- 76 Lee JH, Kim SY, Kil IS, Park JW. Regulation of ionizing radiation-induced apoptosis by mitochondrial
NADP⁺-dependent isocitrate dehydrogenase. *J Biol Chem* 2007; **282**:13385–94.
- 77 Hunter C, Smith R, Cahill DP, et al. A hypermutation phenotype and somatic MSH6 mutations in
recurrent human malignant gliomas after alkylator chemotherapy. *Cancer Res* 2006; **66**: 3987–91.
- 78 Cammack KM, Antoniou E, Hearne L, Lamberson WR. Testicular gene expression in male mice
divergent for fertility after heat stress. *Theriogenology* 2009; **71**: 651–61.
- 79 Kim N, Park WY, Kim JM, et al. Gene expression of AGS cells stimulated with released proteins by
Helicobacter pylori. *J Gastroenterol Hepatol* 2008; **23**: 643–51.
- 80 Baumann F, Leukel P, Doerfelt A, et al. Lactate promotes glioma migration by TGF β 2-dependent
regulation of matrix metalloproteinase-2. *Neuro Oncol* 2009; **11**:368–80.
- 81 Semenza GL. HIF-1 and human disease: one highly involved factor. *Genes Dev* 2000;**14**:1983–91.
- 82 Schlisio S. Neuronal apoptosis by prolyl hydroxylation: implication in nervous system tumors and
the warburg conundrum. *J Cell Mol Med* 2009; **13**: 4104–12.
- 83 Matsumoto K, Obara N, Ema M, et al. Antitumor effects of 2-oxoglutarate through inhibition of
angiogenesis in a murine tumor model. *Cancer Sci* 2009; **100**: 1639–47.
- 84 Lee S, Nakamura E, Yang H, et al. Neuronal apoptosis linked to EglN3 prolyl hydroxylase and
familial pheochromocytoma genes: developmental culling and cancer. *Cancer Cell* 2005; **8**: 155–67.

Chapter Three

Segregation of non-p.R132H mutations in *IDH1* in distinct molecular subtypes of glioma

Nanne K. Kloosterhof, Lonneke A.M. Gravendeel, Linda B.C. Bralten¹, Ronald van Marion, Hendrikus Jan Dubbink, Winand Dinjens, Fonne E. Bleeker, Casper C. Hoogenraad, Erna Michiels, Johan M. Kros, Martin J. van den Bent, Peter A.E. Sillevs Smitt and Pim J. French

Human Mut. 2010 Mar;31(3):E1186-99

Abstract

Mutations in the gene encoding the isocitrate dehydrogenase 1 gene (*IDH1*) occur at a high frequency (up to 80%) in many different subtypes of glioma. In this study, we have screened for *IDH1* mutations in a cohort of 496 gliomas. *IDH1* mutations were most frequently observed in low grade gliomas with c.395G>A (p.R132H) representing >90% of all *IDH1* mutations. Interestingly, non-p.R132H mutations segregate in distinct histological and molecular subtypes of glioma. Histologically, they occur sporadically in classic oligodendrogliomas and at significantly higher frequency in other grade II and III gliomas. Genetically, non-p.R132H mutations occur in tumors with *TP53* mutation, are virtually absent in tumors with loss of heterozygosity on 1p and 19q and accumulate in distinct (gene-expression profiling based) intrinsic molecular subtypes. The *IDH1* mutation type does not affect patient survival. Our results were validated on an independent sample cohort, indicating that the *IDH1* mutation spectrum may aid glioma subtype classification. Functional differences between p.R132H and non-p.R132H mutated *IDH1* may explain the segregation in distinct glioma subtypes.

Introduction

The most common type of primary brain tumor (~40%) are gliomas. Based on their histological appearance, gliomas can be divided into three distinct types of tumors according to the standard WHO classification (Kleihues and Cavenee 2000): Astrocytic tumors (75%), pure oligodendroglial tumors (ODs) and mixed oligoastrocytic tumors (MOAs) (25%). Tumors are further classified into grades II, III (anaplastic) and IV (Glioblastomas, GBMs) depending on the number of malignant features present. Despite advances in neurosurgery, chemotherapy and radiotherapy the prognosis for most glioma patients remains dismal (Stupp et al., 2005).

Recently, a genetic screen identified somatic mutations in the isocitrate dehydrogenase 1 gene (*IDH1*; MIM# 147700) in glioblastomas (Parsons et al., 2008). *IDH1* catalyzes the oxidative decarboxylation of isocitrate to α -ketoglutarate and uses NADP(+) as the electron acceptor (Geisbrecht and Gould 1999; Margittai and Banhegyi 2008). Additional analysis showed that *IDH1* mutations occur at a very high frequency (up to 80%) in all grade II and III gliomas (astrocytic, oligodendrocytic and oligoastrocytic) and secondary GBMs (Balss et al., 2008; Parsons, et al., 2008; Yan et al., 2009; Dubbink et al., 2009; Watanabe et al., 2009a; Ichimura et al., 2009; Sanson et al., 2009; Sonoda et al., 2009). *IDH1* mutations do not occur at significant frequencies in other tumor types, with the notable exception of acute myeloid leukemia (AML) (Bleeker et al., 2009; Yan, et al., 2009; Mardis et al., 2009). The reported mutations in *IDH1* all result in a reduced enzymatic activity towards its native substrate, isocitrate (Yan, et al., 2009; Ichimura, et al., 2009; Zhao et al., 2009).

Mutations in the *IDH1* gene are heterozygous and virtually always affect only a single residue (arginine 132) which is replaced by a histidine in approximately 90% of tumors (c.395G>A resulting in p.R132H (Balss, et al., 2008; Ichimura, et al., 2009; Yan, et al., 2009; Sanson, et al., 2009). However, non-p.R132H mutations in the *IDH1* gene (e.g. p.R132C) have been reported to accumulate at higher frequencies in histological subtypes of glioma (Hartmann et al., 2009), in astrocytomas of Li-Fraumeni patients (Watanabe et al., 2009b) and in patients with AML (Mardis, et al., 2009). Distinct mutations within the

same gene but affecting the same codon therefore appear to segregate in distinct tumor subtypes.

In this study, we demonstrate that non-p.R132H mutations specifically accumulate in distinct histological subtypes of glioma. Because histological classification of gliomas is subject to significant interobserver variability (Kros et al., 2007), we also used molecular markers (TP53; MIM# 191170), 1p/19q LOH and intrinsic molecular subtypes) to identify the glioma subtypes. Our results demonstrate that non-p.R132H mutations indeed segregate in distinct histological, genetic and molecular subtypes of gliomas.

Materials and methods

Samples

Glioma samples were collected from five hospitals in the Netherlands (Erasmus MC, Rotterdam; UMCU, Utrecht; NCI and VUMC, Amsterdam; RUNMC, Nijmegen) from patients, operated from 1989-2009. Use of patient material was approved by the Institutional Review Board. All samples are listed in Supp. Table S1. Histological diagnoses were made on formalin-fixed, paraffin-embedded Haematoxylin & Eosin sections and were reviewed by the neuropathologist (J.M.K.). Genomic DNA from snap frozen or formalin fixed, paraffin embedded tissue samples was isolated as described (Gravendeel et al., 2009; Dubbink, et al., 2009). Of the 496 glioma samples reported in this study, 247 were derived from a series of gliomas of all histologies (set A) (Gravendeel, et al., 2009), 54 from a series of low grade astrocytomas (set B) (Dubbink, et al., 2009), 24 were derived from samples operated in Rotterdam that were included in EORTC 26951 (set C) (van den Bent et al., 2006) and 171 novel glioma samples (set D). The IDH1 status of 297 samples was described previously (Gravendeel, et al., 2009; Dubbink, et al., 2009). IDH1 (NM_005896.2, GI:28178824) mutational status of the remaining 199 samples was determined as described (Bleeker, et al., 2009), see also Supp. Table S2.

1p/19q status was determined in 317 samples. 1p19q LOH was determined by fluorescent in-situ hybridization (FISH) (Kouwenhoven et al., 2006), inferred from genotyping arrays or by microsatellite analysis. Microsatellites were amplified by PCR on 20 nanogram genomic DNA, using a fluorescently labeled forward primer and a reversed primer. Allelic losses were statistically determined as described and scored by two independent researchers (French et al., 2005). TP53 (NM_000546.4, GI:187830767) status was determined in 169 samples. Primers and cycling conditions to determine the TP53 mutation status are stated in the Supp. Table S2.

Statistical analysis

Comparison between frequencies of different groups was assessed using the Fisher exact test. The significance of IDH1 mutation type was assessed by univariate and multivariate analysis using Cox Regression. Differences between Kaplan-Meier survival curves were calculated by the Log-rank (Mantel-Cox) test. Survival time was defined as the period from date of surgery to date of death. If date of death was not available, date of last follow-up was used.

Results and discussion

Dataset

We have screened for mutations in IDH1 in a large cohort of 496 glioma samples. In this dataset, a total of 246 mutations in the IDH1 gene were identified (49.6%). The IDH1 mutation frequency for all grades II and III gliomas was high and ranged from 49% in anaplastic oligoastrocytic tumors to 79% in low grade oligodendrogliomas (Table 1). The frequency of genetic changes in our sample cohort is similar to reported by others (Balss, et al., 2008; Ichimura, et al., 2009; Yan, et al., 2009; Hartmann, et al., 2009; Sonoda, et al., 2009). The frequency of IDH1 mutations in grade II gliomas (76%, n=110/144) was higher than in grade III tumors (58%, n=102/177, P<0.001) (see also (Sanson, et al., 2009)). More specifically, low grade oligodendrogliomas (79%, n=34/43) and oligoastrocytomas (79%, n=22/28) have a higher IDH1 mutation frequency than their corresponding grade III tumors (60%, n=64/106 and 49%, n=19/39 respectively P<0.05). A similar difference in frequency can also be extracted from at least two external sample cohorts (Hartmann, et al., 2009; Watanabe, et al., 2009a).

The observation of a higher mutation incidence in lower grade tumors has thus far been described for only a few genes (see e.g. (Knowles 2007)). This differential frequency indicates that low grade tumors can accumulate distinct genetic changes and thus represent a different disease entity. Moreover, such differential frequency indicates that the IDH1 mutation status can, at least to some extent, serve as a marker for low grade gliomas (see also Jones et al., 2008; Korshunov et al., 2009).

Table 1. The frequency of IDH1 (NM_005896.2, GI:28178824) mutations, LOH on 1p and 19q and mutations in TP53 (NM_000564.4, 187830767) in different histological.

	n	p.R132H	p.R132X	IDH1	1p/19q	no loss	nd	TP53	TP53	nd
ODII	43	34	0	9	21	9	13	0	6	37
ODIII	106	63	1	42	57	31	18	7	18	81
OAI	28	21	1	6	6	10	12	1	3	24
OAI	39	15	4	20	3	23	13	8	2	29
AII	73	48	6	19	2	53	18	29	18	26
AIII	32	15	4	13	1	18	13	12	6	14
GBM	175	31	3	141	10	73	92	27	32	116
total	496	227	19	250	100	0	179	84	85	0

ODII/ODIII: grade II/III oligodendroglioma, OAI/OAI: grade II/III oligoastrocytoma, AII/AIII: grade II/III astrocytoma, GBM: glioblastoma. nd: not determined.

Non-p.R132H mutations in IDH1 segregate in distinct glioma subtypes

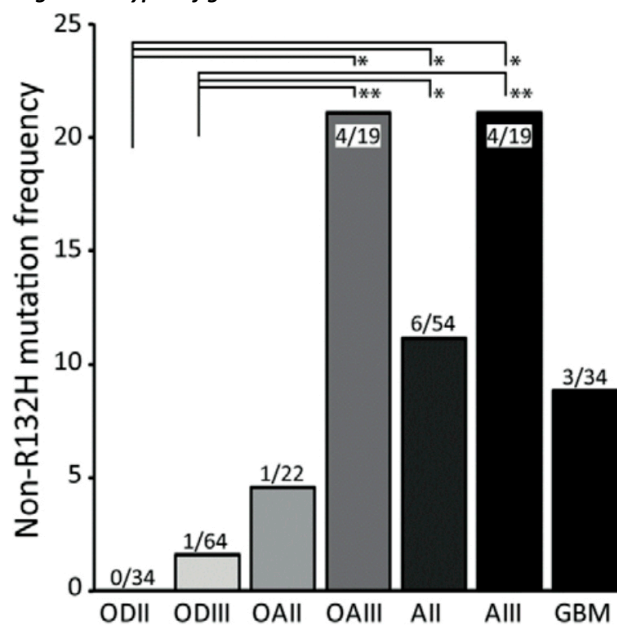
The majority of mutations (92.3%) in the IDH1 gene were heterozygous c.395G>A missense mutations that result in an arginine to histidine substitution on position 132 (p.R132H). However, 19/246 mutations (7.7%) were non-p.R132H mutations: Single nucleotide changes that result in different amino acid substitutions albeit on the same position. Similar to reported, c.394C>T (p.R132C) was the second most common mutation type in our sample cohort and was identified in nine gliomas. Other non-p.R132H mutations were p.R132S (n=5), p.R132G (n=3), p.R132L (n=1) and p.R132P (n=1).

When focusing on non-p.R132H IDH1 mutations in our dataset, we observed that in classical oligodendrogliomas (combined grades II and III), only one out of the total of 98 IDH1 mutations (1.0%) was non-p.R132H (Figure 1). A significantly larger proportion of non-p.R132H mutations was present in oligoastrocytic tumors (5/41, P<0.01) and in

astrocytic tumors (10/73, $P < 0.001$). Significance remained within the different tumor grades (Figure 1). These results indicate that, although non-p.R132H mutations are rare, they are not uniformly distributed across the different histological subtypes of glioma.

We aimed to confirm the differential distribution of non-p.R132H mutations using objective molecular markers. We first screened for combined LOH on 1p and 19q; chromosomal losses that are frequently observed in oligodendrogliomas and relatively rare in astrocytic tumors (Ohgaki and Kleihues 2009; Bromberg and van den Bent 2009)). These losses are caused by an unbalanced translocation between chromosomes 1 and 19 [t(1;19)(q10,p10)] (Griffin et al., 2006; Jenkins et al., 2006). In our entire dataset, 1p/19q LOH was determined in 317 (63.9%) samples. Of the tumors with combined 1p/19q LOH ($n=100$), a mutation in the IDH1 gene was detected in 75 samples (75%). In these 75 samples, only one non-p.R132H mutation was identified (1.3%, Figure 2). Conversely, in tumors that have retained 1p and/or 19q ($n=217$), the proportion of non-p.R132H mutations was significantly higher, 13/106 (12.3%, $P < 0.01$). Non-p.R132H mutations therefore segregate in tumors that do not show combined 1p/19q LOH.

Figure 1: Distribution of non-p.R132H mutations in IDH1 in different histological subtypes of glioma.



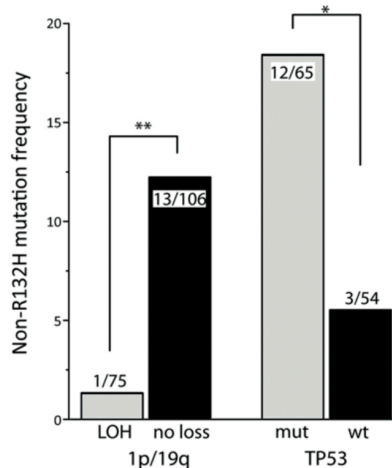
Plotted is the relative frequency of non-p.R132H mutations in IDH1 mutated histological subtypes of glioma. Absolute numbers for each subtype is stated in/above individual bars. For example, IDH1 mutations are observed in 54 grade II astrocytomas. Of these, six are non-p.R132H. As can be seen, non-p.R132H mutations are sporadically observed in oligodendrogliomas and more frequent in oligoastrocytomas and astrocytomas. *: $P < 0.05$, **: $P < 0.01$, Fishers' exact test.

We then correlated the type of IDH1 mutation to the TP53 mutation status. TP53 mutations are frequently observed in astrocytomas and secondary glioblastomas but relatively rare in oligodendrogliomas and primary glioblastomas (Collins 2004; Ohgaki and Kleihues 2009). In our entire dataset, TP53 mutation status was determined in 169 samples (34.1 %). Of the tumors with a mutation in TP53 ($n=84$), a mutation in the IDH1 gene was detected in 65 samples (77.4%). Non-p.R132H mutations were identified in 12 of these 65 samples (17.9%, Figure 2). Conversely, in tumors with wt TP53 ($n=85$), the proportion of non-p.R132H mutations was significantly lower (3/54) (5.6%, $P < 0.05$). Non-p.R132H mutations therefore accumulate in tumors with a mutation in the TP53 gene.

Finally, we determined whether non-p.R132H mutations segregate in intrinsic, gene expression based-, molecular subtypes of glioma. In a recent study, we identified seven intrinsic glioma subtypes based on gene expression profiles of 276 gliomas of all histological subtypes and grades (Gravendeel, et al., 2009). As reported, IDH1 mutations

were most frequently observed in clusters 9 and 17 (27/40 and 22/32 respectively). When focusing on the non-p.R132H mutations (n=8) in this cohort, they were relatively rare in cluster 9 (n=1/27, 3.7%) and more frequent in cluster 17 (5/22, 22.7%, P=0.05). Other non-R132 samples were identified in clusters that have relatively few IDH1 mutations; one in cluster 0 and one in cluster 18 (Gravendeel, et al., 2009). Non-p.R132H mutations therefore appear not to be uniformly distributed across intrinsic molecular subtypes of glioma.

Figure 2: The frequency of non-p.R132H mutations in IDH1 is correlated to distinct genetic changes in gliomas.



Non-p.R132H mutations are more prevalent in gliomas that do not show combined LOH on 1p and 19q (left) and in gliomas with a TP53 mutation (right). Absolute numbers for non-p.R132H mutations/total number of IDH1 mutations are stated in/above the individual bars. *: P<0.05, **: P<0.01, Fishers' exact test.

Validation of non-p.R132H segregation

The segregation of non-p.R132H mutations into distinct

molecular subtypes of gliomas was validated on a recently described independent cohort of glioma samples (Ichimura, et al., 2009). In this study, a total of 119 mutations in IDH1 were identified across various histological subtypes, nine of which were non-p.R132H. Non-p.R132H mutations are clearly more prevalent in IDH1 mutated astrocytomas (7/45) compared to IDH1 mutated oligodendrogliomas (0/35, P<0.05). Furthermore, a significantly higher proportion of non-p.R132H mutations was observed in tumors with both IDH1 and TP53 mutation (8/65) compared to tumors with wt TP53 (1/52, P<0.05). Finally, all non-p.R132H mutations were identified in tumors that have retained 1p and 19q (9/74 vs. 0/45, P<0.05). In summary, non-p.R132H mutations are more prevalent in IDH1 mutated astrocytomas, gliomas with TP53 mutation and gliomas that have retained 1p and 19q in this external dataset. These data therefore confirm our hypothesis that

non-p.R132H mutations in IDH1 are more prevalent in distinct subtypes of gliomas.

There are two possible explanations for the differential distribution of non-p.R132H mutations in glioma subtypes. First, it is possible that (epi)genetic differences between tumor types (e.g. differences in DNA repair due to e.g. MGMT (MIM# 156569) promoter methylation) result in the preferential accumulation of distinct mutations (see e.g. (Greenman et al., 2007)). For example, MGMT promoter methylation is associated with transition type mutations in TP53 in colorectal cancer and in gliomas (Esteller et al., 2001; Nakamura et al., 2001). Indeed, a higher percentage of oligodendroglial tumors show MGMT promoter hypermethylation compared to astrocytic tumors (Wick et al., 2009; Jeuken et al., 2007; Yang et al., 2009). Differences in the MGMT promoter methylation status between glioma subtypes may therefore explain the differential distribution of non-p.R132H mutations in IDH1. However, the transition/transversion ratio in IDH1 (i.e. p.R132H,C/p.R132S,G,L,P) between GBMs, astrocytic tumors (AII/III), oligoastrocytic tumors (OAI/III) or oligodendrocytic tumors (ODII/III) is similar (2/32, 5/68, 2/39 and 1/97 respectively). We also failed to observe a difference in transition/transversion ratio in the

TP53 gene in the respective histological subgroups (14/12, 26/13, 8/1 and 5/2). The transition/transversion ratio in the TP53 gene between R132H and non-R132H mutated samples is also similar (39/15 and 8/3 respectively). Any possible difference in DNA repair between tumor types therefore is not reflected by a difference in the type of mutations acquired.

A second tentative possibility is that different mutations have different functional properties. For example, non-p.R132H mutations may show some residual activity towards isocitrate either in cis (activity of the mutated enzyme itself) or in trans (by influencing the activity of the remaining wt enzyme (Zhao, et al., 2009)). Alternatively, a recent study described that mutated IDH1 is able to convert α -ketoglutarate into 2-hydroxyglutarate (Dang et al., 2009). Interestingly, different IDH1 mutation types showed a differential activity towards α -ketoglutarate. Whether this differential activity can explain the differential distribution of specific types of IDH1 mutations requires further detailed analysis.

References

- Balss J, Meyer J, Mueller W, Korshunov A, Hartmann C, von Deimling A. 2008. Analysis of the IDH1 codon 132 mutation in brain tumors. *Acta Neuropathol* 116(6):597-602.
- Bleeker FE, Lamba S, Leenstra S, Troost D, Hulsebos T, Vandertop WP, Frattini M, Molinari F, Knowles M, Cerrato A, Rodolfo M, Scarpa A, Felicioni L, Buttitta F, Malatesta S, Marchetti A, Bardelli A. 2009. IDH1 mutations at residue p.R132 (IDH1(R132)) occur frequently in high-grade gliomas but not in other solid tumors. *Hum Mutat* 30(1):7-11.
- Bromberg JE, van den Bent MJ. 2009. Oligodendrogliomas: molecular biology and treatment. *Oncologist* 14(2):155-63.
- Collins VP. 2004. Brain tumours: classification and genes. *J Neurol Neurosurg Psychiatry* 75 Suppl 2:ii2-11.
- Dang L, White DW, Gross S, Bennett BD, Bittinger MA, Driggers EM, Fantin VR, Jang HG, Jin S, Keenan MC, Marks KM, Prins RM, Ward PS, Yen KE, Liao LM, Rabinowitz JD, Cantley LC, Thompson CB, Vander Heiden MG, Su SM. 2009. Cancer-associated IDH1 mutations produce 2-hydroxyglutarate. *Nature*.
- Dubbink HJ, Taal W, van Marion R, M. KJ, van Heuvel I, Bromberg JE, Zonnenberg BA, Zonnenberg CBL, Postma TJ, Gijtenbeek JMM, Boogerd W, Groenendijk FH, Sillevs Smitt PA, Dinjens W, van den Bent MJ. 2009. IDH1 mutations in astrocytomas predict survival but not response to temozolomide. *Neurology* in press.
- Esteller M, Risques RA, Toyota M, Capella G, Moreno V, Peinado MA, Baylin SB, Herman JG. 2001. Promoter hypermethylation of the DNA repair gene O(6)-methylguanine-DNA methyltransferase is associated with the presence of G:C to A:T transition mutations in p53 in human colorectal tumorigenesis. *Cancer Res* 61(12):4689-92.
- French PJ, Swagemakers SMA, Nagel JHA, Kouwenhoven MCM, Brouwer E, van der Spek P, Luider TM, Kros JM, van den Bent MJ, Sillevs Smitt PA. 2005. Gene expression profiles associated with treatment response in oligodendrogliomas. *Cancer Res* 65(24):11335-44.
- Geisbrecht BV, Gould SJ. 1999. The human PICD gene encodes a cytoplasmic and peroxisomal NADP(+)-dependent isocitrate dehydrogenase. *J Biol Chem* 274(43):30527-33.
- Gravendeel LA, Kouwenhoven MC, Gevaert O, de Rooij JJ, Stubbs AP, Duijm JE, Daemen A, Bleeker FE, Bralten LB, Kloosterhof NK, De Moor B, Eilers PH, van der Spek PJ, Kros JM, Sillevs Smitt PA, van den Bent MJ, French PJ. 2009. Intrinsic gene expression profiles of gliomas are a better predictor of survival than histology. *Cancer Res* 69(23):9065-72.
- Greenman C, Stephens P, Smith R, Dalgliesh GL, Hunter C, Bignell G, Davies H, Teague J, Butler A, Stevens C, Edkins S, O'Meara S, Vastrik I, Schmidt EE, Avis T, Barthorpe S, Bhamra G, Buck G, Choudhury B, Clements J, Cole J, Dicks E, Forbes S, Gray K, Halliday K, Harrison R, Hills K, Hinton J, Jenkinson A, Jones D, Menzies A, Mironenko T, Perry J, Raine K, Richardson D, Shepherd R, Small A, Tofts C, Varian J, Webb T, West S, Widaa S, Yates A, Cahill DP, Louis DN, Goldstraw P, Nicholson AG, Brasseur F, Looijenga L, Weber BL, Chiew YE, DeFazio A, Greaves MF, Green AR, Campbell P, Birney

- E, Easton DF, Chenevix-Trench G, Tan MH, Khoo SK, Teh BT, Yuen ST, Leung SY, Wooster R, Futreal PA, Stratton MR. 2007. Patterns of somatic mutation in human cancer genomes. *Nature* 446(7132):153-8.
- Griffin CA, Burger P, Morsberger L, Yonescu R, Swierczynski S, Weingart JD, Murphy KM. 2006. Identification of del(1;19)(q10;p10) in five oligodendrogliomas suggests mechanism of concurrent 1p and 19q loss. *J Neuropathol Exp Neurol* 65(10):988-94.
- Hartmann C, Meyer J, Balss J, Capper D, Mueller W, Christians A, Felsberg J, Wolter M, Mawrin C, Wick W, Weller M, Herold-Mende C, Unterberg A, Jeuken JW, Wesseling P, Reifenberger G, von Deimling A. 2009. Type and frequency of IDH1 and IDH2 mutations are related to astrocytic and oligodendroglial differentiation and age: a study of 1,010 diffuse gliomas. *Acta Neuropathol* 118(4):469-74.
- Ichimura K, Pearson DM, Kocialkowski S, Backlund LM, Chan R, Jones DT, Collins VP. 2009. IDH1 mutations are present in the majority of common adult gliomas but are rare in primary glioblastomas. *Neuro Oncol*.
- Jenkins RB, Blair H, Ballman KV, Giannini C, Arusell RM, Law M, Flynn H, Passe S, Felten S, Brown PD, Shaw EG, Buckner JC. 2006. A t(1;19)(q10;p10) mediates the combined deletions of 1p and 19q and predicts a better prognosis of patients with oligodendroglioma. *Cancer Res* 66(20):9852-61.
- Jeuken JW, Cornelissen SJ, Vriezen M, Dekkers MM, Errami A, Sijben A, Boots-Sprenger SH, Wesseling P. 2007. MS-MLPA: an attractive alternative laboratory assay for robust, reliable, and semiquantitative detection of MGMT promoter hypermethylation in gliomas. *Lab Invest* 87(10):1055-65.
- Jones DT, Kocialkowski S, Liu L, Pearson DM, Backlund LM, Ichimura K, Collins VP. 2008. Tandem duplication producing a novel oncogenic BRAF fusion gene defines the majority of pilocytic astrocytomas. *Cancer Res* 68(21):8673-7.
- Kang MR, Kim MS, Oh JE, Kim YR, Song SY, Seo SI, Lee JY, Yoo NJ, Lee SH. 2009. Mutational analysis of IDH1 codon 132 in glioblastomas and other common cancers. *Int J Cancer* 125(2):353-5.
- Kleihues P, Cavenee WK. 2000. World Health Organization Classification of Tumours of the Nervous System. Lyon: WHO/IARC.
- Knowles MA. 2007. Role of FGFR3 in urothelial cell carcinoma: biomarker and potential therapeutic target. *World J Urol* 25(6):581-93.
- Korshunov A, Meyer J, Capper D, Christians A, Remke M, Witt H, Pfister S, von Deimling A, Hartmann C. 2009. Combined molecular analysis of BRAF and IDH1 distinguishes pilocytic astrocytoma from diffuse astrocytoma. *Acta Neuropathol* 118(3):401-5.
- Kouwenhoven MC, Kros JM, French PJ, Biemond-ter Stege EM, Graveland WJ, Taphoorn MJ, Brandes AA, van den Bent MJ. 2006. 1p/19q loss within oligodendroglioma is predictive for response to first line temozolomide but not to salvage treatment. *Eur J Cancer* 42(15):2499-503.
- Kros JM, Gorlia T, Kouwenhoven MC, Zheng PP, Collins VP, Figarella-Branger D, Giangaspero F, Giannini C, Mokhtari K, Mork SJ, Paetau A, Reifenberger G, van den Bent MJ. 2007. Panel review of anaplastic oligodendroglioma from European Organization For Research and Treatment of Cancer Trial 26951: assessment of consensus in diagnosis, influence of 1p/19q loss, and correlations with outcome. *J Neuropathol Exp Neurol* 66(6):545-51.
- Mardis ER, Ding L, Dooling DJ, Larson DE, McLellan MD, Chen K, Koboldt DC, Fulton RS, Delehaunty KD, McGrath SD, Fulton LA, Locke DP, Magrini VJ, Abbott RM, Vickery TL, Reed JS, Robinson JS, Wylie T, Smith SM, Carmichael L, Eldred JM, Harris CC, Walker J, Peck JB, Du F, Dukes AF, Sanderson GE, Brummett AM, Clark E, McMichael JF, Meyer RJ, Schindler JK, Pohl CS, Wallis JW, Shi X, Lin L, Schmidt H, Tang Y, Haipek C, Wiechert ME, Ivy JV, Kalicki J, Elliott G, Ries RE, Payton JE, Westervelt P, Tomasson MH, Watson MA, Baty J, Heath S, Shannon WD, Nagarajan R, Link DC, Walter MJ, Graubert TA, DiPersio JF, Wilson RK, Ley TJ. 2009. Recurring mutations found by sequencing an acute myeloid leukemia genome. *N Engl J Med* 361(11):1058-66.
- Margittai E, Banhegyi G. 2008. Isocitrate dehydrogenase: A NADPH-generating enzyme in the lumen of the endoplasmic reticulum. *Arch Biochem Biophys* 471(2):184-90.
- Nakamura M, Watanabe T, Yonekawa Y, Kleihues P, Ohgaki H. 2001. Promoter methylation of the DNA repair gene MGMT in astrocytomas is frequently associated with G:C-> A:T mutations of the TP53 tumor suppressor gene. *Carcinogenesis* 22(10):1715-9.
- Ohgaki H, Kleihues P. 2005. Population-based studies on incidence, survival rates, and genetic alterations in astrocytic and oligodendroglial gliomas. *J Neuropathol Exp Neurol* 64(6):479-89.
- Ohgaki H, Kleihues P. 2009. Genetic alterations and signaling pathways in the evolution of gliomas. *Cancer*

Sci.

- Parkin DM, Bray F, Ferlay J, Pisani P. 2005. Global cancer statistics, 2002. *CA Cancer J Clin* 55(2):74-108.
- Parsons DW, Jones S, Zhang X, Lin JC, Leary RJ, Angenendt P, Mankoo P, Carter H, Siu IM, Gallia GL, Olivi A, McLendon R, Rasheed BA, Keir S, Nikolskaya T, Nikolsky Y, Busam DA, Tekleab H, Diaz LA, Jr., Hartigan J, Smith DR, Strausberg RL, Marie SK, Shinjo SM, Yan H, Riggins GJ, Bigner DD, Karchin R, Papadopoulos N, Parmigiani G, Vogelstein B, Velculescu VE, Kinzler KW. 2008. An integrated genomic analysis of human glioblastoma multiforme. *Science* 321(5897):1807-12.
- Sanson M, Marie Y, Paris S, Idbaih A, Laffaire J, Ducray F, El Hallani S, Boisselier B, Mokhtari K, Hoang-Xuan K, Delattre JY. 2009. Isocitrate dehydrogenase 1 codon 132 mutation is an important prognostic biomarker in gliomas. *J Clin Oncol* 27(25):4150-4.
- Sonoda Y, Kumabe T, Nakamura T, Saito R, Kanamori M, Yamashita Y, Suzuki H, Tominaga T. 2009. Analysis of IDH1 and IDH2 mutations in Japanese glioma patients. *Cancer Sci* 100(10):1996-8.
- Stupp R, Mason WP, van den Bent MJ, Weller M, Fisher B, Taphoorn MJ, Belanger K, Brandes AA, Marosi C, Bogdahn U, Curschmann J, Janzer RC, Ludwin SK, Gorlia T, Allgeier A, Lacombe D, Cairncross JG, Eisenhauer E, Mirimanoff RO. 2005. Radiotherapy plus concomitant and adjuvant temozolomide for glioblastoma. *N Engl J Med* 352(10):987-96.
- van den Bent MJ, Carpentier AF, Brandes AA, Sanson M, Taphoorn MJ, Bernsen HJ, Frenay M, Tijssen CC, Grisold W, Sipos L, Haaxma-Reiche H, Kros JM, van Kouwenhoven MC, Vecht CJ, Allgeier A, Lacombe D, Gorlia T. 2006. Adjuvant procarbazine, lomustine, and vincristine improves progression-free survival but not overall survival in newly diagnosed anaplastic oligodendrogliomas and oligoastrocytomas: a randomized European Organisation for Research and Treatment of Cancer phase III trial. *J Clin Oncol* 24(18):2715-22.
- Watanabe T, Nobusawa S, Kleihues P, Ohgaki H. 2009a. IDH1 mutations are early events in the development of astrocytomas and oligodendrogliomas. *Am J Pathol* 174(4):1149-53.
- Watanabe T, Vital A, Nobusawa S, Kleihues P, Ohgaki H. 2009b. Selective acquisition of IDH1 R132C mutations in astrocytomas associated with Li-Fraumeni syndrome. *Acta Neuropathol* 117(6):653-6.
- Wick W, Hartmann C, Engel C, Stoffels M, Felsberg J, Stockhammer F, Sabel MC, Koeppen S, Ketter R, Meyermann R, Rapp M, Meisner C, Kortmann RD, Pietsch T, Wiestler OD, Ernemann U, Bamberg M, Reifenberger G, von Deimling A, Weller M. 2009. NOA-04 Randomized Phase III Trial of Sequential Radiochemotherapy of Anaplastic Glioma With Procarbazine, Lomustine, and Vincristine or Temozolomide. *J Clin Oncol*.
- Yan H, Parsons DW, Jin G, McLendon R, Rasheed BA, Yuan W, Kos I, Batinic-Haberle I, Jones S, Riggins GJ, Friedman H, Friedman A, Reardon D, Herndon J, Kinzler KW, Velculescu VE, Vogelstein B, Bigner DD. 2009. IDH1 and IDH2 mutations in gliomas. *N Engl J Med* 360(8):765-73.
- Yang SH, Kim YH, Kim JW, Park CK, Park SH, Jung HW. 2009. Methylation Status of the O6- Methylguanine-Deoxyribonucleic Acid Methyltransferase Gene Promoter in World Health Organization Grade III Gliomas. *J Korean Neurosurg Soc* 46(4):385-8.
- Zhao S, Lin Y, Xu W, Jiang W, Zha Z, Wang P, Yu W, Li Z, Gong L, Peng Y, Ding J, Lei Q, Guan KL, Xiong Y. 2009. Glioma-derived mutations in IDH1 dominantly inhibit IDH1 catalytic activity and induce HIF-1alpha. *Science* 324(5924):261-5.

Chapter Four

IDH1 R132H Decreases Proliferation of Glioma Cell Lines In Vitro and In Vivo

Nanne K. Kloosterhof, Linda B. C. Bralten, Rutger Balvers, Andrea Sacchetti, Lariesa Lapre, Martine Lamfers, Sieger Leenstra, Hugo de Jonge, Johan M. Kros, Erwin E. W. Jansen, Eduard A. Struys, Cornelis Jakobs, Gajja S. Salomons, Sander H. Diks, Maikel Peppelenbosch, Andreas Kremer, Casper C. Hoogenraad, Peter A. E. Sillevs Smitt and Pim J. French
Ann Neurol 2011 Mar;69(3):455-463

Abstract

Objective: A high percentage of grade II and III gliomas have mutations in the gene encoding isocitrate dehydrogenase (IDH1). This mutation is always a heterozygous point mutation that affects the amino acid arginine at position 132 and results in loss of its native enzymatic activity and gain of alternative enzymatic activity (producing D-2-hydroxyglutarate). The objective of this study was to investigate the cellular effects of R132H mutations in IDH1.

Methods: Functional consequences of mutations were examined among others using Fluorescenceactivated cell sorting, kinome and expression arrays, biochemical assays, and intracranial injections on 3 different (glioma) cell lines with stable overexpression of IDH1R132H.

Results: IDH1R132H overexpression in established glioma cell lines in vitro resulted in a marked decrease in proliferation, decreased Akt phosphorylation, altered morphology, and a more contact-dependent cell migration. The reduced proliferation is related to accumulation of D-2-hydroxyglutarate that is produced by IDH1R132H. Mice injected with IDH1R132H U87 cells have prolonged survival compared to mice injected with IDH1wt or green fluorescent protein–expressing U87 cells.

Interpretation: Our results demonstrate that IDH1R132H dominantly reduces aggressiveness of established glioma cell lines in vitro and in vivo. In addition, the IDH1R132H-IDH1wt heterodimer has higher enzymatic activity than the IDH1R132H-IDH1R132H homodimer. Our observations in model systems of glioma might lead to a better understanding of the biology of IDH1 mutant gliomas, which are typically low grade and often slow growing.

Introduction

Gliomas are histologically classified into astrocytic, oligodendroglial, and oligoastrocytic tumors. They are further subdivided into low grade (grade II), ana-plastic (grade III), or glioblastoma multiforme (grade IV), depending on the presence or absence of malignant features. Mutations in the gene encoding isocitrate dehydrogenase 1 (IDH1) are very common in all grade II and III gliomas, often occurring at frequencies >70%.^{1,2} The IDH1 mutation frequency is inversely correlated to tumor grade,^{3,4} with the lowest frequency observed in glioblastoma multiformes.⁵ IDH1 mutations are always heterozygous missense mutations affecting the arginine at position 132. In >90% of the IDH1 mutations in gliomas, this arginine is replaced by a histidine (R132H mutation).^{1,6}

IDH1 mutations are an early event in tumorigenesis; they arise even before TP53 mutations or loss of 1p and 19q.7 Patients with IDH1 mutations are generally younger, and mutations are associated with prolonged survival.^{3,4,8–11} Mutations in the homologous IDH2 gene were also identified, although these occur at much lower frequencies in gliomas (0–6%).^{1,12–15} The only other tumor type in which regular IDH1 and IDH2 mutations are detected is acute myeloid leukemia (AML).¹⁶ IDH1 catalyses the oxidative decarboxylation of isocitrate into α -ketoglutarate (α KG), thereby using nicotinamide adenine dinucleotide phosphate (NADP) as an electron acceptor.¹⁷ The mutated IDH1 enzyme (R132H, IDH1R132H) shows a strongly decreased enzymatic

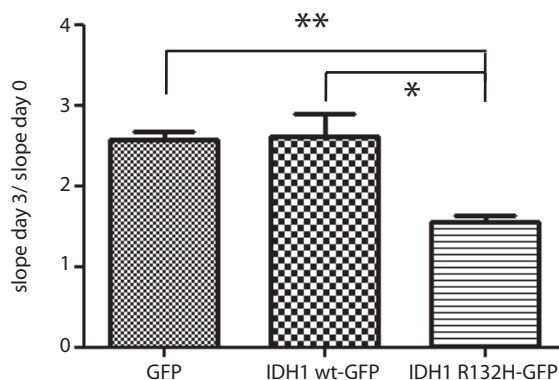
activity toward isocitrate, leading to lower aKG production, thereby increasing hypoxia inducible factor 1a levels.^{15,18,19} In addition, IDH1R132H has an altered enzymatic activity and uses aKG as a substrate to produce D-2-hydroxyglutarate (D-2HG).²⁰⁻²² Although it is clear that IDH1R132H has altered enzymatic activity, little is known about how the altered enzymatic activity contributes to tumor formation.

In this study, we have therefore studied the cellular IDH1R132H and functional effects of in vitro and in vivo. Our results show that IDH1R132H expression decreases proliferation rates and alters the morphology and migration pattern of these cells. Although the reduced aggressiveness/proliferation found in our study was identified in established cell lines that are different from the in vivo growing tumors, our results may help to understand the biology of IDH1 mutated gliomas, which are associated with improved outcome and are predominantly low grade.

Materials and Methods

IDH1 mutation analysis was performed using forward and reverse primers as described,³ and IDH1R132H IDH1wt were cloned into pEGFP-C2bio, which contains a biotin tag before the green fluorescent protein (GFP) tag. U87, U138, or HEK stable cell lines overexpressing, IDH1R132H-GFP pressing IDH1wt-GFP, or GFP were selected for using Geneticin (Gibco, Invitrogen, Breda, the Netherlands). Morphology analysis, scratch assay, WST proliferation assay,²³ fluorescence-activated cell sorting (FACS) cell cycle analysis, and Ki67 staining and apoptosis assay were performed as described in the Supporting Information Methods. Cells plated in a 6-well plate were labeled with 1mM bromodeoxyuridine

Figure 1: Glioma cells expressing mutant IDH1 show reduced proliferation in vitro.

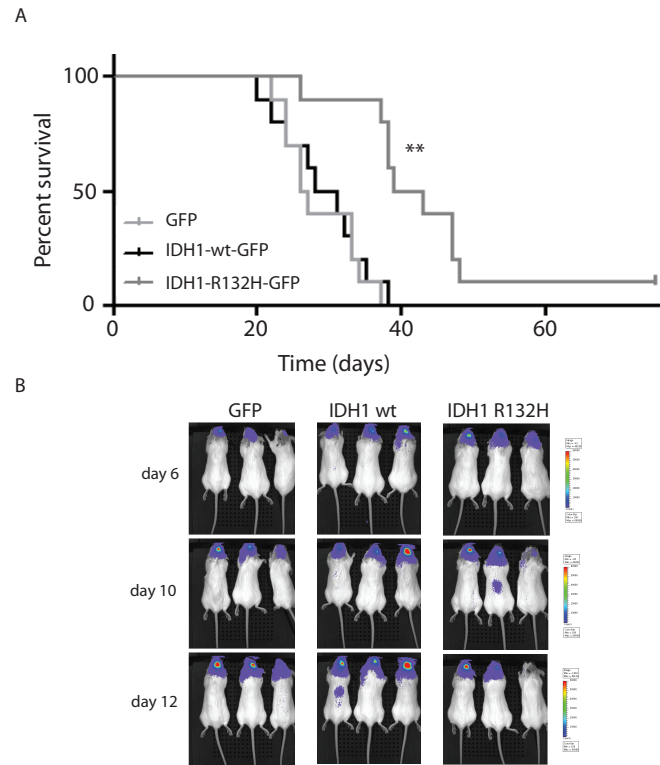


WST-1 proliferation data of stable U87 cells expressing green fluorescent protein (GFP), IDH1wt-GFP, or IDH1R132H-GFP are shown. Error bars represent the standard deviation. *p < 0.05, **p < 0.01. wt = wild type.

(BrdU) (BD Biosciences, Breda, the Netherlands) for 2 hours. Cells were fixed and stained using the BrdU In-Situ Detection kit (BD Biosciences) according to the manufacturer's instructions. Visualization of BrdU-labeled cells was performed using biotin-conjugated anti-BrdU (1:10) and allophycocyanin-conjugated streptavidin (1:400). Visualization of intracranially injected U87 cells was performed using a mouse antivimentin antibody (DAKO, Heverlee, Belgium) and Alexa568-conjugated antimouse antibody (Invitrogen) at 1:300 and 1:500 dilutions, respectively. Sections were counterstained using 4,6-diamidino-2-phenylindole (DAKO).

EGFP-C2-bio-IDH1wt or EGFP-C2-bio-IDH1R132H in combination with BirA were transiently expressed by HEK cells, and purified using Streptavidin Dynabeads M-280 (Invitrogen) and a Magna-Sep (Invitrogen). Enzyme measurements of isolated

Figure 2: Glioma cells expressing mutant IDH1 show reduced proliferation in vivo.



(
A) Survival curve of 10 mice injected with U87-IDH1wt-GFP (black line), 10 mice injected with U87-IDH1R132H-GFP (dark gray line), and 10 mice injected with U87-GFP (light gray line). The mice injected with U87-IDH1R132H-GFP have a significantly longer survival ($p < 0.01$); 1 mouse survived >75 days. (B) IVIS imaging on day 6, 10, and 12 of mice injected with U87 cells expressing GFP (left), IDH1wt-GFP (middle), and IDH1R132H-GFP (right). Notice in the right panel that the initial tumor burden in the rightmost mouse decreases. GFP = green fluorescent protein; wt = wild type. [Color figure can be viewed in the online issue, which is available at www.annalsofneurology.org.]

considered that (1) had a $>20\%$ difference in expression level in $-$ expressing cells IDH1wt-GFP compared to $-$ expressing cells (in both U87 and U138), (2) had the same direction of difference between IDH1R132H-GFP-expressing and GFP-expressing cells, and (3) had expression of the gene in both of the 2 compared groups (MAS 5.0 > 30 and RMA > 7.0).

For kinome analysis stable U87 cell lines were used. Pepchip kinomics arrays (Pepscan, Lelystad, the Netherlands) were hybridized according to the manufacturer's protocol and as described in Parikh et al²⁷ and Sikkema et al²⁸). Pathway analysis was performed using the Ingenuity Pathways Analysis tool (Ingenuity Systems, Mountain View, CA). To compare groups, 2-sided Student t-tests were used; otherwise, the statistical test used is stated in the text. For more detailed information see also Supporting Information Methods.

recombinant enzymes, of the stable cell lines and in primary tumors, were performed as described (see also Supporting Information Methods).

Intracranial injections were performed with the U87 stable cell lines. C.B-17/Icr-Hantmhsd-Prkdc SCID mice (Harlan) were stereotactically injected with 1×10^5 tumor cells according to a protocol previously described.²⁴ Tumor growth was measured 3x/wk in the IVIS 200 system (Xenogen, Alameda, CA).

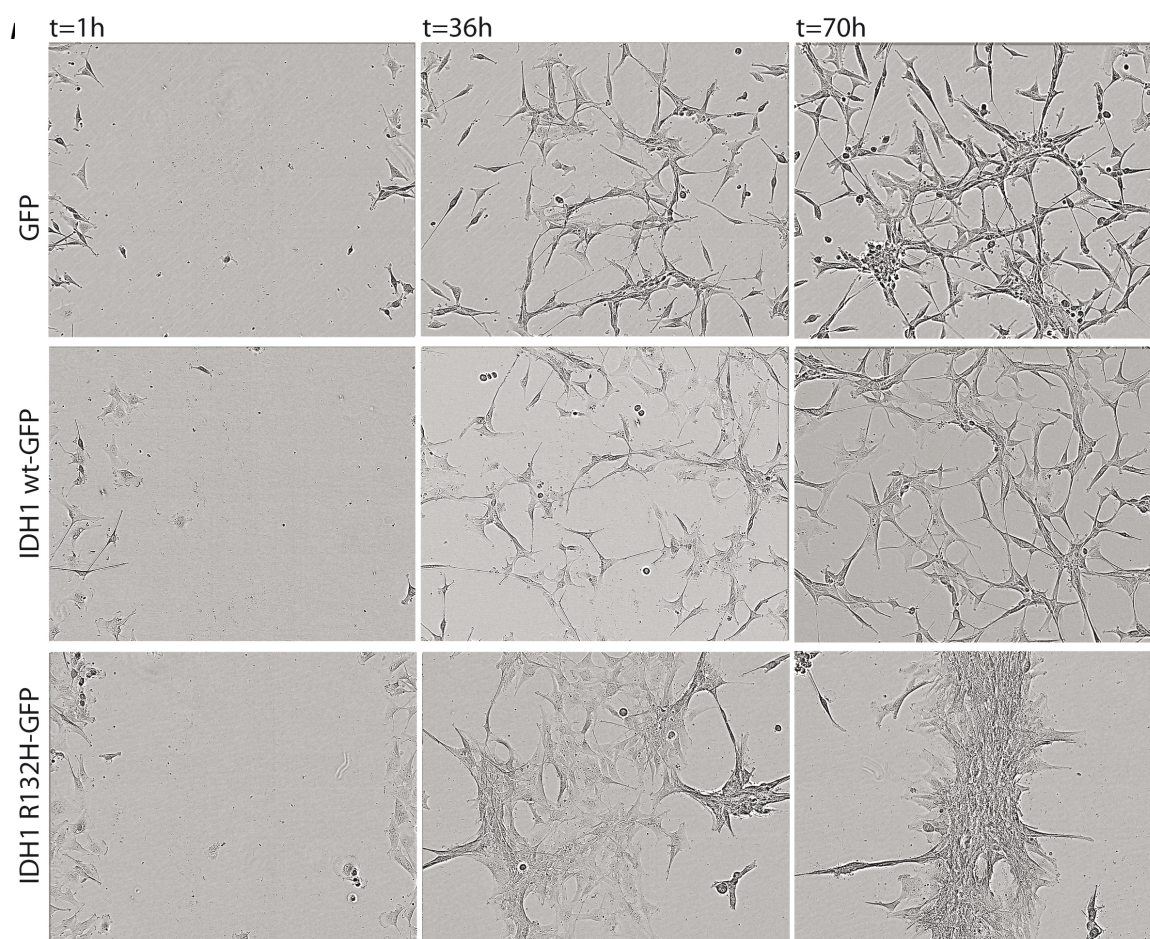
L-2-HG and D-2-HG were measured as described.²⁵ Both L-2-HG and D-2-HG had no effect on the pH of the medium in the concentrations used in this study. Stable U87 and U138 cell lines were used for mRNA expression analysis on U133

Plus2 arrays (Affymetrix, Santa Clara, CA). Data were normalized using both the MAS5.0 (Affymetrix) and Robust Multi-array Average (RMA) algorithms.²⁶ Only genes were

Results

Proliferation

Three independent cell lines (U87, U138, and HEK) were created that stably overexpress IDH1R132H-GFP, IDH1wt-GFP, or GFP. In all 3 cell lines, we observed a IDH1R132H-GFP decreased proliferation rate of the expressing cell lines compared to control (IDH1wt-GFP-expressing or GFP-expressing) cell lines. The decreased proliferation was observed by WST assays (Fig 1 and Supporting Information Fig 1) and confirmed by FACS cell cycle analysis (U87). For example, FACS analysis on exponentially growing cells showed that the percentages of cells in S-phase, G2, or mitosis were lower in IDH1R132H-GFPIDH1wt-GFP-expressing cells than in expressing or GFP-expressing cells (18.3% vs 22.5% and 22.4%, respectively, $p < 0.05$, Mann-Whitney U test). IDH1R132HGFP-expressing cells also had concurrent fewer IDH1wt-GFP. Ki67-positive cells compared to -expressing cells (33.6% and 45.5%) and had a reduced number of BrdU-positive (proliferating) cells in IDH1R132HGFP compared to IDH1wt-GFP cells (17.5% vs 19.2%) as determined by FACS



Scratch assay results of U87 cells overexpressing gamma-fetoprotein (GFP), IDH1wt-GFP, or IDH1R132H-GFP are shown. The U87 cells overexpressing IDH1R132H-GFP show a reduced motility and cluster tightly together on the scratched surface area (see also Supporting Information Videos 1–3). wt = wild type.

analysis. The decreased proliferation was not due to differences in apoptosis. Our data therefore demonstrate that established cell lines expressing IDH1R132H show lower proliferation rates due to a reduced cell cycle activity.

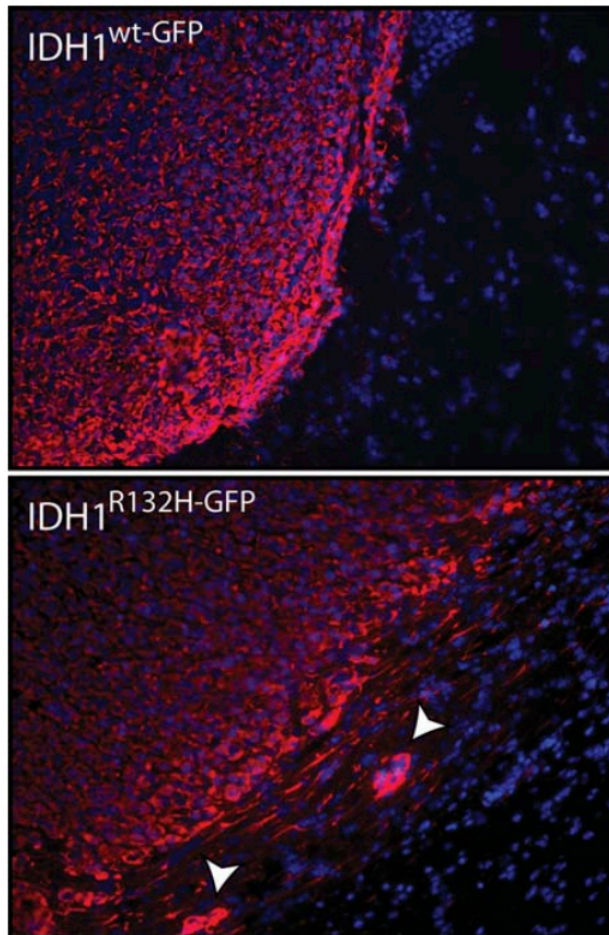
To determine whether the reduced proliferation rate of IDH1R132H-GFP-expressing cells is also observed in vivo, we performed intracranial injection in mice with our 3 U87 cell lines. Mice injected with IDH1R132H-GFP-expressing cells had significantly better survival (mean 40.3 ± 6.9 days) than both the control groups injected with cells expressing either IDH1wt-GFP (mean 29 ± 5.8 days, $p = 0.0012$) or GFP (mean 28.6 ± 5.2 days, $p = 0.00058$) (Fig 2). The difference in survival was obvious, and histological analysis of 1 of the mice injected with IDH1R132H-GFP-expressing cells revealed complete absence of tumor at 75 days, whereas the initial IVIS measurements did detect tumor burden (see Fig 2 and Supporting Information Fig 2). Immunohistochemistry showed a reduced GFP staining in some of the IDH1R132H-GFP-induced but none of the IDH1wt-GFP-induced tumors, indicating that IDH1R132H-GFP expression is, at least partially, lost in the absence of selection pressure (Supporting Information Fig 3). Mutant tumor cells were present as indicated by elevated D-2-HG levels (see below). The reduced proliferation of IDH1R132H-GFP-expressing cells in vitro therefore is also apparent in vivo following intracranial injection of IDH1R132H-GFP-expressing U87 cells.

To further investigate the cellular consequences of the IDH1R132H mutation, we performed a cell migration assay. Cells expressing IDH1R132H-GFP showed a different and more clusterlike (adherent to other cells) migration pattern, ultimately resulting in a tightly squeezed line of cells in the middle of the scratched region (Fig 3 and Supporting Information Videos 1–3). When counting individual cells ($n = 20$) in the scratched region, the overall motility was significantly less in U87 cells expressing IDH1R132H-GFP than in U87 cells expressing IDH1wt-GFP or GFP ($18.0 \pm 2.1 \mu\text{m/h}$ vs 26.3 ± 3.3 and 27.5 ± 3.9 respectively, both $p < 0.0001$). IDH1R132H-GFP-expressing U87 cells also show an altered migration in vivo following intracranial injection; clusters of vimentin-positive infiltrative foci were approximately twice as frequent in the tumors expressing IDH1R132H-GFP as in those expressing IDH1wt-GFP in vivo (Fig 4). Such an increase in infiltrative foci in U87 cells has also been observed by others.²⁹ The IDH1R132H mutation therefore is not only associated with a reduced proliferation rate but also associated with an altered cellular migration pattern in an established glioma cell line. Whether these 2 are correlated remains to be investigated.

Altered Enzymatic Activity of IDH1R132H-GFP Is Increased in the Presence of IDH1wt-GFP

Thus far, all reported enzymatic experiments have been performed using extracts of cells overexpressing wild-type or mutant IDH1.^{15,18} Similar to the findings reported by these groups, our cell lines stably expressing IDH1R132HGFP also show reduced enzymatic activity toward isocitrate and increased activity toward αKG compared to IDH1wt-GFP (Fig 5 and Supporting Information Figs 4 and 5). Patient-derived tumors with IDH1 mutations ($n = 5$, all R132H) also showed reduced enzymatic activity toward isocitrate ($p = 0.037$) (see Supporting Information Figures 5 and 6).

Figure 4: Glioma cells expressing mutant IDH1 have an altered migration pattern in vivo.



Intracranially injected U87 cell tumors expressing IDH1R132H-GFP (bottom panel) are characterized by the presence of infiltrative foci (arrowheads). Such foci were observed much less frequently in tumors expressing IDH1wt-GFP (top panel). Red = vimentin; blue = 4,6-diamidino-2-phenylindole; wt = wild type; GFP = green fluorescent protein. [Color figure can be viewed in the online issue, which is available at www.annalsofneurology.org.]

indicate that the presence of IDH1bio-wt-GFP increases the enzymatic activity of IDH1bio-R132H-GFP toward α KG.

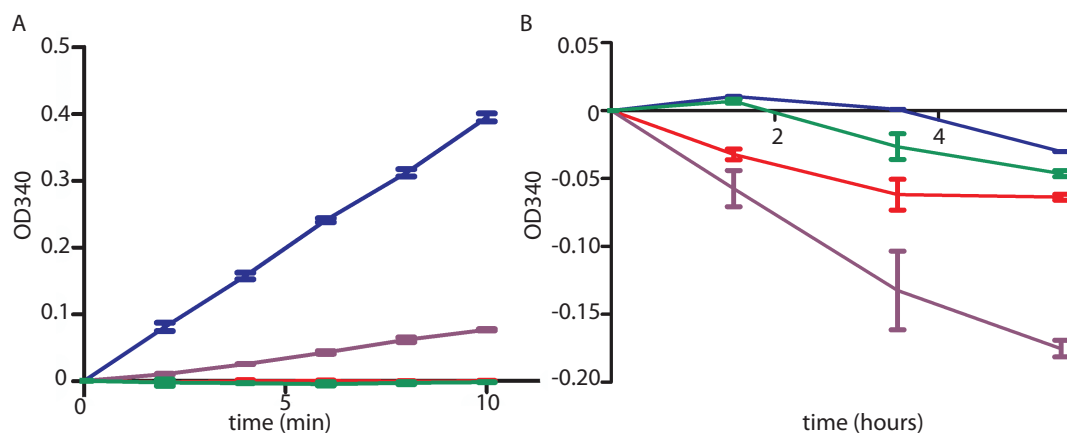
2-Hydroxyglutarate Reduces Proliferation

Our next experiments were aimed at determining whether the reduced proliferation rate of IDH1R132H-GFP-expressing cells is a consequence of the D-2-HG produced by the mutant enzyme. In our U87 cell lines, D-2-HG concentrations are strongly increased, both in cell pellets (68 μ mol/mg protein) and in the medium (55 μ mol/l) (Supporting Information Fig 7). L-2-HG levels were not affected by IDH1R132H-GFP expression. Similar increases were observed in cell extracts of intracranially injected tumors (26.9 μ mol/l vs 1.35 μ mol/l, $p = 0.014$, see also Supporting Information Fig 7).

Subsequently we sought to examine whether the altered enzymatic activity of IDH1R132H could be recapitulated in a purified protein system with our constructs. For these experiments, we generated constructs in which a biotag was added to the N-terminal end of the protein. Biotagged constructs could then be purified following biotinylation and streptavidin-conjugated magnetic beads. As reported using extracts of cell lines, IDH1bio-wt-GFP had enzymatic activity toward isocitrate and not toward α KG and vice versa for IDH1bio-R132H-GFP. The activity was dose dependent for both isocitrate and enzyme concentration (not shown). A 1:1 mixture of IDH1wt-GFP and IDH1R132H-GFP showed intermediate activity toward isocitrate (see Fig 5). Surprisingly, in this purified protein system, the IDH1bio-R132H-GFP activity was more active toward α KG in the presence of IDH1biowt-GFP enzyme. More α KG is converted in these mixture experiments, although they contained only half of the IDH1bio-R132H-GFP of the nonmixture experiments (all experiments contained equimolar amounts of enzyme). These results

The concentrations of D-2-HG measured in pellets and media were used to spike this metabolite into the medium of U87 cells expressing GFP. Both D-2-HG and L-2-HG reduced the proliferation of these cells in a dose-dependent way as measured by FACS cell cycle analysis (Fig 6). The percentage of cells in G2-SM phase was reduced from 20.1% to 15.2% and 7.7% ($p = 0.018$ and $p = 0.037$, respectively) by the addition of 3 and 6mmol/l D-2-HG. This was confirmed by WST analysis using 30mmol/l D-2-HG (46% decrease in growth compared to U87 without D-2-HG, $p < 0.001$). A reduction in cellular proliferation was also observed when performing a BrdU proliferation assay; the number of BrdU-positive U87 cells was reduced from 26.6% to 23.4% in the presence of 1.2mM D-2-HG. Similar percentages of BrdU-positive U87 cells have been observed by others.³⁰ These results indicate that the reduced proliferation rate observed in U87 cells in vitro is at least partly mediated by the accumulation of D-2-HG.

Figure 5: Wild-type (wt)-mutant IDH1 dimers are enzymatically more active toward α -ketoglutarate than mutant IDH1.



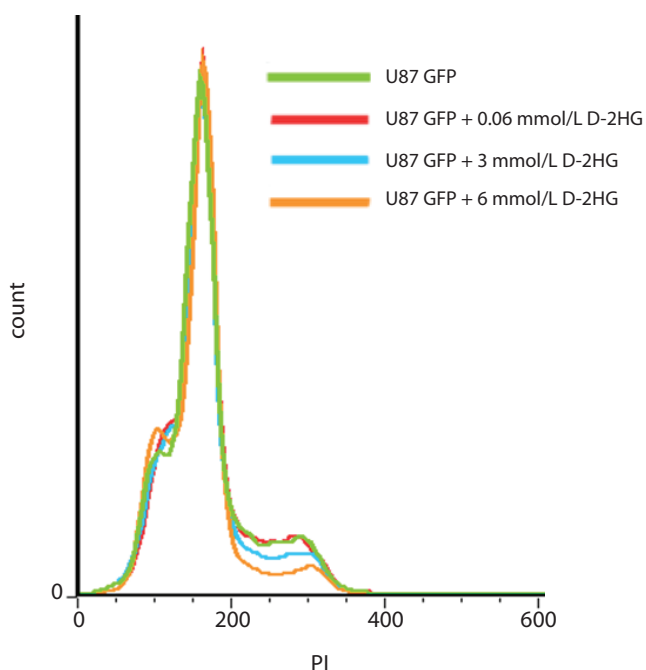
(A) Enzymatic activity of purified enzyme as measured by nicotinamide adenine dinucleotide phosphate hydrogen (NADPH) production (expressed by OD340) in the presence of isocitrate and NADP; IDH1wt-GFP (blue line) and IDH1R132H-GFP (red line) or a 1:1 mixture of both (purple line). Green fluorescent protein (GFP) (green line) is used as a control. (B) Enzymatic activity as measured by NADPH use in the presence of α -ketoglutarate of IDH1wt-GFP (blue line), IDH1R132H-GFP (red line), a 1:1 mixture of IDH1wt-GFP and IDH1R132H-GFP (purple line), and GFP (green line). Error bars represent the standard error of the mean.

The decrease in proliferation was not accompanied by an increase in apoptosis as determined by FACS analysis; the number of annexin V-positive cells in U87 cells was not increased in the presence of D-2-HG (5.5%, 5.2%, and 5.9% for 0.12, 0.6, and 1.2mM D-2-HG, respectively) compared to control U87 cells (6.9%). These results are in line with our observation that IDH1R132H-GFP-expressing cells do not show an increase in apoptosis (see above) despite having elevated levels of D-2-HG.

Downstream Pathway Analysis

It is unknown which oncogenic pathways are affected by IDH1R132H and D-2-HG. We therefore performed expression profiling to further analyze the downstream pathways. Only 7 genes (Table) were identified that show an IDH1R132H-GFP-associated differential expression of >20% in both U87 and U138 cells. Ingenuity pathway analysis indicated that these genes are not significantly linked to any canonical pathway, but can be linked to a single network involved in tumor morphology, cellular development, and cellular growth and proliferation (Supporting Information Fig 8). However, the number of differentially

Figure 6: D-2-hydroxyglutarate (D-2HG) reduces proliferation of glioma cells.



Dose-dependent effects of D-2-hydroxyglutarate on the cell cycle of U87 cells expressing green fluorescent protein (GFP) as measured by fluorescence-activated cell sorting are shown. PI = propidium iodide.

As AKT1 activation is positively correlated with cell proliferation, kinome profiling confirms the reduced proliferation observed in IDH1R132H-GFP-expressing U87 cells.

Discussion

To our knowledge, we are the first to describe the cellular effects of IDH1R132H-GFP expression in established cell lines. Our data strongly indicate that IDH1R132HGFP reduces the proliferation rate of various cell lines, as is demonstrated by WST assays, FACS cell cycle analysis, and Ki67 staining. These results were supported morphologically (visualized by a reduced population of elongated, actively dividing, cells) and by kinome profiling (as indicated by a reduced AKT activation). The reduced proliferation in vitro was confirmed in vivo following intracranial injection of IDH1R132H-GFP-expressing cells.

It is possible that the reduced proliferation rate in established glioma cell lines explains why only 1 tumor cell line expressing IDH1R132H has been reported,^{31,32} although xenografts of glioblastomas with IDH1 mutations have been described.⁵ In fact, we examined 13 primary cell cultures on serum propagated from IDH1 mutated gliomas. No primary tumor cell culture bearing the IDH1 mutation could be established from any of these gliomas. A reduced presence of the IDH1 mutation was already visible in the first passage of these cells as a reduced peak on sequence chromatograms (R.B. and M.L., unpublished observations). However, a correlation between difficulties of culturing IDH1 mutated gliomas and reduced proliferation in established cell lines should be treated with caution, as many other factors might contribute to poor growth of (lower grade) gliomas in vitro.

expressed genes is too few to significantly address downstream pathway activation.

Kinome profiling on our three U87 cell lines was then performed to further examine the pathways affected by IDH1R132H-GFP. Seven kinases were significantly differentially activated between IDH1R132H-GFP-expressing cells and both IDH1wt-GFP-expressing and GFP-expressing cells ($p < 0.05$) (see Table). One of the most differentially activated kinases was AKT1, showing less activity in IDH1R132H-GFP-expressing cells. Immunocytochemistry using phospho-AKT specific antibodies confirmed the reduced AKT1 activity in IDH1R132HGFP expressing cells (Supporting Information Fig 9).

It is interesting that the effects of IDH1R132H were so apparent although the mutation was introduced into highly malignant glioma cell lines. This demonstrates the dominant nature of mutant IDH1 in established cell lines. If mutant IDH1 is also causal for reduced proliferation in gliomas, it might explain why IDH1R132H is inversely correlated with tumor grade and why IDH1R132H is an independent favorable prognostic marker in glioma patients.^{1,3,4} However, it is possible that the effect of IDH1R132H expression observed in this study is associated with its expression in highly malignant cell lines that have a distinct set of genetic changes (see, eg, Clark et al³³). Therefore, the effect of IDH1R132H expression on nonmalignant cell types, low-grade gliomas, and/or cancer stem cells remains to be determined.

Table 1: Differentially Expressed Genes and Activated Kinases in Mutant IDH1-Expressing Cell Lines

Gene	Expression in mutant	Fold change
<i>BTG3</i>	Overexpressed	1.672
<i>CCNG1</i>	Overexpressed	1.514
<i>CD99</i>	Overexpressed	1.727
<i>SERPINE1</i>	Overexpressed	2.865
<i>HNRPDL</i>	Underexpressed	0.714
<i>PPP1CB</i>	Underexpressed	0.703
<i>TMED7</i>	Underexpressed	0.540

Kinase	Activation in mutant	Fold change
Activin A receptor, type 1	Higher	2.15
MARK	Higher	1.62
AKT1	Lower	0.82
MAPK4	Lower	0.66
Ribosomal protein S6 alpha 4	Lower	0.64
SHP2	Lower	<<
TAO kinase 2	Lower	0.66

Gene = Differentially expressed genes in IDH1R132H-GFP-expressing cell lines (U87 and U138) compared to IDH1wt-GFP expressing cell lines. Kinase = Differentially activated kinases in IDH1R132H-GFP expressing U87 cell lines compared to IDH1wt-GFP-expressing and GFP-expressing U87 cell lines. < = no expression detectable anymore. wt = wild type; GFP =Green fluorescent protein

Our results appear contradictory, with a presumed oncogenic role of IDH1R132H and D-2-HG as an oncometabolite.^{20,22,34} However, our results may be explained if IDH1 mutation only has a favorable role in tumor initiation, but is unfavorable for tumor progression. Indeed, IDH1R132H is the first hit,⁷ does not accumulate secondary to tumor formation, and anecdotally is lost in part of the tumor after malignant progression.³⁵

However, our results may also be explained if IDH1R132H does not contribute to tumor formation, or if effects observed in this study are specific to the cell lines used. A causal role has not yet been established. Alternative functions of IDH1R132H can also explain a possible role in oncogenesis.

A similar discussion can be held on D-2-HG as an oncometabolite. IDH1 or IDH2 mutations result in an increase in D-2-HG in serum and tumors of AML^{21,22} and glioma²⁰ patients (see also Supporting Information Fig 7), whereas we demonstrate that D-2-HG reduces the proliferation rate of glioma cells. These results appear contradictory to a presumed role of D-2-HG as an oncometabolite, but it is possible that D-2-HG only plays a role in tumor initiation. However, accumulation of D-2-HG is also not associated with brain tumor formation (whereas L-2-HG is),³⁶ which might suggest D-2-HG has no tumor-initiating

capacities and is solely an inevitable byproduct. If so, mutated IDH1 or IDH2 has oncogenic properties not associated with D-2-HG. It has been reported that the IDH1 and IDH2 mutation spectra differ across the various diseases (glioma, AML and D-2-HG aciduria).^{6,13,36,37} It is tempting to speculate that these oncogenic properties vary across the different IDH1 and IDH2 mutations.

To further elucidate a possible function of mutant IDH1, we have recently performed methylation profiling (Infinium Human methylation 27 arrays [Illumina, San Diego, CA]) on a panel of 68 anaplastic oligodendrogliomas and oligoastrocytomas (P.J.F., manuscript in preparation). In this study, the CpG island methylator phenotype (CIMP) was highly correlated with the presence of IDH1 mutation. These data are in line with the recently suggested hypothesis that IDH1 induces promoter methylation.³⁸ However, not all IDH1 mutated tumors are CIMP positive, nor is the effector gene TET2 differentially expressed between IDH1wt-GFP-expressing and IDH1R132H-GFP-expressing U87 and U138 cells. It therefore remains to be determined whether IDH1 mutations also result in promoter methylation in glioma.

Our purified enzyme system allowed us to examine the properties of wild-type–mutant enzyme mixtures. Interestingly, our results show that the 1:1 mixture of IDH1bio-wt-GFP-expressing and IDH1bio-R132H-GFP expressing cells has the highest reductive enzymatic activity. The altered enzymatic activity therefore is stimulated by the presence of wild-type enzyme. To our knowledge, this is the first paper to examine the altered enzymatic activity of IDH1R132H-GFP in a purified protein system. Others have studied and reported on IDH1 mutated enzymes from cell lysates that also contain endogenous IDH1²² or have not tested the enzymatic activity toward αKG of the combination of IDH1 mutant and wild-type enzyme.^{19,21} The increased alternative enzyme activity could be explained by the fact that IDH1 functions as a dimer. In this model, the αKG produced by wild-type IDH1 in wild-type–mutant heterodimers improves substrate availability for mutant IDH1. Alternatively, heterodimers confer a more active conformational state of mutant IDH1.

IDH1 can only function as a dimer,¹ and therefore it is possible that wt-IDH1 enzymes in wt-mutant IDH1 heterodimers may induce a different conformational state than IDH1 mutant homodimers. Such an altered state can result in increased activity of the mutant enzyme. The increased alternative enzyme activity of the wild-type–mutant combination is in line with the observation that virtually all IDH1 mutations are heterozygous.

In conclusion, IDH1R132H-GFP-expressing cell lines show a reduced proliferation rate in vitro and better survival in vivo. Our results obtained in model systems of glioma may help explain the biology of IDH1 mutated gliomas, which are typically low grade and slow growing.

Supplementary Information accompanies the paper on the Annals of Neurology website

References

1. Kloosterhof NK, Bralten LB, Dubbink HJ, et al. Isocitrate dehydrogenase- 1 mutations: a fundamentally new understanding of diffuse glioma? *Lancet Oncol* 2011;12:83–91.
2. Yan H, Bigner DD, Velculescu V, Parsons DW. Mutant metabolic enzymes are at the origin of gliomas. *Cancer Res* 2009;69: 9157–9159.

3. Gravendeel LA, Kouwenhoven MC, Gevaert O, et al. Intrinsic gene expression profiles of gliomas are a better predictor of survival than histology. *Cancer Res* 2009;69:9065–9072.
4. Sanson M, Marie Y, Paris S, et al. Isocitrate dehydrogenase 1 codon 132 mutation is an important prognostic biomarker in gliomas. *J Clin Oncol* 2009;27:4150–4154.
5. Parsons DW, Jones S, Zhang X, et al. An integrated genomic analysis of human glioblastoma multiforme. *Science* 2008;321:1807–1812.
6. Gravendeel LA, Kloosterhof NK, Bralten LB, et al. Segregation of non-p.R132H mutations in IDH1 in distinct molecular subtypes of glioma. *Hum Mutat* 2010;31:E1186–E1199.
7. Watanabe T, Nobusawa S, Kleihues P, Ohgaki H. IDH1 mutations are early events in the development of astrocytomas and oligodendrogliomas. *Am J Pathol* 2009;174:1149–1153.
8. Nobusawa S, Watanabe T, Kleihues P, Ohgaki H. IDH1 mutations as molecular signature and predictive factor of secondary glioblastomas. *Clin Cancer Res* 2009;15:6002–6007.
9. van den Bent MJ, Dubbink HJ, Marie Y, et al. IDH1 and IDH2 mutations are prognostic but not predictive for outcome in anaplastic oligodendroglial tumors: a report of the European Organization for Research and Treatment of Cancer Brain Tumor Group. *Clin Cancer Res* 2010;16:1597–1604.
10. Weller M, Felsberg J, Hartmann C, et al. Molecular predictors of progression-free and overall survival in patients with newly diagnosed glioblastoma: a prospective translational study of the German Glioma Network. *J Clin Oncol* 2009;27:5743–5750.
11. Wick W, Hartmann C, Engel C, et al. NOA-04 randomized phase III trial of sequential radiochemotherapy of anaplastic glioma with procarbazine, lomustine, and vincristine or temozolomide. *J Clin Oncol* 2009;27:5874–5880.
12. Balss J, Meyer J, Mueller W, et al. Analysis of the IDH1 codon 132 mutation in brain tumors. *Acta Neuropathol* 2008;116:597–602.
13. Hartmann C, Meyer J, Balss J, et al. Type and frequency of IDH1 and IDH2 mutations are related to astrocytic and oligodendroglial differentiation and age: a study of 1,010 diffuse gliomas. *Acta Neuropathol* 2009;118:469–474.
14. Sonoda Y, Kumabe T, Nakamura T, et al. Analysis of IDH1 and IDH2 mutations in Japanese glioma patients. *Cancer Sci* 2009; 100:1996–1998.
15. Yan H, Parsons DW, Jin G, et al. IDH1 and IDH2 mutations in gliomas. *N Engl J Med* 2009;360:765–773.
16. Mardis ER, Ding L, Dooling DJ, et al. Recurring mutations found by sequencing an acute myeloid leukemia genome. *N Engl J Med* 2009;361:1058–1066.
17. Bolduc JM, Dyer DH, Scott WG, et al. Mutagenesis and Laue structures of enzyme intermediates: isocitrate dehydrogenase. *Science* 1995;268:1312–1318.
18. Ichimura K, Pearson DM, Kocialkowski S, et al. IDH1 mutations are present in the majority of common adult gliomas but rare in primary glioblastomas. *Neuro Oncol* 2009;11:341–347.
19. Zhao S, Lin Y, Xu W, et al. Glioma-derived mutations in IDH1 dominantly inhibit IDH1 catalytic activity and induce HIF-1 α . *Science* 2009;324:261–265.
20. Dang L, White DW, Gross S, et al. Cancer-associated IDH1 mutations produce 2-hydroxyglutarate. *Nature* 2010;465:966.
21. Gross S, Cairns RA, Minden MD, et al. Cancer-associated metabolite 2-hydroxyglutarate accumulates in acute myelogenous leukemia with isocitrate dehydrogenase 1 and 2 mutations. *J Exp Med* 2010;207:339–344.
22. Ward PS, Patel J, Wise DR, et al. The common feature of leukemia-associated IDH1 and IDH2 mutations is a neomorphic enzyme activity converting α -ketoglutarate to 2-hydroxyglutarate. *Cancer Cell* 2010;17:225–234.
23. Bralten LB, Gravendeel AM, Kloosterhof NK, et al. The CASPR2 cell adhesion molecule functions as a tumor suppressor gene in glioma. *Oncogene* 2010;29:6138–6148.
24. Lamfers ML, Idema S, Bosscher L, et al. Differential effects of combined Ad5-delta 24RGD and radiation therapy in in vitro versus in vivo models of malignant glioma. *Clin Cancer Res* 2007;13:7451–7458.
25. Struys EA, Jansen EE, Verhoeven NM, Jakobs C. Measurement of urinary D- and L-2-hydroxyglutarate enantiomers by stable-isotope-dilution liquid chromatography-tandem mass spectrometry after derivatization with diacetyl-L-tartaric anhydride. *Clin Chem* 2004;50:1391–1395.
26. Irizarry RA, Hobbs B, Collin F, et al. Exploration, normalization, and summaries of high density

- oligonucleotide array probe level data. *Biostatistics* 2003;4:249–264.
27. Parikh K, Peppelenbosch MP, Ritsema T. Kinome profiling using peptide arrays in eukaryotic cells. *Methods Mol Biol* 2009;527: 269–280, x.
 28. Sikkema AH, Diks SH, den Dunnen WF, et al. Kinome profiling in pediatric brain tumors as a new approach for target discovery. *Cancer Res* 2009;69:5987–5995.
 29. Delamarre E, Taboubi S, Mathieu S, et al. Expression of integrin alpha6beta1 enhances tumorigenesis in glioma cells. *Am J Pathol* 2009;175:844–855.
 30. Lu Y, Jiang F, Jiang H, et al. Gallic acid suppresses cell viability, proliferation, invasion and angiogenesis in human glioma cells. *Eur J Pharmacol* 2010;641:102–107.
 31. Bleeker FE, Lamba S, Leenstra S, et al. IDH1 mutations at residue p.R132 (IDH1(R132)) occur frequently in high-grade gliomas but not in other solid tumors. *Human Mutat* 2009;30:7–11.
 32. Kelly JJ, Blough MD, Stechishin OD, et al. Oligodendroglioma cell lines containing t(1;19)(q10;p10). *Neuro Oncol* 2010 Apr 13.
 33. Clark MJ, Homer N, O'Connor BD, et al. U87MG decoded: the genomic sequence of a cytogenetically aberrant human cancer cell line. *PLoS Genet* 2010;6:e1000832.
 34. Dang L, Jin S, Su SM. IDH mutations in glioma and acute myeloid leukemia. *Trends Mol Med* 2010;16:387–397.
 35. Pusch S, Sahm F, Meyer J, et al. Glioma IDH1 mutation patterns off the beaten track. *Neuropathol Appl Neurobiol* 2010 Sep 27. [Epub ahead of print].
 36. Kranendijk M, Struys EA, van Schaftingen E, et al. IDH2 mutations in patients with D-2-hydroxyglutaric aciduria. *Science* 2010;330: 336.
 37. Paschka P, Schlenk RF, Gaidzik VI, et al. IDH1 and IDH2 mutations are frequent genetic alterations in acute myeloid leukemia and confer adverse prognosis in cytogenetically normal acute myeloid leukemia with NPM1 mutation without FLT3 internal tandem duplication. *J Clin Oncol* 2010;28:3636–3643.
 38. Figueroa ME, Abdel-Wahab O, Lu C, et al. Leukemic IDH1 and IDH2 mutations result in a hypermethylation phenotype, disrupt TET2 function, and impair hematopoietic differentiation. *Cancer Cell* 2010;18:553–56

Chapter Five

Mutation specific functions of *EGFR* result in a mutation-specific downstream pathway activation

Nanne K. Kloosterhof, Lale Erdem, Jeroen de Vrij, Niek Maas, Johan Hoeksel, Valeska van Breughel, Yassar Atlasi, Jeroen Demmers, Linda Bralten, Andrea Sacchetti, Ton van Agthoven, Johan M. Kros, Erna Michiels, Peter Sillevius Smitt, Pim J. French

Manuscript in preparation

Abstract

Background: *EGFR* is frequently mutated in various types of cancer. Interestingly however, specific mutations within *EGFR* are restricted to specific tumour types. Here, we have examined whether functional differences underlie this tumor-type specific mutation spectrum.

Methods: We have determined whether specific mutations in *EGFR* (*EGFR*, *EGFRvIII* and *EGFR-L858R*) have differences in binding partners, downstream activation of gene expression, loading into the exosomal compartment, and growth and migration.

Results: Using biotin pulldown and subsequent mass spectrometry we were able to detect mutation specific binding partners for *EGFR*. Of these, the dedicator of cytokinesis 4 (*DOCK4*) and *UGGT1* associate specifically with *EGFRvIII* but not with *EGFR-L858R*. We also demonstrate that each mutation induces the expression of a specific set of genes, likely caused by the activation of mutation specific molecular pathways. Finally, we demonstrate using stably expressing cell lines that *EGFRvIII* and *EGFR-L858R* display reduced growth and migration compared to *EGFR* Wildtype expressing cells.

Conclusion: Our results indicate that there are distinct functional differences between different *EGFR* mutations. This indicates that not all mutations of *EGFR* can be considered identical but should be approached as distinct problems. The functional differences between different mutations can lead to the identification of mutation-specific targeting of *EGFR* in cancer.

Introduction

The epidermal growth factor receptor (*EGFR*) is a receptor tyrosine kinase that is localised on the cell membrane. *EGFR* binds several growth factors such as epidermal growth factor (*EGF*) and transforming growth factor (*TGF*) α . Growth factor binding results in dimerisation and activation of a number of different signal transduction pathways including the RAS-MAPK/ERK, JAK-STAT, PI3-K-AKT-mTOR - and the JNK pathways. (1) Activation of these *EGFR*-mediated pathways ultimately results in a cellular growth and/or differentiation response. (1, 2)

Activating mutations of the *EGFR* gene are found in several types of cancer, such as breast, lung, brain, gastric, and head and neck. Elevated levels of *EGFR* in cancer are also frequently associated with poor prognosis. (3, 4) Although the *EGFR* gene is mutated at high frequency in the various cancer types, the type of mutation differs per tumour. For example, the most frequent mutation in *EGFR* is the c.2573T>G which results in the substitution of a leucine for an arginine at amino acid 858 (*L858R*). This is found in ~17% of all pulmonary adenocarcinomas but has thusfar never been identified in glioblastomas (*GBMs*). (5-7) The *EGFR* alterations found in *GBMs* are gene amplifications often followed by a deletion of exons 2-7 (also known as *EGFRvIII*) and is found in ~30% of all *GBMs*, it has been reported in frequency up to 50-60% in *GBMs* with *EGFR* amplification. (8) Such intragenic deletions are not found in pulmonary adenocarcinomas. (9) A tumour specific mutation spectrum is not unique to *EGFR*, it is found in other causal cancer genes such as *IDH1* and *PIK3CA*. (10, 11) One of the explanations for this differential mutation spectrum is that each mutation activates a unique set of signal transduction pathways. Here, we have tested this hypothesis by screening for functional differences between wt-*EGFR*, *EGFR L858R* and *EGFRvIII*. Our results demonstrate that each mutation has a unique set of

binding partners, induce expression of a different set of genes and activate a different signal transduction pathway. Our results suggest that EGFR mutants cannot be considered identical but should be investigated as a group of unique but closely related proteins. It is possible that different tumour types depend on the pathways activated by the tumor-type specific mutations. Better understanding of the effects of specific *EGFR* mutations therefore may lead to the development of mutation specific targeted therapies.

Materials and methods

Generation of the constructs

EGFRvIII and EGFR L858R were obtained from Addgene, plasmid 20737, and plasmid 11012, EGFR wildtype was a gift from Ton van Agthoven. (12, 13) The EGFR fragments were cloned into pcDNA3.1/CT-GFP-TOPO (Invitrogen cat no: K4820-01). A biotin tag was added to the construct at the 3' before the GFP. These constructs were used to stably transfect HOG cells, human glioma cells. One day after transfection the cultures were supplemented with geneticin. After at least 5 weeks FACS sorting was performed on the cell lines to select for GFP expressing cells. The cells were further cultured under standard conditions, Dulbecco's modified Eagle's medium with 10% fetal calf serum, antibiotics and geneticin and at 37°C and 5% CO₂.

FACS sorting

Cells were analyzed and sorted with a BD FACS Aria III (Beckton Dickinson, NJ, USA). Live/dead discrimination was performed using Hoechst 33258 (Sigma-Aldrich). GFP fluorescence was detected using a 488 nm laser and emission filters LP520 + BP530/30. Hoechst 33258 fluorescence was detected using 405 nm laser and BP450/40 emission filter. Sorting was performed with a 100 µm nozzle and a pressure of 20 PSI, keeping both unsorted sample and sorted cells at 4 degrees Celcius during the entire procedure.

Migration and proliferation

Migration and proliferation assays were performed using an Incucyte (Essen Bioscience, Ann Arbor, MI). Proliferation experiments were done in four separate experiments. The cells were monitored for at least 90 hours and a picture was taken either every two or three hours. Migration was done in two separate experiment and the cells were monitored for 64 and 69 hours with a picture taken every three hours. For both experiments we determined the slope in the linear phase for each location, took a picture and performed a t-test to determine the significance compared to GFP.

Biotin pulldown

Constructs containing *bio-GFP-EGFR*, *bio-GFP-EGFR L858R* and *bio-GFP-EGFRvIII* were transfected into HEK cell lines using Polyethylenimine "Max" (Polysciences, Eppelheim, Germany). The EGFR wildtype and mutants were isolated using Dynabeads (Life Technologies, Carlsbad, CA, USA) as described previously. (14) The purified proteins were subsequently incubated for 2 hours with lysate from CRL5908 cells, an adenocarcinoma cell line, washed and subsequently loaded on a SDS page gel.

Mass spectrometric analysis

The isolated protein was incubated with cell lysate from the CRL5908 cell line, a lung cancer cell line containing an EGFR L858R mutation. Using sodium dodecyl sulfate polyacrylamide gel electrophoresis (SDS-PAGE) the samples were separated by MW. Nanoflow LC-MS/MS analysis was performed essentially as described by van den Berg et al. (15) Analysis of the mass spectrometry data was performed in two steps. The initial step was to discard all proteins found in a pulldown of eGFP (results in supplementary table 1). The remaining proteins with the highest mascot score and biggest difference in mascot score between the EGFR constructs were selected (table 1).

Western blot

Western blots were performed essentially as described previously in Bralten et al.(14) Antibodies used were DDX21 (Sigma, Zwijndrecht, Nederland, HPA036592)(1:500); UGGT1 (Sigma, Zwijndrecht, Nederland, HPA012761)(1:100), DOCK4 (Sigma, Zwijndrecht, Nederland, WH0009732M1)(1:100) ARHGEF5 (Abcam, Cambridge, UK, Ab42695) (1:100) EGFR (Cell Signaling, Boston, MA, USA, 4267)(1:1000) and GFP (Abcam, Cambridge, UK, Ab290-50)(1:5000).

Immunofluorescence

For immunofluorescence (IF) of the cell culture, cells were cultured on glass slides. Snap frozen tumours were obtained from the Erasmus MC glioma tissue bank. 5µm sections were cut. The antibodies used were for DOCK4 (Abcam, Cambridge, UK, ab85723) (1:100) and for EGFR (DAKO, Heverlee, Belgium, M3563) (1:200).

Transcriptome analysis

Cells were transfected 20 hours prior to sorting using the previously described constructs or biotin-GFP. Transfections were performed in triplicate. After FACS sorting the cells were snap frozen in liquid nitrogen and stored at -80°C. RNA extraction was performed using TriZol (Invitrogen). All samples were analysed using the Bioanalyzer, the RIN scores were 8.5 to 10. RNA was hybridized onto U133 plus2 arrays (Affymetrix) by AROS Applied Biotechnology (Aarhus, Denmark) according to manufacturer's protocol.

Results

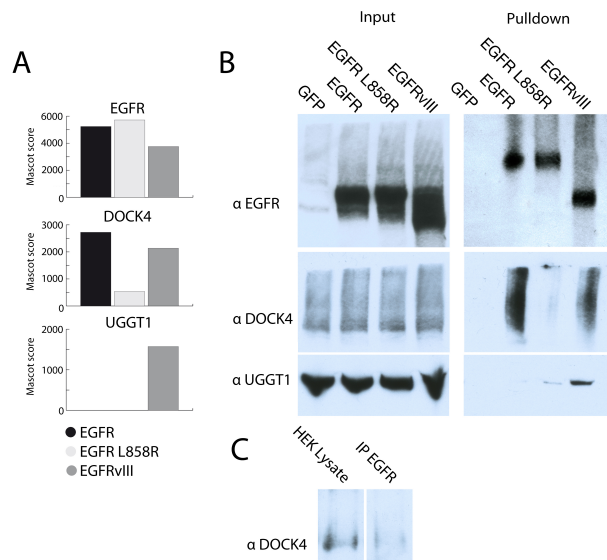
EGFR, EGFR L858R and EGFRvIII have unique binding partner

Our first experiment was aimed to determine whether different mutations in EGFR have different binding partners. For this we performed a biotin-pulldown of mutated EGFR constructs and identified a number of candidate proteins that bind to the various EGFR constructs. The candidate binding proteins include known EGFR interacting proteins such as SOS1, CBL and ELMO2 (supplementary table 1). We then screened the MS data to see whether there are proteins that show selective binding to specific EGFR constructs. This resulted in a list of potential novel binding proteins for EGFR with some showing differential binding, including DOCK4, UGGT1, MYCBP2, DDX21 and ARHGEF5.

For DOCK4 for example, we identified fewer peptides for EGFR L858R-bio-GFP (11 hits) compared to EGFR wt-bio-GFP and EGFRvIII-bio-GFP (54 and 46 hits respectively). Mascot

scores (a measure of the probability of identifying a protein) show a similar ratio, a score of 536 for EGFR L858R-bio-GFP and scores of 2725 and 2136 for EGFR wt-bio-GFP and EGFRvIII-bio-GFP respectively. Similarly for UGGT1, only peptides were identified by pulldown using EGFRvIII-bio-GFP (31 hits) whereas no hits were found for EGFR wt-bio-

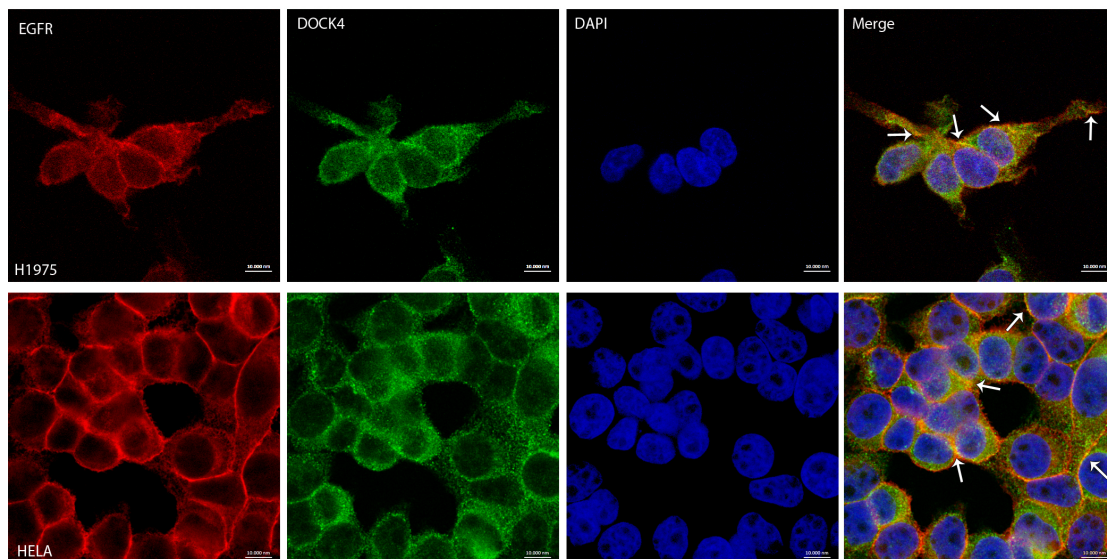
Figure 1: EGFR mutation-specific protein-protein interactions.



A) The Mascot scores of EGFR, DOCK4 and UGGT1 are derived from table 1. As can be seen the Mascot scores indicate mutation specific association with DOCK4 and UGGT1. B) Western blots against UGGT1, DOCK4 and EGFR (as control) of the input (left) and after the streptavidin pulldown of bio-EGFR constructs (right). As can be seen, the Western blot data are highly similar to the MS data and confirm differential binding of proteins to specific mutations in EGFR. C) DOCK4 co-immunoprecipitates with EGFR after pulldown of native EGFR in HEK cells.

GFP or EGFR L858R-bio-GFP. The MASCOT score was 1573 for EGFRvIII-bio-GFP, no MASCOT score were assigned to EGFR wt-bio-GFP and EGFR L858R-bio-GFP respectively.

Figure 2: Immunofluorescence for DOCK4 and EGFR in H1975 and HELA cell lines



DOCK4 colocalises with EGFR. Confocal microscopy pictures for immunofluorescent staining of H1975 and HELA cells against EGFR (red), DOCK4 (green), DAPI and a merge picture. Some areas of colocalization can be seen in the merged picture for both cell lines, some areas of colocalization have been pointed out with arrows in the merge panel.

We then performed western blots on independent biotin pulldowns (at least two pulldowns/protein) to confirm the differential binding of these two proteins. Western

blot results confirmed the mass spectrometry results that DOCK4 binds preferentially to EGFRvIII-bio-GFP and to a lesser extent to EGFR wt-bio-GFP but not to EGFR L858R-bio-GFP (figure 1). To further confirm the binding of DOCK4 to wt-EGFR we performed a co-immunoprecipitation using anti-EGFR antibodies in non-transfected HEK cells. Also under these conditions, DOCK4 co-precipitated with EGFR (figure 1c). These results confirm the identification of DOCK4 as a novel binding partner of EGFR. DOCK4 and EGFR are also colocalised, both in established cell lines H1975 and HELA cells as in glioblastoma tissue sections (Figure 2 and supplementary figure 1).

Table 1: Mass spectrometry results for EGFR, DOCK4 and UGGT1.

	Hits			MASCOT score		
	EGFR	EGFR L858R	EGFRvIII	EGFR	EGFR L858R	EGFRvIII
EGFR	71	78	52	5239	5717	3754
DOCK4	54	11	46	2725	536	2136
UGGT1			31			1573

Table 1: The number of hits and the MASCOT score for EGFR, and DOCK4 and UGGT1. The latter two were found in the pull-down of bio-GFP-EGFR-wt, bio-GFP-EGFR L858R and bio-GFP-EGFRvIII and we could confirm selective binding to EGFR.

Table 2: Survival associated with the most differently expressed probes associated with EGFR.

		Average survival			Average expression			
		Lower 75	Upper 75	p-value	EGFR	EGFR L858R	EGFRvIII	eGFP
ARC	210090_at	4.88	0.93	1.59E-07	6.76	9.28	6.31	5.75
C11orf96	227099_s_at	1.20	6.46	7.27E-09	10.31	12.00	9.49	8.48
EGFR	201983_s_at	1.58	1.14	0.15	14.27	14.41	14.42	6.11
EGFR	210984_x_at	1.60	1.05	0.11	10.02	10.81	9.02	5.53
EGFR	211607_x_at	1.79	1.05	3.20E-03	9.55	10.38	8.64	5.52
EGR1	201693_s_at	4.00	1.10	3.10E-04	8.91	10.93	7.77	6.04
EGR1	201694_s_at	4.00	1.18	1.32E-04	11.18	12.64	10.16	8.22
EGR1	227404_s_at	3.80	1.13	1.78E-05	9.43	10.70	8.44	6.49
EGR2	205249_at	3.30	1.18	1.33E-03	7.59	9.41	6.79	6.11
EGR3	206115_at	2.32	1.25	0.02	7.07	9.36	6.16	5.57
ETV5	203349_s_at	3.52	1.64	0.42	8.58	9.33	8.04	5.51
FOS	209189_at	2.87	1.26	6.37E-03	7.05	9.09	7.21	5.17
HSPA6	213418_at	6.82	0.80	1.40E-09	8.13	9.32	6.74	4.81
MAFF	36711_at	3.24	1.19	5.74E-03	8.48	9.77	8.73	6.11
MAP2K5	211371_at	0.97	1.85	0.04	8.77	9.19	8.78	3.46
RAP1A	1555339_at	1.61	1.44	0.42	4.92	4.68	7.01	13.44
RAP1A	1555340_x_at	1.79	1.18	0.14	5.53	5.09	7.35	14.28
SOCS3	227697_at	6.58	0.86	3.56E-10	4.90	5.59	9.12	4.53
TAC1	206552_s_at	1.58	1.31	0.94	6.65	8.21	6.04	4.73
TFPI2	209278_s_at	4.01	1.16	1.28E-04	6.58	8.72	5.61	5.35

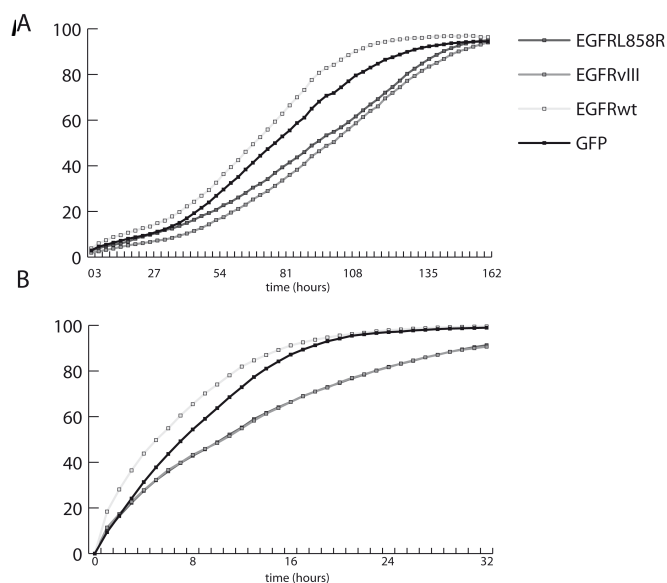
List of the 20 probes with the largest absolute difference between EGFR, EGFR L858R or EGFRvIII and GFP. For each probe the 75 highest and 75 lowest expressing samples were taken from a previously described datasets of human gliomas (Gravendeel et.al.) and an average survival was calculated. A t-test was performed to determine whether the survival was significantly different between the two groups. For all probes that display a significantly different survival, $p < 0.01$, the expression for the EGFR transfected samples is higher than in the GFP control. All but one probe with a significantly different survival display a decreased survival for increased expression.

Transcriptome analysis

We hypothesized that any differential pathway activation by the various EGFR mutants would ultimately result in the induction of a unique set of genes. We have therefore performed gene expression profiling for HEK cells 20 hours after transient transfection with *EGFR-bio-GFP*, *EGFRvIII-bio-GFP*, *EGFR L858R-bio-GFP*, or *GFP* constructs, $n=3$ for each condition. Analysis identified 151, 140 and 688 probes that were differentially

expressed more than 2 fold in *EGFR*, *EGFR-vIII* and *EGFR L858R* transfected cell lines compared to *GFP* (table 2 and supplementary table 2).

Most of the 20 probes with the largest difference in RNA levels between GFP and one of the EGFR constructs have an increased expression in the *EGFR* transfected cells, three of which were *EGFR*. To determine whether these probes are also clinically relevant, we examined the survival associated with expression of these probes in a dataset containing 273 gliomas of all histological subtypes.(16) For this exploratory analysis, we have taken the 75 highest and lowest expressing tumours for each probe and determined whether the survival for these two groups was statistically different (at $p < 0.01$). A total of 12 probes were associated with survival, of which eleven were negatively correlated with survival and one probe positively correlated with survival. (see table 2). The 11/20 ratio was a significant enrichment for genes inversely correlated with survival: In this entire dataset 11636/54675 probesets were negatively correlated with survival and 8649/54675 were positively correlated.



liferation and migration.

Two graphs showing the proliferation (A) and migration (B) of the stably transfected HOG cells with EGFR wt-bio-GFP, EGFRvIII-bio-GFP, EGFR L858R-bio-GFP and bio-GFP. The upper graph displays the proliferation of the stably transfected cell lines over a period of 162 hours. In our experiments we consistently found that the two EGFR mutants, vIII and L858R grew slower than GFP. A difference in proliferation between bio-EGFRwt and bio-GFP expressing cells was not consistent in all experiments. The lower graph display a decreased migration when comparing the slope between 6 and 21 hours for bio- EGFRvIII and bio-EGFR- L858R, compared to the bio-GFP control (both $p < 0.001$) or compared to bio-EGFR-wt cells. (also both $P < 0.001$) Migration of EGFR-wt-bio-GFP cells was not significantly different from bio-GFP controls ($P = 0.58$). The lines of EGFRvIII-bio-GFP and EGFR L858R-bio-GFP strongly overlap in this figure and appears as one line.

Mutations in EGFR differentially affect cell growth and migration

Because our results indicate that each mutation has unique molecular properties, we determined whether the various forms of EGFR also differentially affect cell physiology. For this, we created human glioma, HOG, cells stably expressing *EGFR wt-bio-GFP*, *EGFRvIII-bio-GFP*, *EGFR L858R-bio-GFP* or *bio-GFP*. HOG cells stably expressing *EGFRvIII-bio-GFP* and *EGFR L858R-bio-GFP* showed a decreased proliferation compared to the *bio-GFP* control whereas *EGFR wt-bio-GFP* had a growth rate that was comparable to the *bio-*

GFP control. *EGFRvIII-bio-GFP* and *EGFR L858R-bio-GFP* showed a similar reduction in proliferation. The differences between constructs were consistently observed over multiple experiments (n=4). (figure 3).

In a wound healing assay, the *EGFR L858-bio-GFP* and *EGFRvIII-bio-GFP* stably transfected HOG cells had a significantly slower migration compared to *EGFR wt-bio-GFP* and *bio-GFP* cells ($P < 0.001$, for all comparisons figure 3). *EGFRvIII-bio-GFP* and *EGFR L858R-bio-GFP* had a similar rate of migration. There was no difference in the migration between *EGFR wt-bio-GFP* and *bio-GFP* control cells. The difference between constructs was consistently observed in two experiments (n=2).

These experiments, demonstrate that different mutations in *EGFR* differentially affect cell physiology.

Discussion

In this paper we have generated various mutational constructs of *EGFR*. Our data demonstrate that different mutations in *EGFR* associate with different proteins. For example, DOCK4 doesn't bind to *EGFR L858R* but it binds to *EGFRwt* and *EGFRvIII* while UGGT1 binds to *EGFRvIII* and *EGFR L858R* but not to *EGFRwt*. In addition to the mutation specific protein associations, different mutations in *EGFR* also result in the induction of a unique transcriptional response. Interestingly, the expression of many of these genes is negatively correlated to patient survival. Finally, mutations in *EGFR* differentially affect cell growth and migration resulting in a decreased growth and migration for *EGFRvIII* and *EGFR L858R*.

Our experiments demonstrate that DOCK4 associates with *EGFRvIII* and, to a lesser extent, *EGFR wt* but not with *EGFR L858R*. DOCK4 reduces invasion and cell growth and is mutated in various tumours. (17) Rescue of these tumors with wildtype DOCK4 results in reduced growth and invasion. (17) DOCK4 is a binding partner of ELMO2, a protein that is involved in cell migration. (18) Of note, ELMO2 was also identified as an *EGFR* binding partner in this study. Furthermore, an ILK/ELMO2 complex is also known to be stimulated by *EGFR* resulting in migration. (19) As our experiments show that cell lines expressing *EGFRvIII* have a different speed of migration compared to *EGFRwt* cells, these results are in line with the observation that *EGFRvIII* and *EGFRwt* differentially associate with proteins like DOCK4 that are involved in cellular migration.

DOCK4 also functions as a scaffold protein within the Wnt signaling pathway and is essential for activation of this pathway in vivo. (20) There are several reports that provide evidence for crosstalk between *EGFR* and the WNT signaling. In *Drosophila* for example, phyllopod is a downstream activator of *EGFR* and inhibits the WNT signaling. Furthermore, Wnt3a activates proliferation and motility through *EGFR* and via the ERK pathway. (21) Our data suggest that DOCK4 is another link between these two pathways.

UGGT1 is a relatively unknown protein that plays a role in the ER preventing incorrectly folded proteins to leave it. (22) Recent research has found that in the *L858R* mutation in *EGFR* reduces the disorganised conformation of the intracellular domain. (23) It is possible that the disorganised intracellular domain of *EGFR L858R* and *EGFRvIII* result in an association UGGT1.

Although several groups have reported that mutations in *EGFR* induce proliferation, our data shows that EGFRvIII and EGFR L858R display a reduced proliferation compared to both EGFRwt and control cells. (24) It has been reported that, in some cell lines with high expression of EGFR, stimulation by EGF results in decreased proliferation, cell adhesion and increase in apoptosis. (25) As EGFRvIII and EGFR L858R are constitutively active, this could explain why the cell lines containing these mutations show a reduced proliferation.

Previous research has shown that expression of either EGFRvIII or EGFR L858R results in an increased migration capacity compared to EGFR wildtype. (26, 27) Our migration assays were performed in HOG cells, which originated from an oligodendroglioma whereas other groups have used different cell lines. It is therefore possible that effects of EGFR mutations on migration are dependent on the cell line used.

Our data is in-line with observations made by other groups who have shown that EGFR-wt and EGFRvIII have different functional consequences. For example, EGFR associates with Cbl proteins whereas EGFRvIII does not, ultimately resulting in a reduced degradation rate of EGFRvIII. (28, 29) In our experiments however, Cbl proteins do not show mutation specific binding. This difference is likely due to the fact that (differential) binding to Cbl proteins occurs only after stimulation with EGF; in these experiments we did not stimulate cells with EGF. Different mutations in EGFR also induce phosphorylation of different substrates and depend on different downstream pathways: EGFRvIII nuclear signalling via STAT5 depends on SRC family kinases, EGFRwt does not (30, 31). EGFR-vIII but not EGFR-L858R is imported into the nucleus where it affects DNA repair in response to ionizing radiation. (32) Our data expand on these observations by performing a detailed characterization of the mutation specific pathways that are affected.

Mutation specific pathway activation, such as reported here for EGFR, has also been reported for other causal cancer genes. For example, NRD1, a protein associated specifically with the R273H mutation in TP53, promotes invasion. (33, 34) In addition, the TP53 R267P mutation activates the p21 promoter whereas the TP53 O278S does not. (34) In PIK3CA there are two common types of mutations, those located in the kinase domain and those located in the helical domain, that differentially downstream AKT signalling. (11) Furthermore, one specific PIK3CA mutant, E545K displays directional migration whereas another mutant, H1047R, does not. (35)

In summary, our results show that EGFR and the mutants EGFRvIII and EGFR L858R are not identical when it comes to binding, migration, proliferation and gene expression. Mutations within a single protein therefore should not be considered identical. As each mutation in EGFR activates unique downstream pathways, it is possible that EGFR inhibitors do not equally inhibit these mutation specific pathways. Our data therefore argue for mutation specific targeted therapies.

References

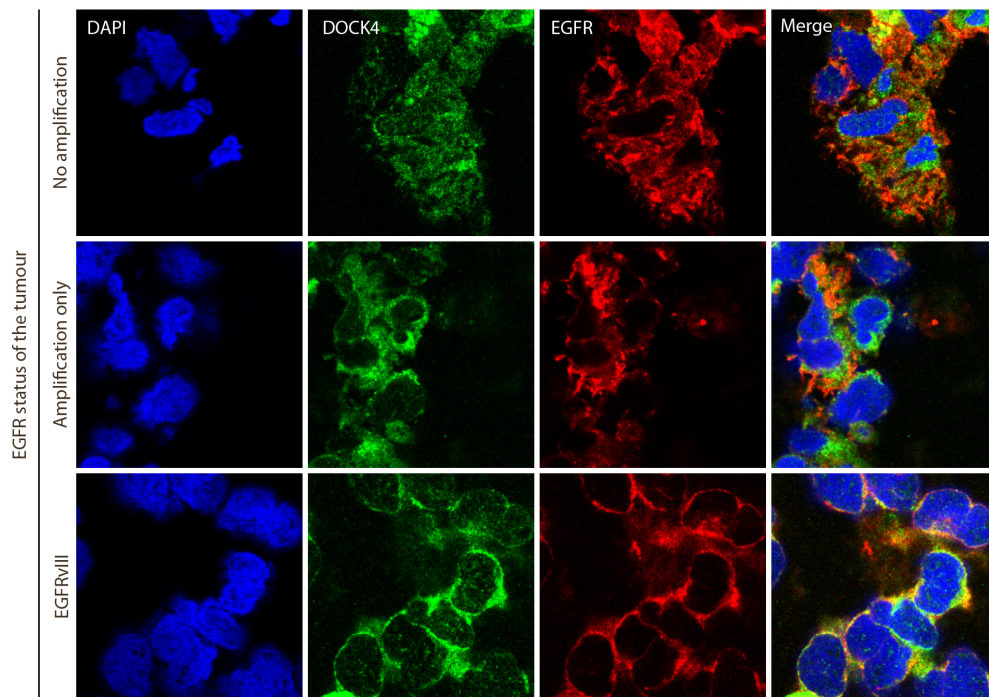
1. Alberts B, Wilson JH, Hunt T. Molecular biology of the cell. 5th ed. New York: Garland Science; 2008.
2. Liu P, Cleveland T, Bouyain S, Byrne PO, Longo PA, Leahy DJ. A single ligand is sufficient to activate EGFR dimers. Proc Natl Acad Sci U S A. Jul 3;109(27):10861-6.

3. van den Bent MJ, Brandes AA, Rampling R, Kouwenhoven MC, Kros JM, Carpentier AF, et al. Randomized phase II trial of erlotinib versus temozolomide or carmustine in recurrent glioblastoma: EORTC brain tumor group study 26034. *J Clin Oncol*. 2009 Mar 10;27(8):1268-74.
4. Nicholson RI, Gee JM, Harper ME. EGFR and cancer prognosis. *Eur J Cancer*. 2001 Sep;37 Suppl 4:S9-15.
5. Bamford S, Dawson E, Forbes S, Clements J, Pettett R, Dogan A, et al. The COSMIC (Catalogue of Somatic Mutations in Cancer) database and website. *Br J Cancer*. 2004 Jul 19;91(2):355-8.
6. Nyati MK, Morgan MA, Feng FY, Lawrence TS. Integration of EGFR inhibitors with radiochemotherapy. *Nat Rev Cancer*. 2006 Nov;6(11):876-85.
7. Gajiwala KS, Feng J, Ferre R, Ryan K, Brodsky O, Weinrich S, et al. Insights into the Aberrant Activity of Mutant EGFR Kinase Domain and Drug Recognition. *Structure*. Feb 5;21(2):209-19.
8. Comprehensive genomic characterization defines human glioblastoma genes and core pathways. *Nature*. 2008 Oct 23;455(7216):1061-8.
9. Pines G, Kostler WJ, Yarden Y. Oncogenic mutant forms of EGFR: lessons in signal transduction and targets for cancer therapy. *FEBS Lett*. Jun 18;584(12):2699-706.
10. Gravendeel AM, Kloosterhof NK, Bralten LB, Marion Rv, Dubbink HJ, Dinjens WN, et al. Segregation of non-R132H mutations in IDH1 into distinct molecular subtypes of glioma. *Human Mutation*. 2009;in press.
11. Ross RL, Askham JM, Knowles MA. PIK3CA mutation spectrum in urothelial carcinoma reflects cell context-dependent signaling and phenotypic outputs. *Oncogene*. Feb 7;32(6):768-76.
12. Li L, Dutra A, Pak E, Labrie JE, 3rd, Gerstein RM, Pandolfi PP, et al. EGFRvIII expression and PTEN loss synergistically induce chromosomal instability and glial tumors. *Neuro Oncol*. 2009 Feb;11(1):9-21.
13. Greulich H, Chen TH, Feng W, Janne PA, Alvarez JV, Zappaterra M, et al. Oncogenic transformation by inhibitor-sensitive and -resistant EGFR mutants. *PLoS Med*. 2005 Nov;2(11):e313.
14. Bralten LB, Kloosterhof NK, Balvers R, Sacchetti A, Lapre L, Lamfers M, et al. IDH1 R132H decreases proliferation of glioma cell lines in vitro and in vivo. *Ann Neurol*. Mar;69(3):455-63.
15. van den Berg DL, Snoek T, Mullin NP, Yates A, Bezstarosti K, Demmers J, et al. An Oct4-centered protein interaction network in embryonic stem cells. *Cell Stem Cell*. Apr 2;6(4):369-81.
16. Gravendeel LA, Kouwenhoven MC, Gevaert O, de Rooij JJ, Stubbs AP, Duijm JE, et al. Intrinsic Gene Expression Profiles of Gliomas Are a Better Predictor of Survival than Histology. *Cancer Res*. 2009 Nov 17.
17. Yajnik V, Paulding C, Sordella R, McClatchey AI, Saito M, Wahrer DC, et al. DOCK4, a GTPase activator, is disrupted during tumorigenesis. *Cell*. 2003 Mar 7;112(5):673-84.
18. Hiramoto-Yamaki N, Takeuchi S, Ueda S, Harada K, Fujimoto S, Negishi M, et al. Ephexin4 and EphA2 mediate cell migration through a RhoG-dependent mechanism. *J Cell Biol*. Aug 9;190(3):461-77.
19. Ho E, Dagnino L. Emerging role of ILK and ELMO2 in the integration of adhesion and migration pathways. *Cell Adh Migr*. May-Jun;6(3):168-72.
20. Upadhyay G, Goessling W, North TE, Xavier R, Zon LI, Yajnik V. Molecular association between beta-catenin degradation complex and Rac guanine exchange factor DOCK4 is essential for Wnt/beta-catenin signaling. *Oncogene*. 2008 Oct 2;27(44):5845-55.
21. Hu T, Li C. Convergence between Wnt-beta-catenin and EGFR signaling in cancer. *Mol Cancer*.9:236.
22. Ritter C, Helenius A. Recognition of local glycoprotein misfolding by the ER folding sensor UDP-glucose:glycoprotein glucosyltransferase. *Nat Struct Biol*. 2000 Apr;7(4):278-80.
23. Shan Y, Eastwood MP, Zhang X, Kim ET, Arkhipov A, Dror RO, et al. Oncogenic mutations counteract intrinsic disorder in the EGFR kinase and promote receptor dimerization. *Cell*. May 11;149(4):860-70.
24. Wang MY, Lu KV, Zhu S, Dia EQ, Vivanco I, Shackelford GM, et al. Mammalian target of rapamycin inhibition promotes response to epidermal growth factor receptor kinase inhibitors in PTEN-deficient and PTEN-intact glioblastoma cells. *Cancer Res*. 2006 Aug 15;66(16):7864-9.
25. Zhao X, Dai W, Zhu H, Zhang Y, Cao L, Ye Q, et al. Epidermal growth factor (EGF) induces apoptosis in a transfected cell line expressing EGF receptor on its membrane. *Cell Biol Int*. 2006 Aug;30(8):653-8.
26. Kapoor GS, O'Rourke DM. SIRPalpha1 receptors interfere with the EGFRvIII signalosome to inhibit glioblastoma cell transformation and migration. *Oncogene*. Jul 22;29(29):4130-44.

27. Chung BM, Dimri M, George M, Reddi AL, Chen G, Band V, et al. The role of cooperativity with Src in oncogenic transformation mediated by non-small cell lung cancer-associated EGF receptor mutants. *Oncogene*. 2009 Apr 23;28(16):1821-32.
28. Schmidt MH, Furnari FB, Cavenee WK, Bogler O. Epidermal growth factor receptor signaling intensity determines intracellular protein interactions, ubiquitination, and internalization. *Proc Natl Acad Sci U S A*. 2003 May 27;100(11):6505-10.
29. Han W, Zhang T, Yu H, Foulke JG, Tang CK. Hypophosphorylation of residue Y1045 leads to defective downregulation of EGFRvIII. *Cancer Biol Ther*. 2006 Oct;5(10):1361-8.
30. Chumbalkar V, Latha K, Hwang Y, Maywald R, Hawley L, Sawaya R, et al. Analysis of phosphotyrosine signaling in glioblastoma identifies STAT5 as a novel downstream target of DeltaEGFR. *J Proteome Res*. Mar 4;10(3):1343-52.
31. Latha K, Li M, Chumbalkar V, Gururaj A, Hwang Y, Dakeng S, et al. Nuclear EGFRvIII-STAT5b complex contributes to glioblastoma cell survival by direct activation of the Bcl-XL promoter. *Int J Cancer*. Feb 1;132(3):509-20.
32. Liccardi G, Hartley JA, Hochhauser D. EGFR nuclear translocation modulates DNA repair following cisplatin and ionizing radiation treatment. *Cancer Res*. Feb 1;71(3):1103-14.
33. Vogelstein B, Sur S, & Prives, C. . p53 : The Most Frequently Altered Gene in Human Cancers. *Nature Education*. 2010; 3(9):6.
34. Vaughan CA, Frum R, Pearsall I, Singh S, Windle B, Yeudall A, et al. Allele specific gain-of-function activity of p53 mutants in lung cancer cells. *Biochem Biophys Res Commun*. Nov 9;428(1):6-10.
35. Pang H, Flinn R, Patsialou A, Wyckoff J, Roussos ET, Wu H, et al. Differential enhancement of breast cancer cell motility and metastasis by helical and kinase domain mutations of class IA phosphoinositide 3-kinase. *Cancer Res*. 2009 Dec 1;69(23):8868-76.

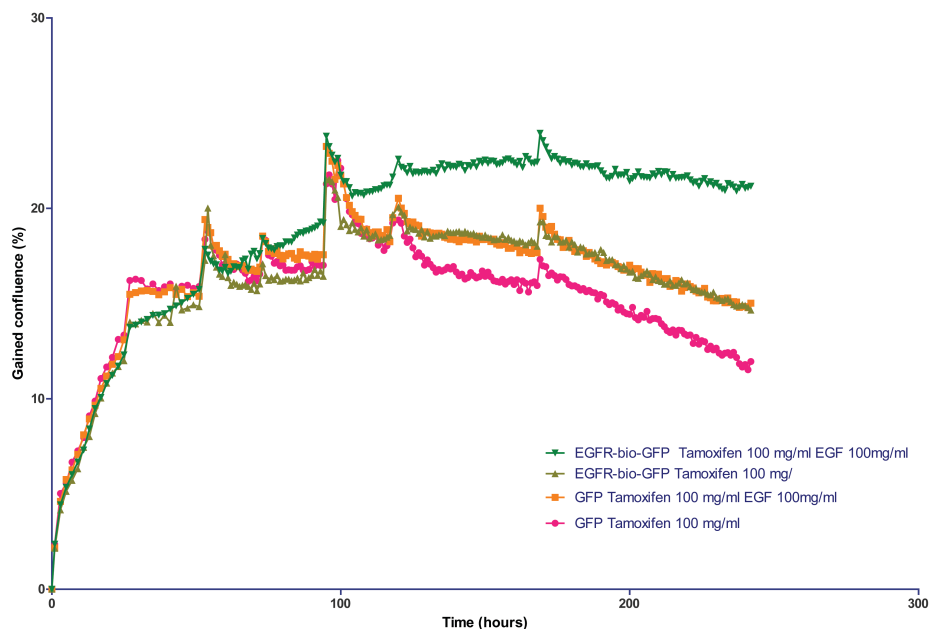
Supplementary figures and tables

Supplementary figure 1: Immunofluorescence staining for DOCK4 and EGFR in human glioma tissue samples



DOCK4 seems to colocalise with EGFR in tumour samples. We have looked at three glioblastoma samples, one without EGFR alterations, one with EGFR amplification and the last one with EGFR amplification and EGFRvIII.

Supplementary figure 2: Growth in ZR751 cells after Tamoxifen treatment with or without EGF rescue



Supplementary figure 2: In order to determine if the biotin and GFP tag did not interfere with the functionality of the constructs we transfected wildtype EGFR-biotin-GFP in ZR751 cells. After 24 hours they were subjected to 100mg/ml Tamoxifen. Cells were incubated either with or without EGF (concentration 100 mg/ml) and with or without Tamoxifen. Functional EGFR should be able to rescue these cells and allow growth. Growth was measured using an Incucyte (Essen instruments, Hertfordshire, UK) for 242 hours. We can conclude from this that the addition of biotin-GFP does not interfere with the regular function of EGFR.

Supplementary table 1: Proteins found in EGFR pulldown

EGFR	DNM2	SPTLC2	ARL1	SHROOM3
SOS1	IPO9	UBE3C	CORO1C	BAG5
DOCK4	ALDH3B1	DDX20	TMOD3	RRAS2
ARHGEF5	NF1	PIK3CA	AP1G1	PPP2CA
CBL	VAPA	DNAJC30	S100A7	SC4MOL
PIK3R1	STAT3	DNAJB14	MAPK1	OSTC
ELMO2	UPP1	AP1S2	AP3S1	DHRS7B
AP2A1	EIF2B3	HADHA	OPA1	WDR6
UBASH3B	NGLY1	TBRG4	SDF2L1	RANGAP1
IPO5	AP2S1	TUBGCP2	WWOX	CAV1
AP2B1	NCDN	P14	CBX3	SACM1L
PKP3	XIAP	VCP	DHCR24	C8orf55
GRB2	MAP4K5	AP1G2	DHRS2	AP1S1
ATXN10	LAMB3	XPO5	TMEM43	DNAJC7
TNPO1	CDC37	TMCO1	TOMM20	EIF2S3
VAV3	LTN1	VPS28	NPEPPS	ARF6
IFI16	IPO4	BANF1	STAT1	RPS5
XPO1	TSG101	NUP93	GNB1	SSR3
ERRFI1	AP1M1	DNAJC16	NUMB	SNRPE
SAAL1	HSPB1	ABLIM3	TRPM1	MYADM
HKDC1	PLK1	CLN6	OCIAD2	SLC39A11
HEATR3	SUPT16H	RAC1	DCAF7	SERBP1
AP2M1	GALNT3	DGKA	SSRP1	GRB7
CRKL	SEC61A1	LAD1	CANX	
CKAP4	FAM125A	ECH1	EIF6	
PIK3CB	EIF2B4	RP9	CTNND1	

A list of proteins found to be present in either EGFR, EGFRvIII or in EGFR L858R but not in a GFP control.

Supplementary table 2: A list of probes that display at least a 2-fold difference compared to GFP

Probe Set ID	EGFR	EGFR L858R	EGFRvIII	Present
1555929_s_at	1	1		1
1556054_at		1		1
1556347_at		1		1
1556462_a_at		1		1
1556543_at		1		1
1557240_a_at		1		1
1557270_at		1		1
1557422_at		1		1
1557543_at		1		1
1557738_at		1		1
1557780_at		1		1
1558048_x_at	1	1		1
1558250_s_at		1		1
1558714_at		1	1	1
1558739_at		1		1
1558740_s_at		1		1
1558854_a_at		1		1
1558877_at		1		1
1559156_at		1		1
1559214_at	1	1	1	1
1559360_at		1		1
1559391_s_at		1		1
1559410_at		1		1
1559524_at		1		1
1559723_s_at		1		1
1559916_a_at		1		1
1560049_at		1		1
1560082_at		1		1
1560271_at		1	1	1
1560659_at		1		1

1560763_at		1		1
1561155_at		1		1
1561195_at		1		1
1562280_at		1		1
1563217_at		1		1
1563494_at		1		1
1564378_a_at		1		1
1565689_at	1	1		1
1565830_at	1	1		1
1565886_at		1		1
1566163_at		1		1
1568408_x_at	1	1	1	1
1568799_at		1		1
1569180_at		1		1
1569181_x_at		1		1
1569482_at	1	1	1	1
1570143_at		1		1
206548_at	1	1		1
213605_s_at		1		1
214731_at		1		1
214862_x_at		1		1
215592_at	1	1	1	1
216000_at		1		1
216683_at		1		1
217164_at		1		1
220728_at		1		1
220915_s_at		1		1
222227_at	1	1	1	1
222371_at		1		1
224254_x_at		1		1
224549_x_at		1		1
225193_at		1		1
225239_at		1	1	1
226341_at		1		1
226458_at		1		1
226848_at		1		1
227062_at		1		1
227576_at		1		1
227663_at		1		1
227943_at	1	1	1	1
228216_at		1		1
228387_at		1		1
228390_at		1		1
228465_at		1		1
228539_at		1		1
228623_at		1		1
228919_at		1		1
229072_at	1			1
229206_at		1		1
229243_at		1		1
229298_at		1		1
229315_at		1		1
229366_at		1		1
229413_s_at			1	1
229434_at		1		1
229455_at		1		1
229470_at		1		1
229483_at		1		1
229692_at		1		1
229869_at		1		1
229970_at	1	1		1
230312_at		1		1
230653_at		1		1
230657_at	1			1
230791_at		1		1
230961_at		1		1
231165_at		1		1
231502_at		1		1
231597_x_at	1	1		1
231964_at	1	1		1
232134_at		1		1
232174_at		1		1
232257_s_at	1			1

232372_at	1	1	1	1
232431_at	1	1	1	1
232453_at		1	1	1
232511_at		1		1
232565_at		1		1
232628_at	1	1		1
232653_at		1		1
232726_at		1		1
232744_x_at		1		1
232773_at		1		1
232793_at		1		1
232889_at		1		1
233036_at		1		1
233090_at		1		1
233152_x_at	1	1		1
233300_at		1		1
233518_at		1		1
233611_at		1		1
233713_at		1		1
233908_x_at		1	1	1
233921_s_at		1	1	1
234562_x_at		1		1
234675_x_at		1		1
234723_x_at		1		1
234989_at		1		1
235028_at		1		1
235224_s_at		1		1
235274_at		1		1
235286_at	1	1	1	1
235456_at	1			1
235555_at		1	1	1
235581_at	1			1
235693_at		1		1
235701_at		1		1
235705_at		1		1
235782_at		1		1
235786_at	1	1		1
235803_at		1		1
235919_at	1	1		1
235926_at		1		1
235947_at	1	1		1
235985_at		1		1
236032_at		1		1
236099_at			1	1
236103_at		1		1
236170_x_at	1	1		1
236194_at		1		1
236220_at		1		1
236229_at		1		1
236379_at		1		1
236404_at		1		1
236472_at		1		1
236750_at		1		1
236924_at		1		1
237001_at		1		1
237007_at		1		1
237269_at	1	1	1	1
237301_at	1			1
237310_at		1		1
237330_at		1		1
237388_at		1		1
237483_at		1		1
237789_at		1		1
238000_at		1		1
238595_at		1		1
238651_at		1		1
238729_x_at		1		1
238774_at		1		1
238883_at		1		1
238913_at		1		1
238919_at		1		1
238932_at	1	1		1
239049_at		1		1

239227_at		1		1
239347_at		1		1
239409_at	1	1		1
239516_at		1		1
239630_at		1		1
239673_at		1		1
239862_at		1		1
239907_at		1		1
239934_x_at		1		1
239946_at	1	1	1	1
240143_at		1		1
240170_at		1		1
240326_at		1		1
240421_x_at		1		1
240557_at	1	1		1
240558_at		1		1
240721_at	1	1		1
240798_at	1	1		1
241506_at		1		1
241569_at		1		1
241681_at		1		1
241773_at		1		1
241786_at		1		1
241838_at		1		1
241853_at		1		1
241858_at		1		1
241863_x_at		1		1
241893_at	1	1	1	1
242008_at		1		1
242052_at		1		1
242110_at		1		1
242239_at		1		1
242270_at		1		1
242273_at	1	1		1
242310_at		1		1
242434_at	1	1		1
242440_at		1		1
242457_at		1		1
242471_at		1		1
242563_at		1		1
242598_at		1		1
242671_at		1		1
242708_at	1	1		1
242715_at		1		1
242801_at		1		1
242824_at		1		1
242827_x_at		1		1
242836_at		1		1
242859_at		1		1
242894_at		1		1
242920_at		1		1
242968_at		1		1
242989_at		1		1
243003_at		1		1
243006_at		1		1
243008_at		1		1
243009_at		1		1
243016_at	1	1		1
243416_at		1		1
243431_at		1	1	1
243509_at	1	1	1	1
243527_at		1		1
243561_at		1		1
243736_at		1		1
243751_at		1		1
243768_at		1		1
243915_at		1		1
243934_at	1	1		1
243964_at		1	1	1
244112_x_at		1		1
244341_at		1		1
244383_at		1		1
244414_at		1		1

244433_at		1		1
244551_at		1		1
244610_x_at		1		1
244726_at		1		1
244803_at		1		1
244813_at		1		1
244845_at		1		1
228124_at		1		1
226030_at		1		1
213808_at		1		1
230634_x_at		1		1
225701_at			1	1
232184_at		1		1
216550_x_at		1		1
1556361_s_at		1		1
1569607_s_at			1	1
1561079_at		1		1
220940_at	1	1	1	1
227337_at		1		1
201012_at		1		1
210090_at		1		1
205239_at		1		1
1553349_at		1		1
220468_at		1		1
210718_s_at		1		1
242727_at		1		1
219996_at		1		1
219918_s_at	1	1		1
1554980_a_at		1	1	1
202672_s_at		1	1	1
205704_s_at		1		1
1553959_a_at	1	1		1
1559078_at		1		1
1555372_at		1		1
203140_at		1		1
1554443_s_at		1		1
201170_s_at		1		1
225144_at		1		1
207186_s_at		1		1
230056_at		1		1
238545_at	1	1	1	1
238890_at		1		1
209183_s_at			1	1
1559265_at		1		1
1559266_s_at		1		1
238593_at		1		1
227099_s_at	1	1	1	1
218723_s_at		1		1
215087_at	1	1		1
208109_s_at	1	1		1
239208_s_at		1		1
220770_s_at		1		1
212913_at		1		1
239297_at	1			1
231270_at		1	1	1
239106_at		1		1
1554327_a_at		1		1
240983_s_at		1		1
219342_at		1		1
238549_at		1		1
239014_at		1		1
232362_at	1	1		1
205899_at		1		1
204490_s_at		1		1
203252_at	1	1	1	1
202284_s_at		1		1
228482_at			1	1
212501_at	1	1	1	1
204203_at		1	1	1
205046_at	1	1	1	1
205250_s_at		1		1
224150_s_at		1		1
219270_at	1	1	1	1

226350_at		1		1
239436_at		1		1
242492_at		1		1
223500_at		1		1
204573_at		1		1
225557_at		1	1	1
209101_at		1		1
206085_s_at		1	1	1
217127_at	1	1	1	1
201289_at		1		1
210764_s_at		1		1
209158_s_at		1		1
1562209_at	1			1
1554049_s_at		1	1	1
242428_at		1		1
209383_at	1	1	1	1
225434_at		1		1
204383_at		1		1
239730_at	1	1	1	1
32032_at		1		1
242539_at	1	1		1
230229_at		1		1
203791_at		1		1
200664_s_at	1	1		1
200666_s_at	1	1		1
223054_at		1	1	1
1554462_a_at		1	1	1
202842_s_at		1	1	1
202843_at	1	1	1	1
1558080_s_at			1	1
214844_s_at		1		1
205493_s_at		1		1
232098_at		1		1
208891_at	1	1	1	1
208892_s_at	1	1	1	1
208893_s_at	1	1	1	1
228116_at		1		1
201983_s_at	1	1	1	1
210984_x_at	1	1	1	1
211607_x_at	1	1	1	1
201693_s_at	1	1	1	1
201694_s_at	1	1	1	1
227404_s_at	1	1	1	1
205249_at	1	1		1
206115_at	1	1		1
207768_at		1		1
205222_at		1		1
214314_s_at		1		1
227491_at		1		1
203499_at		1		1
227449_at		1		1
206852_at		1		1
229288_at		1		1
238533_at		1		1
241252_at		1		1
221911_at	1	1		1
211603_s_at		1		1
203348_s_at	1	1	1	1
203349_s_at	1	1	1	1
216375_s_at		1		1
230102_at	1	1	1	1
204363_at		1		1
229512_at		1		1
217966_s_at		1		1
217967_s_at		1	1	1
223791_at		1		1
219895_at		1		1
228587_at		1		1
225667_s_at		1		1
236976_at		1		1
244071_at		1	1	1
236994_at		1		1
228427_at			1	1

242828_at		1		1
239005_at		1		1
229246_at		1		1
210414_at		1		1
209189_at	1	1	1	1
202768_at		1		1
218880_at		1	1	1
205140_at		1		1
230964_at		1		1
206109_at		1	1	1
227499_at		1		1
239082_at		1		1
213524_s_at		1		1
207574_s_at		1		1
209304_x_at		1		1
209305_s_at		1		1
213560_at		1		1
221577_x_at	1	1	1	1
204472_at		1		1
1560133_at		1		1
222710_at			1	1
213212_x_at		1		1
208798_x_at		1		1
208311_at		1		1
210999_s_at		1		1
235405_at		1		1
215470_at		1		1
226606_s_at	1	1	1	1
227235_at	1	1		1
209315_at		1		1
232975_at		1		1
225989_at		1		1
217168_s_at	1	1	1	1
221606_s_at		1		1
207165_at		1		1
209709_s_at		1		1
225107_at		1		1
231786_at		1		1
238808_at		1		1
214457_at	1	1	1	1
210189_at		1		1
211936_at	1	1	1	1
230031_at	1	1	1	1
117_at	1	1		1
213418_at	1	1	1	1
221667_s_at		1		1
200825_s_at	1	1	1	1
202081_at		1		1
201631_s_at		1		1
203153_at		1		1
219174_at		1		1
210095_s_at		1		1
204912_at		1		1
206924_at		1		1
207160_at		1		1
207375_s_at		1		1
222062_at		1		1
214705_at		1		1
210587_at	1	1	1	1
202794_at		1		1
237056_at			1	1
201625_s_at		1		1
220225_at		1		1
232352_at		1		1
203337_x_at	1	1	1	1
240037_at		1		1
201473_at		1		1
223584_s_at		1		1
223412_at		1		1
219615_s_at		1		1
212188_at		1		1
212192_at		1		1
1555897_at		1		1

214295_at		1		1
215268_at		1		1
212779_at		1		1
204444_at		1		1
228377_at		1		1
210634_at		1		1
232297_at		1		1
1561206_at		1		1
201596_x_at		1		1
1556616_a_at	1	1	1	1
227074_at		1		1
233512_at		1		1
1554609_at		1		1
215287_at		1		1
241535_at		1		1
222947_at		1		1
240382_at		1		1
221973_at	1	1	1	1
221919_at		1		1
240908_at		1		1
239017_at	1	1		1
213703_at	1	1	1	1
220609_at		1		1
1557113_at		1		1
229007_at		1		1
1556064_at		1		1
232182_at	1	1		1
65588_at		1		1
236181_at	1	1		1
242329_at		1	1	1
1558688_at	1	1	1	1
228908_s_at		1		1
1557765_at	1	1	1	1
1558404_at			1	1
239343_at		1		1
224686_x_at		1		1
1559580_at		1		1
241792_x_at		1		1
242389_at		1		1
223687_s_at		1		1
228841_at		1		1
240344_x_at		1		1
226748_at		1		1
205193_at	1	1	1	1
36711_at	1	1	1	1
226206_at		1		1
224558_s_at		1		1
202655_at	1	1	1	1
211371_at	1	1	1	1
205192_at		1		1
205027_s_at		1		1
235421_at		1		1
213132_s_at		1		1
200798_x_at		1		1
225955_at		1		1
232194_at		1		1
225316_at	1	1		1
232568_at		1		1
210694_s_at		1		1
1569652_at		1		1
224873_s_at		1		1
220346_at	1			1
228846_at		1		1
215318_at		1		1
228529_at		1		1
212803_at		1		1
221207_s_at	1	1		1
242121_at		1		1
225786_at		1		1
200632_s_at		1		1
224565_at	1	1	1	1
224566_at		1	1	1
226103_at	1	1		1

228933_at		1		1
221348_at		1		1
213479_at		1		1
206645_s_at		1		1
229422_at		1		1
1557071_s_at		1		1
223535_at		1		1
224938_at		1		1
205728_at		1		1
213825_at	1	1	1	1
1554008_at			1	1
1564494_s_at		1		1
210941_at	1	1	1	1
228640_at	1	1		1
203378_at	1			1
226119_at		1		1
229287_at		1		1
222380_s_at		1		1
214582_at		1		1
222317_at	1	1		1
208658_at			1	1
211048_s_at	1		1	1
241801_at		1		1
217996_at		1		1
217997_at		1		1
209803_s_at		1		1
202924_s_at		1		1
1560556_a_at		1		1
233241_at		1		1
213677_s_at		1		1
223568_s_at			1	1
226150_at	1	1	1	1
226384_at			1	1
228108_at		1		1
202014_at		1	1	1
37028_at		1	1	1
1555783_x_at		1		1
235987_at		1		1
1552348_at	1	1	1	1
211756_at		1		1
238695_s_at		1	1	1
208393_s_at		1		1
209349_at		1		1
1555339_at	1	1	1	1
1555340_x_at	1	1	1	1
1557432_at		1		1
1553185_at		1		1
1553186_x_at		1		1
230563_at		1		1
205178_s_at		1		1
212783_at		1		1
228455_at	1	1	1	1
219754_at		1		1
214409_at	1			1
234297_at	1	1		1
1553713_a_at		1		1
1570253_a_at	1	1	1	1
223169_s_at			1	1
1556088_at		1		1
213959_s_at	1			1
230469_at	1	1		1
219957_at		1		1
204351_at			1	1
236487_at	1	1		1
218681_s_at	1	1	1	1
202375_at	1		1	1
222385_x_at		1		1
215028_at		1		1
226492_at		1		1
202319_at	1			1
223394_at		1		1
223195_s_at		1		1
223196_s_at		1	1	1

212177_at		1		1
212179_at		1		1
1570507_at		1		1
242963_at		1		1
230165_at	1	1		1
235425_at		1		1
203320_at		1		1
226673_at			1	1
205234_at		1	1	1
209610_s_at	1	1	1	1
212810_s_at	1	1	1	1
212811_x_at	1	1	1	1
200924_s_at		1		1
212944_at		1	1	1
1569940_at		1		1
206566_at		1		1
212290_at		1		1
212292_at		1		1
212295_s_at		1		1
207528_s_at		1		1
235518_at		1		1
204368_at		1		1
1553055_a_at			1	1
1557078_at	1	1	1	1
207069_s_at		1		1
215623_x_at	1			1
203372_s_at			1	1
203373_at			1	1
206359_at			1	1
227697_at		1	1	1
225728_at		1		1
227426_at		1		1
230337_at		1		1
204915_s_at		1		1
226913_s_at		1		1
232529_at	1	1		1
204011_at		1		1
221489_s_at	1	1		1
227288_at		1		1
223821_s_at		1		1
223822_at		1		1
206552_s_at	1	1	1	1
1569566_at		1		1
238067_at		1		1
226126_at		1		1
208089_s_at		1		1
232692_at		1		1
209277_at		1		1
209278_s_at	1	1		1
209651_at		1		1
242163_at		1		1
201666_at		1		1
212194_s_at		1		1
235798_at		1		1
219253_at		1		1
236219_at	1			1
222690_s_at			1	1
218368_s_at		1		1
207536_s_at		1	1	1
206907_at		1		1
238520_at		1		1
202241_at		1		1
1555788_a_at	1	1	1	1
218145_at	1	1	1	1
210705_s_at	1	1	1	1
221897_at		1		1
230280_at		1		1
227236_at		1		1
215898_at		1		1
203234_at		1		1
212980_at		1		1
233595_at		1		1
213686_at		1		1

227988_s_at		1		1
235023_at		1		1
1557132_at		1		1
1554140_at	1			1
1554141_s_at	1			1
229816_at	1			1
213425_at		1		1
200670_at	1	1	1	1
224590_at		1		1
231211_s_at	1	1	1	1
1554036_at		1		1
1554037_a_at		1		1
228715_at		1		1
215427_s_at		1	1	1
235133_at	1	1		1
229240_at		1		1
243835_at		1		1
222186_at		1		1
201531_at		1		1
227796_at		1		1
235408_x_at		1		1
238631_at		1		1
228157_at		1		1
228185_at		1		1
231864_at		1		1
228927_at		1		1
213124_at		1	1	1
220444_at		1		1
204175_at		1		1
227822_at		1		1
235079_at		1		1
221645_s_at		1		1
1569157_s_at			1	1
226808_at		1		1
222814_s_at		1	1	1
1562988_at	1	1	1	1

Supplementary table 2: A list of probes that were differentially expressed more than 2 fold in EGFR, EGFR-vIII and EGFR L858R compared to GFP. A '1' means that this probe is expressed more than 2-fold for that construct. The last column indicates whether this probe was expressed more than 2-fold in any of the EGFR constructs.

Discussion

In this thesis we have described several genetic changes that occur in brain tumors and how they functionally contribute to tumorigenesis. In chapter two we have described *IDH1* mutations in detail and compared them to known information in the literature. (1) In chapter three we performed an in-depth analysis of *IDH1* mutations examining how the different genetic alterations compare to histology, other mutations and molecular subgroups. (2) Chapter four described the functional consequences of *IDH1* mutations in vitro and in vivo. (3) In chapter five we describe that different mutations within a single gene can have different molecular effects.

Supgroups of brain tumours

Brain tumors are a complex heterogeneous group of diseases. Therefore, researchers have focused on histologically or molecularly defined subgroups to determine subtype-specific driver mutations, mutually exclusive mutations or whether specific mutations occur together. One of the drawbacks of using molecular subgroups is the lack of consensus definitions, unlike the WHO classification for histology. For example, in gliomas there are currently four commonly used gene-expression based classifications and for medulloblastomas there are three, although in medulloblastoma one consensus classification is currently agreed on. (4-10) Also, different molecular methods for classification do not yield identical results. For example, the subgroups found by mRNA profiling in glioma have only partial overlap with subgroups found using methylation profiling. Therefore it is unlikely that a single classification will hold for every question. Potentially different, or novel, classifications are required for different situations, for example when identifying predictive response markers.

In chapter one we describe the presence of subtype-specific splice variants in medulloblastomas. The functional relevance of these specific splice variants remains to be determined but if they are required for tumor growth they can form novel targets for treatment. (11, 12) Although the frequency of any alteration in a tumour is not a marker for impact on the tumour, it does indicate relevance for the tumour. A frequently mutated gene indicates that this specific alteration is essential for a tumour type; however, a low frequency does not indicate a low impact on the tumour. In addition, since a tumour evolves, any alteration can be used to mark progression. The splice variants that we have identified in medulloblastomas occur in multiple samples, therefore they may be important for the disease. To determine importance, causality in e.g. cell growth, migration or gene expression assays is required.

Another question is whether we should focus our future research on single events, such as alternatively spliced genes, or rather on the interaction between commonly found alterations. Since a tumour is a complex interaction between multiple mutations it remains to be seen whether an increase in commonly used readout parameters will hold true in the interaction. For example, the different mutations differentially affect migration of cancer cells. It remains to be determined what the net effect is when these mutations co-occur in a single cancer cell. Classical molecular biological techniques, such as cell lines and animal models, can be used to investigate such interactions. Although these experiments will be more elaborate and costly, and difficult to setup, these should not be reasons not to perform these potentially interesting experiments.

High throughput screening, such as performed in chapter one, has so far giving us a limited number of that are mutated at high frequency mutations in glioma: *IDH1* in 2008 in low grade glioma and *FUBP1* and *CIC* in oligodendroglioma in 2011. (13, 14) Our own findings with exon arrays did not identify frequent novel mutations. (15, 16) Novel techniques give a wealth of publically available information; optimal usage of this information will be a challenge. Nonetheless, it is a potential treasure trove for a better understanding of the tumours. Using clusters of genes mutated together in a single tumour, might give a better understanding of how mutations interact. Using this data, heuristic approaches are most feasible allowing a starting point for future experiments.

IDH1

In gliomas, mutations in the *IDH1* gene almost always result, on protein level, in an arginine to histidine substitution at amino acid 132. (17) In this thesis, we demonstrate that in glioma alternative mutations affecting codon R132, non-R132H mutation, are more frequent in astrocyomas grade III and oligoastrocyomas grade III than in oligodendrogliomas. Furthermore, these non-R132H mutations are frequently found in combination with TP53 mutations.

Using the molecular classification, as described by Gravendeel *et al*, we do not observe a significant differential segregation, $p=0.05$, of the ratio of R132H/non-R132H mutations between molecular subtypes 5/22 for Intrinsic glioma subtypes (IGS)-17 and 1/27 for IGS-9. (2, 9) As both non-R132H and R132H mutations are found in the same molecular subtype, those tumours seem to be molecularly similar. Therefore, the effect of non-R132H mutations on the molecular signature is likely to be small, although the frequency

Table 1: Frequency distribution of non-R132H mutations in tumours

		Solitary central and periosteal cartilaginous tumours ^{22,23}		Ollier disease ^{23,27}		Maffucci syndrome ^{23,27}		AML ²⁴		Glioma ^{25,39,40}		Intrahepatic cholangiocarcinoma ²⁶	
		%	n	%	n	%	n	%	n	%	n	%	n
IDH1													
R132	H	17%	18	22%	14	0%	0	53%	59	91%	1478	0%	0
	C	46%	50	72%	46	100	17	31%	35	5%	77	55%	12
	G	19%	21	3%	2	0%	0	8%	9	2%	34	32%	7
	S	10%	11	2%	1	0%	0	4%	5	2%	27	5%	1
	L	8%	9	2%	1	0%	0	4%	4	1%	13	9%	2
	V										0%	1	
Total		109		64		17		112		1630		22	
IDH2													
R140	Q	0%	0	0%	0	0%	0	73%	122	0%*	0	**	
R172	K	0%	0	0%	0	0%	0	26%	44	60%	24	45%	5
	M	17%	2	0%	0	0%	0	1%	1	23%	9	0%	0
	W	0%	0	0%	0	0%	0	0%	0	13%	5	45%	5
	G	8%	1	0%	0	0%	0	0%	0	5%	2	0%	0
	S	75%	9	100	2	0%	0	0%	0	0%	0	0%	0
	N	0%	0	0%	0	0%	0	0%	0	0%	0	9%	1
Total		12		2		0		167		40		11	

Frequency of mutations found in IDH1 for codon R132, and codons R140 and R172 for IDH2 (* - the analysis of the mutations did not always include R140 as it became known at a later time, ** - not investigated)

of non-R132H mutations is too low to draw definite conclusions.

The differential distribution of mutations between IGS-9 and 17 may be due to tumour subtype specific differences in DNA repair or a different type of genetic stress. However, it is also possible that R132H and non-R132H are functionally different. If so, the next step in IDH1 research would be comparable to what we have done with EGFR as described in chapter five: functional analysis of different mutations. One could investigate with a thorough bioinformatical analysis if multiple mutations are associated, in different tumours, with gene expression or methylation patterns.

Recently an IDH1-R132H conditional knock-in mouse model has been described. (18) In this model increased number of haematopoietic progenitor cells was found after Cre expression in haematopoietic cells. An increase in HIF1 α protein levels was also observed in these mice when IDH1 R132H is expressed in Nestin+ cells (i.e. when mice are crossed with mice expressing Cre-recombinase driven by the Nestin promoter). (19) An increase in HIF1a levels was also found by Zhao and colleagues in human brain tumours containing IDH1 mutations. (20) Knock-in mice do not develop glial brain tumours, and the heterozygous knock-ins are lethal just after birth. A reduced cellular proliferation was found in the embryonic brains of mice 5 days after Nestin-cre expression without changes in the number of precursor cells. For example, the ratio between neural stem cells, glial-restricted precursor cells and Promonin-1 and A2B5 negative cells, was not affected. This is in contrast with the haematopoietic mouse model; in this model an increase in the number of precursor cells was identified. Since the double negative group of more differentiated cells contains neural-restricted precursor cells, differentiated neurons, glial cells and some endothelial cells, it remains possible that an increase in the number of progenitor cells is present within one of these subsets of cells. This is specifically possible for the neural restricted precursor cells as they comprise only 10% of the Nestin+ cell population. The differences in the increase in number of progenitor cells between the haematopoietic mouse model and the brain model may however also be an indication that the tumours initiate differently.

Distribution of mutations amongst tumours

IDH1 mutations are not restricted to gliomas; they are also found in acute myeloid leukemia (AML), Maffucci syndrome (MF) and Olliers disease (Oll) (characterized by multiple enchondromas, benign lesions mostly found in the bones of the hands and feet (21)) and intrahepatic cholangiocarcinoma. When looking in detail at *IDH1* mutations in these tumor types, we observe a tumour type specific mutation spectrum. The different mutation frequencies are highlighted in table 1 for codon R132 in *IDH1* and codons R172 and R140 in *IDH2*. (22-27) For example, the *IDH1* R132C mutations are found at high frequency in AML whereas this mutation is rare in gliomas. The R132C mutations are the most common mutation in MF and Oll. The R132H mutations are most frequent in glioma (91%) whereas in Maffucci syndrome so far no R132H mutations have been found. Although the number of Maffucci syndrome tumours is not very high, it is suggestive that not a single mutation has been found ($p < 0.0001$).

It is not unique for mutations to be unevenly distributed between tissues and within a tissue. Using the COSMIC database (www.sanger.ac.uk), we observe that such tumour type specific mutation pattern is also present in various other genes (table 2). In TP53 for

example, the two most frequent mutations occur at the codons encoding for R248 and R273. When we look at the number of mutations per tissue type we see that the ratio between the two mutations for codon 248 is even whereas it is not for codon 273. There are relatively fewer c.816C>T mutations in breast tumours compared to c.818G>A whereas this is the other way round for the gliomas.

For *PTEN* we see a similar issue for codons 130 and 173. A nonsense mutation is the most frequent mutation at codon 130 in gliomas whereas a missense mutation on this codon (R130G) is most common in endometrial cancer. For codon 173, the p.R173C is the most frequent mutation in endometrial cancer whereas the ratio in gliomas is more equal. (Fischer's exact test, p=0.0013)

Different mutations can occur due to external factors, the best known example is the more frequent occurrence of G>A transitions in non-smokers lung cancers whereas transversions G>T and G>C occur more frequently in (former) smokers. (28) In gliomas, the treatment with an alkylating chemotherapy, such as temozolamide, results in G/T mismatches. (29) Such environmental factors can result in a molecularly different tumor type. For example, EGFR is known to be frequently mutated in lung cancer, but the frequency is inversely correlated with smoking. Looking at mutations in EGFR exons 19 and 21, smokers have a lower frequency of mutations (4%) compared to non-smokers (51%). (30)

Table 2. Frequency of different type of TP53 and PTEN mutations subdivided by tumour type.

TP53	p.R248		p.R273	
	c.743G>A	c.742C>T	c.817C>T	c.818G>A
	p.R248Q	p.R248W	p.R273C	p.R273H
Large intestine	131 (25%)	130 (28%)	98 (22%)	121 (24%)
Breast	73 (14%)	57 (12%)	10 (2%)	62 (13%)
CNS	35 (7%)	30 (6%)	110 (25%)	41 (8%)
Glioma	29 (5%)	27 (6%)	106 (24%)	40 (8%)
PNET/Medulloblastoma	6 (1%)	3 (1%)	4 (1%)	1 (<1%)
Total*	534	465	441	496

PTEN	p.R130G		p.R173		p.R233	
	c.388C>G	c.388C>T	c.389G>A	c.517C>T	c.518G>A	c.697C>T
	p.R130G	p.R130*	p.R130Q	p.R173C	p.R173H	p.R233*
Endometrium	66 (88%)	22 (39%)	38 (73%)	12 (40%)	2 (9%)	37 (55%)
CNS	4 (5%)	21 (37%)	3 (6%)	16 (53%)	19 (83%)	11 (16%)
Glioma	4 (5%)	19 (33%)	3 (6%)	16 (53%)	19 (83%)	11 (16%)
PNET/Medulloblastoma	-	2 (4%)	-	-	-	-
Total*	75	57	52	30	23	67

This table describes the number of mutations for TP53 and PTEN mutations subdivided by tumour type.

Only the most frequent tumours associated with the mutation are mentioned in this table. The total describes the total number of mutations described for that particular mutation on sanger.co.uk.

To what extent the different mutations of IDH1 and the difference between IDH1 and IDH2 is due to environmental changes or functional differences is unknown. It is however, quite interesting from a functional perspective to determine this. In IDH1, low frequent mutations such as G97D and R100A result in the increased concentration of 2HG, similar to their more frequent cousin (R132H). It remains to be determined why virtually only

R132H mutations occur. (31) Functional differences could indicate that IDH mutations result into more changes than just an increase in 2HG. One way to do this would be to analyse the previously mentioned haematopoietic mouse model with an R132H mutation. It will be interesting to see whether other mutations (e.g. IDH1-R132C, R140Q in IDH2) will give identical changes. This would allow a better understanding of the function of IDH1 and 2 and provide clues whether these mutations are not identical in function.

EGFR

The study of such different mutations frequencies in different types of tumours at a single codon is interesting as it may indicate mutation specific functional consequences. An example of such mutation specific functional consequences is shown in chapter five. In this chapter we have studied the functional consequences of different activating mutations in *EGFR*. In GBMs, the most common mutation identified is an in frame deletion of exons 2-7. In pulmonary adenocarcinomas, the most common mutation in *EGFR* results in L858R. *EGFRvIII* mutations are not found in lung adenocarcinomas while *EGFR* L858R mutations are never found in GBM. (32-34) Both mutations are constitutively activating. (34)

We have determined that *EGFR*, *EGFRvIII* and *EGFR* L858R have different binding partners and activate a different transcription response. When considering pleiotropy, multiple effects by a single gene, it is perhaps not surprising that different mutations result in different effects. Other groups have found that different mutations in *EGFR* are differently associated with DNA repair and their nuclear translocation is different. (35) Also for TP53, it has been described that different mutations can result in different binding partners, though only one of 15 interacting proteins was reported to result in an altered function resulting in increased invasion. (36) So although a mutation can be different on a genomic level it does not always result in a functional difference on a protein level, and if it does, the consequences for the tumour remain to be seen. The remaining question is: are there functional consequences for the tumour? Some variation in mutation might give rise to actual differences in the tumour while others might have an identical, or very similar, function.

Models and brain tumours

In this thesis we have used various models to investigate brain tumours. We have used various *in silico* methods, cell lines (both primary and established), and mouse models. Models are imperfect; for example, to which extent current models vary from the original tumour remains to be detailed. On average primary cell lines resemble tumours more than established lines, but only a subset of tumours can be propagated *in vitro*. E.g. IDH1 mutations are gone after one to two rounds of cell culture. What is interesting to note, is that when primary tumours are passed on as xenografts, IDH1 mutations are retained. (13) Primary cell lines retain intratumour heterogeneity, which makes them ideal for studying a human tumour but makes reproducibility of results harder and necessitates an increase in number of experiments. Although genetic animal models can give valuable insight in a process, identical mutations in mouse and man will not always give rise to an identical phenotype. For example, APC mutations give rise to colorectal cancer in man but cancer in the small intestines in mice. (37) For each research question different models should be used, not just established cell lines or just primary cell lines.

Although this will make research results more challenging to interpret it should give us better insight into the answers to the research question.

The introduction of targeted therapies has increased the survival of a subset of patients. For example the introduction of EGFR inhibitors has had a major impact on lung tumour patients with EGFR mutations. BRAF inhibitors have increased the survival of patients with melanoma.(38) Although inhibition of a specific protein might only work with specific mutations or in certain types of cancer, as we see no effect for EGFR inhibitors in GBMs, future research in this direction could mean extending the lives of patients.

References

1. Kloosterhof NK, Bralten LB, Dubbink HJ, French PJ, van den Bent MJ. Isocitrate dehydrogenase-1 mutations: a fundamentally new understanding of diffuse glioma? *Lancet Oncol.* Jul 6.
2. Gravendeel AM, Kloosterhof NK, Bralten LB, Marion Rv, Dubbink HJ, Dinjens WN, et al. Segregation of non-R132H mutations in IDH1 into distinct molecular subtypes of glioma. *Human Mutation.* 2009;in press.
3. Bralten LB, Kloosterhof NK, Balvers R, Sacchetti A, Lapre L, Lamfers M, et al. IDH1 R132H decreases proliferation of glioma cell lines in vitro and in vivo. *Ann Neurol.* Mar;69(3):455-63.
4. Thompson MC, Fuller C, Hogg TL, Dalton J, Finkelstein D, Lau CC, et al. Genomics identifies medulloblastoma subgroups that are enriched for specific genetic alterations. *J Clin Oncol.* 2006 Apr 20;24(12):1924-31.
5. Kool M, Koster J, Bunt J, Hasselt NE, Lakeman A, van Sluis P, et al. Integrated genomics identifies five medulloblastoma subtypes with distinct genetic profiles, pathway signatures and clinicopathological features. *PLoS One.* 2008;3(8):e3088.
6. Phillips HS, Kharbanda S, Chen R, Forrest WF, Soriano RH, Wu TD, et al. Molecular subclasses of high-grade glioma predict prognosis, delineate a pattern of disease progression, and resemble stages in neurogenesis. *Cancer Cell.* 2006 Mar;9(3):157-73.
7. Li A, Walling J, Ahn S, Kotliarov Y, Su Q, Quezado M, et al. Unsupervised analysis of transcriptomic profiles reveals six glioma subtypes. *Cancer Res.* 2009 Mar 1;69(5):2091-9.
8. Comprehensive genomic characterization defines human glioblastoma genes and core pathways. *Nature.* 2008 Oct 23;455(7216):1061-8.
9. Gravendeel LA, Kouwenhoven MC, Gevaert O, de Rooi JJ, Stubbs AP, Duijm JE, et al. Intrinsic Gene Expression Profiles of Gliomas Are a Better Predictor of Survival than Histology. *Cancer Res.* 2009 Nov 17.
10. Northcott PA, Korshunov A, Witt H, Hielscher T, Eberhart CG, Mack S, et al. Medulloblastoma comprises four distinct molecular variants. *J Clin Oncol.* Apr 10;29(11):1408-14.
11. French PJ, Peeters J, Horsman S, Duijm E, Siccama I, van den Bent MJ, et al. Identification of differentially regulated splice variants and novel exons in glial brain tumors using exon expression arrays. *Cancer Res.* 2007 Jun 15;67(12):5635-42.
12. Faustino NA, Cooper TA. Pre-mRNA splicing and human disease. *Genes Dev.* 2003 Feb 15;17(4):419-37.
13. Parsons DW, Jones S, Zhang X, Lin JC, Leary RJ, Angenendt P, et al. An integrated genomic analysis of human glioblastoma multiforme. *Science.* 2008 Sep 26;321(5897):1807-12.
14. Bettgowda C, Agrawal N, Jiao Y, Sausen M, Wood LD, Hruban RH, et al. Mutations in CIC and FUBP1 contribute to human oligodendroglioma. *Science.* Sep 9;333(6048):1453-5.
15. Bralten LB, Gravendeel AM, Kloosterhof NK, Sacchetti A, Vrijenhoek T, Veltman JA, et al. The CASPR2 cell adhesion molecule functions as a tumor suppressor gene in glioma. *Oncogene.* Aug 16.
16. Bralten LB, Kloosterhof NK, Gravendeel LA, Sacchetti A, Duijm EJ, Kros JM, et al. Integrated genomic profiling identifies candidate genes implicated in glioma-genesis and a novel LEO1-SLC12A1 fusion gene. *Genes Chromosomes Cancer.* Jun;49(6):509-17.
17. Hartmann C, Meyer J, Balss J, Capper D, Mueller W, Christians A, et al. Type and frequency of IDH1 and IDH2 mutations are related to astrocytic and oligodendroglial differentiation and age: a study of 1,010 diffuse gliomas. *Acta Neuropathol.* 2009 Oct;118(4):469-74.

18. Sasaki M, Knobbe CB, Munger JC, Lind EF, Brenner D, Brustle A, et al. IDH1(R132H) mutation increases murine haematopoietic progenitors and alters epigenetics. *Nature*. Aug 30;488(7413):656-9.
19. Sasaki M, Knobbe CB, Itsumi M, Elia AJ, Harris IS, Chio, II, et al. D-2-hydroxyglutarate produced by mutant IDH1 perturbs collagen maturation and basement membrane function. *Genes Dev*. Sep 15;26(18):2038-49.
20. Zhao S, Lin Y, Xu W, Jiang W, Zha Z, Wang P, et al. Glioma-derived mutations in IDH1 dominantly inhibit IDH1 catalytic activity and induce HIF-1alpha. *Science*. 2009 Apr 10;324(5924):261-5.
21. Kumar V, Cotran RS, Robbins SL. Robbins basic pathology. 7th ed. Philadelphia, PA: Saunders; 2003.
22. Amary MF, Bacsi K, Maggiani F, Damato S, Halai D, Berisha F, et al. IDH1 and IDH2 mutations are frequent events in central chondrosarcoma and central and periosteal chondromas but not in other mesenchymal tumours. *J Pathol*. Jul;224(3):334-43.
23. Pansuriya TC, van Eijk R, d'Adamo P, van Ruler MA, Kuijjer ML, Oosting J, et al. Somatic mosaic IDH1 and IDH2 mutations are associated with enchondroma and spindle cell hemangioma in Ollier disease and Maffucci syndrome. *Nat Genet*. Dec;43(12):1256-61.
24. Paschka P, Schlenk RF, Gaidzik VI, Habdank M, Kronke J, Bullinger L, et al. IDH1 and IDH2 mutations are frequent genetic alterations in acute myeloid leukemia and confer adverse prognosis in cytogenetically normal acute myeloid leukemia with NPM1 mutation without FLT3 internal tandem duplication. *J Clin Oncol*. Aug 1;28(22):3636-43.
25. Kloosterhof NK, Bralten LB, Dubbink HJ, French PJ, van den Bent MJ. Isocitrate dehydrogenase-1 mutations: a fundamentally new understanding of diffuse glioma? *Lancet Oncol*. Jan;12(1):83-91.
26. Wang P, Dong Q, Zhang C, Kuan PF, Liu Y, Jeck WR, et al. Mutations in isocitrate dehydrogenase 1 and 2 occur frequently in intrahepatic cholangiocarcinomas and share hypermethylation targets with glioblastomas. *Oncogene*. Jul 23.
27. Amary MF, Damato S, Halai D, Eskandarpour M, Berisha F, Bonar F, et al. Ollier disease and Maffucci syndrome are caused by somatic mosaic mutations of IDH1 and IDH2. *Nat Genet*. Dec;43(12):1262-5.
28. Riely GJ, Marks J, Pao W. KRAS mutations in non-small cell lung cancer. *Proc Am Thorac Soc*. 2009 Apr 15;6(2):201-5.
29. Hunter C, Smith R, Cahill DP, Stephens P, Stevens C, Teague J, et al. A hypermutation phenotype and somatic MSH6 mutations in recurrent human malignant gliomas after alkylator chemotherapy. *Cancer Res*. 2006 Apr 15;66(8):3987-91.
30. Pham D, Kris MG, Riely GJ, Sarkaria IS, McDonough T, Chuai S, et al. Use of cigarette-smoking history to estimate the likelihood of mutations in epidermal growth factor receptor gene exons 19 and 21 in lung adenocarcinomas. *J Clin Oncol*. 2006 Apr 10;24(11):1700-4.
31. Ward PS, Cross JR, Lu C, Weigert O, Abel-Wahab O, Levine RL, et al. Identification of additional IDH mutations associated with oncometabolite R(-)-2-hydroxyglutarate production. *Oncogene*. May 10;31(19):2491-8.
32. Bamford S, Dawson E, Forbes S, Clements J, Pettett R, Dogan A, et al. The COSMIC (Catalogue of Somatic Mutations in Cancer) database and website. *Br J Cancer*. 2004 Jul 19;91(2):355-8.
33. Nyati MK, Morgan MA, Feng FY, Lawrence TS. Integration of EGFR inhibitors with radiochemotherapy. *Nat Rev Cancer*. 2006 Nov;6(11):876-85.
34. Gajiwala KS, Feng J, Ferre R, Ryan K, Brodsky O, Weinrich S, et al. Insights into the Aberrant Activity of Mutant EGFR Kinase Domain and Drug Recognition. *Structure*. Feb 5;21(2):209-19.
35. Lippardi G, Hartley JA, Hochhauser D. EGFR nuclear translocation modulates DNA repair following cisplatin and ionizing radiation treatment. *Cancer Res*. Feb 1;71(3):1103-14.
36. Coffill CR, Muller PA, Oh HK, Neo SP, Hogue KA, Cheok CF, et al. Mutant p53 interactome identifies nardilysin as a p53R273H-specific binding partner that promotes invasion. *EMBO Rep*. Jul;13(7):638-44.
37. Heyer J, Yang K, Lipkin M, Edelman W, Kucherlapati R. Mouse models for colorectal cancer. *Oncogene*. 1999 Sep 20;18(38):5325-33.
38. Smalley KS, Sondak VK. Melanoma--an unlikely poster child for personalized cancer therapy. *N Engl J Med*. Aug 26;363(9):876-8.
39. Balss J, Meyer J, Mueller W, Korshunov A, Hartmann C, von Deimling A. Analysis of the IDH1 codon 132 mutation in brain tumors. *Acta Neuropathol*. 2008 Dec;116(6):597-602.
40. Yan H, Parsons DW, Jin G, McLendon R, Rasheed BA, Yuan W, et al. IDH1 and IDH2 mutations in gliomas. *N Engl J Med*. 2009 Feb 19;360(8):765-73.

Addendum

Summary

Brain tumours occur either as, *de novo*, or primary brain tumours, or secondary tumours. The latter group consists of metastases from other tumours, such as breast- and lungtumours. Primary braintumours are a heterogenous group consisting of different type of brain tumours. In children, a frequent type of brain tumour are primitive neuro-ectodermal tumours (PNET), other tumours frequently occurring are pilocytic astrocytomas, ependymomas and medulloblastoma. Other tumours occur in adults, mainly meningioma, which are generally benign, and glioma. Glioma is a heterogenous group of tumours. The most frequent types of glioma are oligodendroglioma, astrocytoma, oligoastrocytoma and glioblastoma multiforme (GBM).

In this thesis we investigated both medulloblastoma and glioma. We have walked through the process of finding, describing, investigating and comparing mutations. We have looked for novel mutations in medulloblastoma, and we did functional research in glioma and looked into *IDH1* and *EGFR*.

In chapter one we have investigated 'splicing' in medulloblastoma. Based on gene expression medulloblastoma can be subdivided in four distinct groups, WNT, SHH, group 3 and group 4. We have looked in 117 samples for subgroup specific alterations and compared this with fetal brain tissue. We found group specific alterations mainly in group 3 and the SHH group. They were relatively rare in the WNT group.

In the second chapter we performed a literature study to determine what is known about *IDH1*, in tumours and from other research. In this chapter we have further looked at potential leads for future research.

In chapters three and four we further examine the genetic changes of *IDH1*. In the third chapter we describe that apart from the most frequent mutation, *IDH1 R132H*, other mutations occur on the same codon. These mutations are not normally distributed amongst the different types of glioma. These non-R132H mutations occur more frequently in combination with mutations in TP53. On the other hand, loss of chromosomes 1p and 19q, a frequent occurrence in oligodendroglioma, is inversely correlated with the presence of these non-R132H mutations. The distribution of the non-R132H mutations could indicate a different cause of the mutations, or a functional difference between these mutations.

In the fourth chapter we are digging deeper into the function of the *IDH1 R132H* mutation. We show, that contrary to our expectation, cells containing this mutation display reduced growth. The reduced growth was also observed when using xenografts. Staining for pAkt in these cells confirms reduced activation in these cell lines. Patients with an *IDH1* mutation have an increased survival; our results could give an indication why this could be.

In chapter five we compared different mutations of *EGFR*, *EGFRvIII* and *EGFR L858R*, with each other and compared them with *EGFR* wildtype. *EGFR L858R* occurs frequently in adenocarcinomas of the lung, whereas the *EGFRvIII* mutation occurs most frequently in GBM. Inversly, *EGFRvIII* was never found in lung adenocarcinomas and *EGFR L858R* mutations were never found in GBM. This is an important reason why we looked at these mutations, if there is a functional difference. Firstly we have used mass spectrometry to determine whether there are different binding partners for *EGFR* or its mutants. We found two novel partners, *DOCK4* and *UGGT1*. *DOCK4* does not seem to be binding to *EGFR L858R*, but does however bind to *EGFRvIII* and *EGFR* wildtype. Furthermore, we see a strong difference in growth and migration between the different variants of *EGFR*. The two *EGFR* mutants we investigated, *EGFRvIII* and *EGFR L858R*, display a reduced migration compared to wildtype *EGFR*. In respect to proliferation, the two *EGFR* mutants have reduced proliferation compared to GFP control cells.

In this thesis we describe research starting at the discovery of novel targets, the detailed description of the mutations present to the detailed functional investigations of target genes and proteins.

Samenvatting

Hersentumoren komen in twee varianten voor, *de novo*, of primaire hersentumoren, en secundaire tumoren. De laatste groep tumoren zijn metastasen van andere tumoren, zoals borst- en longtumoren, die naar de hersenen zijn uitgezaaid. Primaire hersentumoren bestaan uit verschillende type tumoren. Bij kinderen komen vaak primitieve neuro-ectodermale tumoren voor, zogenaamde PNETs, maar ook pilocitaire astrocytomen, ependymomen en medulloblastomen. Bij volwassenen komen andere tumoren voor, meningiomen, deze zijn meestal goedaardig, en gliomen. Gliomen bestaan wederom uit zeer diverse soorten tumoren maar de meest voorkomende zijn oligodendrogliomen, astrocytomen, oligoastrocytomen en glioblastomen multiforme (GBM).

In deze thesis hebben wij basaal onderzoek gedaan naar medulloblastomen en gliomen. We hebben het proces van het vinden, het beschrijven, onderzoeken en vergelijken van de mutaties doorlopen. Het onderzoek naar mogelijke nieuwe eiwitten is gedaan in medulloblastomen en het functionele onderzoek is gedaan bij de genen *IDH1* and *EGFR*.

In hoofdstuk twee hebben wij 'splicing' onderzocht bij medulloblastomen. Medulloblastomen zijn op basis van genexpressie onder te verdelen in vier groepen, WNT, SHH, group 3 en group 4. Wij hebben in 117 samples gekeken naar afwijkingen die voorkomen in specifieke subgroepen en dit vergeleken met foetaal hersenweefsel. Wij hebben voornamelijk in groep 3 en in de SHH groep specifieke afwijkingen gevonden. Deze waren relatief zeldzaam in de WNT groep.

In het derde hoofdstuk hebben wij een literatuurstudie gedaan om te bestuderen wat bekend is over *IDH1* in tumoren en van ander onderzoek om zodoende een basis te vormen voor verder onderzoek. In dit hoofdstukken hebben wij verschillende aanknopingspunten voor verder onderzoek uitgewerkt.

In de hoofdstukken vier en vijf gaan wij dieper in op de genetische veranderingen van *IDH1*. In hoofdstuk vier beschrijven wij dat er naast de meest voorkomende mutatie, *IDH1* R132H, andere mutaties op dit codon voorkomen en dat deze niet normaal verdeeld zijn over de verschillende typen hersentumoren. Deze andere, oftewel de niet-R132H mutaties, komen voornamelijk voor in tumoren met een mutatie in het gen *TP53*, dit zijn vaker astrocytomen. Daarentegen komen wij deze mutatie relatief weinig tegen als er een verlies is van chromosomen 1p and 19q, wat vaker voorkomt in oligodendrogliomen. Deze verdeling van mutaties zou er op kunnen wijzen dat er of een verschil is in de oorzaak van deze mutaties of dat er een functioneel verschil is.

In het vijfde hoofdstuk gaan wij dieper in op de functie van de meeste voorkomende mutatie, *IDH1* R132H. Wij laten zien dat, tegen onze verwachting in, cellen met deze mutatie langzamer groeien wanneer er celculturen gebruikt worden maar ook wanneer dit getest wordt met xenografts. Kleuring tegen pAkt bevestigt verminderde activatie bij de mutant cellijnen. Patienten met een *IDH1* mutatie hebben een leven langer, deze resultaten geven aan dat *IDH1* hieraan mogelijk een bijdrage levert.

In hoofdstuk zes van deze thesis vergelijken wij verschillende mutaties van *EGFR*, *EGFRvIII* en *EGFR* L858R, met elkaar en de normale variant. De *EGFR* L858R mutatie komt vaak voor bij adenocarcinomen van de long, terwijl de *EGFRvIII* mutatie voornamelijk bij GBMs voorkomt, andersom zijn deze mutaties nog nooit gevonden. Dat is de reden waarom wij hebben gekeken of er een functioneel verschil is met verschillende technieken. Als eerste hebben wij gekeken of er verschillen zijn met bindingspartners van de eiwitten. Hier hebben wij twee nieuwe partners gevonden, *DOCK4* en *UGGT1*. *DOCK4* bindt niet aan *EGFR* L858R maar wel aan *EGFRvIII* en het wildtype *EGFR*. *UGGT1* bindt ook aan *EGFRvIII*, minder sterk aan *EGFR* L858R en niet aan *EGFR* wildtype. Ook zien wij een verschil in groei en migratie tussen de verschillende varianten van *EGFR*. Wij zien dat zowel *EGFRvIII* als *EGFR*L858R langzamer migreren dan het wildtype *EGFR*. Qua proliferatie zien wij dat dit consequent langzamer is dan onze controle met GFP.

Dit proefschrift beschrijft het proces van het begin van het vinden van een mogelijk interessant gen, de analyse hiervan tot het in detail beschrijven van het gen casu quo eiwit.

PhD portfolio

Name PhD student: Nanne K. Kloosterhof

PhD period: 2008-2012

Research School: Molecular Medicine

Promotor(s): Prof. P.A.E. Sillevius Smitt

Erasmus MC Department:

Supervisors: dr. P.J. French, dr E.M.C. Michiels

Neurology/Paediatric Oncology and

Hematology

PhD Training

Courses

	Year	ECTS
Partek Training Course	2008	0.2 ECTS
Basic and Translational Oncology	2008	0.6 ECTS
Indesign CS5 workshop	2011	0.2 ECTS
Basic Course on 'R'	2011	0.2 ECTS
Research Management for PhD-students	2012	0.2 ECTS

Meetings

Weekly JN1 research meetings	2008-2012	2 ECTS
Biweekly Neurooncology meeting	2008-2012	1 ECTS
Molmed Bridge meetings	2008-2012	0.5 ECTS

(Inter)national conferences

LWNO (oral presentation)	2010	0.4 ECTS
LWNO (oral presentation)	2011	0.4 ECTS
15 th Society for Neuro-Oncology annual meeting (poster)	2010	0.4 ECTS
Molmed day (poster)	2012	0.4 ECTS
Molmed day (poster)	2011	0.4 ECTS
IBTRT conference (oral presentation)	2012	0.4 ECTS

Other activities

Chair Promeras (PhD organisation Erasmus MC)	2009-2011	6 ECTS
Nicky Bakker (HLO student)	2012	1 ECTS

List of publications

Gravendeel, L. A., Kouwenhoven, M. C., Gevaert, O., de Rooi, J. J., Stubbs, A. P., Duijm, J. E., Daemen, A., Bleeker, F. E., Bralten, L. B., **Kloosterhof, N. K.**, De Moor, B., Eilers, P.H., van der Spek, P.J., Kros, J.M., Sillevius Smitt, P.A., van den Bent, M.J., and French, P.J. (2009). Intrinsic gene expression profiles of gliomas are a better predictor of survival than histology. *Cancer Res* 69, 9065-9072.

Bralten, L. B., Gravendeel, A. M., **Kloosterhof, N. K.**, Sacchetti, A., Vrijenhoek, T., Veltman, J. A., van den Bent, M. J., Kros, J. M., Hoogenraad, C. C., Sillevius Smitt, P. A., and French, P. J. (2010). The CASPR2 cell adhesion molecule functions as a tumor suppressor gene in glioma. *Oncogene* 29, 6138-6148.

Bralten, L. B., **Kloosterhof, N. K.**, Gravendeel, L. A., Sacchetti, A., Duijm, E. J., Kros, J. M., van den Bent, M. J., Hoogenraad, C. C., Sillevius Smitt, P. A., and French, P. J. (2010). Integrated genomic profiling identifies candidate genes implicated in glioma-genesis and a novel LEO1-SLC12A1 fusion gene. *Genes Chromosomes Cancer* 49, 509-517.

Kloosterhof, N. K.,* Gravendeel, L. A.,* Bralten, L. B.,* van Marion, R., Dubbink, H. J., Dinjens, W., Bleeker, F. E., Hoogenraad, C. C., Michiels, E., Kros, J. M., *et al.* (2010). Segregation of non-p.R132H mutations in IDH1 in distinct molecular subtypes of glioma. *Hum Mutat* 31, E1186-1199.

Kloosterhof, N. K.,* Bralten, L. B.,* Balvers, R., Sacchetti, A., Lapre, L., Lamfers, M., Leenstra, S., de Jonge, H., Kros, J. M., Jansen, E. E., Struys, E.A., Jakobs, C., Salomons, G.S., Diks, S.H., Peppelenbosch, M., Kremer, A., Hoogenraad, C.C., Sillevius Smitt, P.A., and French, P.J. (2011). IDH1 R132H decreases proliferation of glioma cell lines in vitro and in vivo. *Ann Neurol* 69, 455-463.

Kloosterhof, N. K.,* Bralten, L. B.,* Dubbink, H. J., French, P. J., and van den Bent, M. J. (2011). Isocitrate dehydrogenase-1 mutations: a fundamentally new understanding of diffuse glioma? *Lancet Oncol* 12, 83-91.

Dubuc, A. M., Morrissy, A. S., **Kloosterhof, N. K.**, Northcott, P. A., Yu, E. P., Shih, D., Peacock, J., Grajkowska, W., van Meter, T., Eberhart, C. G., Pfister, S., Marra, M.A., Weiss, W.A., Scherer, S.W., Rutka, J.T., French, P.J., and Taylor, M.D. (2012). Subgroup-specific alternative splicing in medulloblastoma. *Acta Neuropathol* 123, 485-499.

Korpershoek, E., **Kloosterhof, N. K.**, Ziel-van der Made, A., Korsten, H., Oudijk, L., Trapman, J., Dinjens, W. N., and de Krijger, R. R. (2012). Trp53 inactivation leads to earlier pheochromocytoma formation in pten knockout mice. *Endocr Relat Cancer* 19, 731-740.

Northcott, P. A., Shih, D. J., Peacock, J., Garzia, L., Morrissy, A. S., Zichner, T., Stutz, A. M., Korshunov, A., Reimand, J., Schumacher, S. E., Beroukhi, R., Ellison, D. W., Marshall, C. R., Lionel, A. C., Mack, S., Dubuc, A., Yao, Y., Ramaswamy, V., Luu, B., Rolider, A., Cavalli, F. M., Wang, X., Remke, M., Wu, X., Chiu, R. Y., Chu, A., Chuah, E., Corbett, R. D., Hoad, G. R., Jackman, S. D., Li, Y., Lo, A., Mungall, K. L., Nip, K. M., Qian, J. Q., Raymond, A. G., Thiessen, N. T., Varhol, R. J., Birol, I., Moore, R. A., Mungall, A. J., Holt, R., Kawachi, D., Roussel, M. F., Kool, M., Jones, D. T., Witt, H., Fernandez, L. A., Kenney, A. M., Wechsler-Reya, R. J., Dirks, P., Aviv, T., Grajkowska, W. A., Perek-Polnik, M., Haberler, C. C., Delattre, O., Reynaud, S. S., Doz, F. F., Pernet-Fattet, S. S., Cho, B. K., Kim, S. K., Wang, K. C., Scheurlen, W., Eberhart, C. G., Fevre-Montange, M., Jouvett, A., Pollack, I. F., Fan, X., Muraszko, K. M., Gillespie, G. Y., Di Rocco, C., Massimi, L., Michiels, E. M., **Kloosterhof, N. K.**, French, P. J., Kros, J. M., Olson, J. M., Ellenbogen, R. G., Zitterbart, K., Kren, L., Thompson, R. C., Cooper, M. K., Lach, B., McLendon, R. E., Bigner, D. D., Fontebasso, A., Albrecht, S., Jabado, N., Lindsey, J. C., Bailey, S., Gupta, N., Weiss, W. A., Bogner, L., Klekner, A., Van Meter, T. E., Kumabe, T., Tominaga, T., Elbabaa, S. K., Leonard, J. R., Rubin, J. B., Liao, L. M., Van Meir, E. G., Fouladi, M., Nakamura, H., Cinalli, G., Garami, M., Hauser, P., Saad, A. G., Iolascon, A., Jung, S., Carlotti, C. G., Vibhakkar, R., Ra, Y. S., Robinson, S., Zollo, M., Faria, C. C., Chan, J. A., Levy, M. L., Sorensen, P. H., Meyerson, M., Pomeroy, S. L., Cho, Y. J., Bader, G. D., Tabori, U., Hawkins, C. E., Bouffet, E., Scherer, S. W., Rutka, J. T., Malkin, D., Clifford, S. C., Jones, S. J., Korb, J. O., Pfister, S. M., Marra, M. A., and Taylor, M. D. (2012). Subgroup-specific structural variation across 1,000 medulloblastoma genomes. *Nature* 488, 49-56.

Kloosterhof, N. K., de Rooi, J. J., Kros, M., Eilers, P. H., Sillevius Smitt, P. A., van den Bent, M. J., and French, P. J. (2013). Molecular subtypes of glioma identified by genome-wide methylation profiling. *Genes Chromosomes Cancer* 52, 665-674.

*authors contributed equally

About the author

The author studied Biomedical Sciences at the Universiteit Leiden and at the Karolinska Institutet in Stockholm, Sweden. In 2008 he graduated on the master thesis "*Genetic characterization of pheochromocytomas in PTEN/p53 conditional knock-out mice*" under supervision of dr. R.R. de Krijger. In 2008 he started with his PhD research under supervision of dr. E.M.C. Michiels, dr. P.J. French and prof. P.A.E. Sillevs Smitt at the departments of Neurology and Paediatric Oncology and Hematology. Currently he is working at Salm Partners, LLC in Denmark, Wisconsin.